UNIVERSIDAD NACIONAL DE COLOMBIA
SEDE BOGOTÁ
FACULTAD DE INGENIERÍA

Hybrid Optical Fiber-Wireless Communication to Support Tactile Internet

Mónica Andrea Rico Martínez

Universidad Nacional de Colombia
Facultad de Ingeniería
Departamento de Ingeniería Eléctrica y Electrónica
Bogotá, Colombia
2019

Hybrid Optical Fiber-Wireless Communication to Support Tactile Internet

By

Mónica Andrea Rico Martínez

A dissertation submitted in partial satisfaction of the requirements
for the degree of Doctor in Engineering – Electrical Engineering
in the Doctoral School
of the
National University of Colombia at Bogota

Directed by
Dr. Gloria Margarita Varón Durán
Department of Electrical and Electronics Engineering,
National University of Colombia,
Bogotá, Colombia

Co-Directed by
Dr. Idelfonso Tafur Monroy
Department of Electrical Engineering, Electro-Optical Communications Section,
Technische Universiteit Eindhoven, Netherlands

Research Line:
Optoelectronics
Research Group:
Research Group in high frequency electronics and telecommunications CMUN

National University of Colombia
Faculty of Engineering
Department of Electrical and Electronics Engineering
Bogotá, Colombia
2019

To my little princess……

Knowledge once gained casts a faint light beyond its own immediate boundaries

John Tyndall

Acknowledgments
Agradecimientos

En esta sección quiero dar las gracias a todos y cada una de las personas que me encontré en este camino de más de cuatro años y quienes sin duda hicieron parte de este nuevo peldaño en mi vida. Gracias mil!

A mis padres Judith Martinez y Rodrigo Rico, su apoyo emocional y muchas veces también económico fue fundamental para alcanzar este logro. Mamita, gracias por estar siempre escuchando todas mis preocupaciones durante estos años. Papito, gracias por tu apoyo económico, sin tu ayuda no hubiese podido estar un año en Dinamarca y tu apoyo al regresar es también muy importante. Gracias totales.

A mi familia, mi esposo Oscar Martin y mi pequeña hija Isabella Martin Rico. Empecé este camino cuando apenas tú tenías 6 meses de vida, ya hoy eres toda una princesa con 5 años! Ustedes son merecedores de este logro, ustedes me acompañaron, me escucharon y lucharon a mi lado para poder realizar este trabajo. Fue toda una aventura estar un año en Dinamarca y fue todo un acontecimiento separar mi corazón del de ustedes cuando estuve en Francia y en Medellín y cada vez que salía a una conferencia. Amados míos gracias por ser mi felicidad y mi polo a tierra.

A mis directores de tesis: Margarita e Idelfonso. Gracias por guiarme y apoyarme en este largo camino. A Idelfonso, gracias por recibirme en Dinamarca y hacerme parte de su grupo de investigación en otro país, gracias a ello pude realizar gran parte de la parte experimental de este trabajo de investigación. A Margarita, gracias por la paciencia, el tiempo que has dedicado a leer este documento y la forma como me has orientado para hacerlo cada vez mejor. Gracias infinitas por la confianza, por abrirme las puertas y la oportunidad tanto en DTU como en la Universidad Nacional. De ustedes me llevo su ejemplo y les dejo mi total gratitud.

Agradezco a todos y cada uno de los integrantes de CMUN de la Universidad Nacional. Realmente conocí personas maravillosas que además de apoyarme también me brindaron su amistad. A Santiago, Andrés y Sebastián, gracias por hacerme pasar momentos muy alegres e integrarme cuando llegué al CMUN. A Camilo, Daniel, y otra vez Santi gracias por el apoyo en toda la experimentación. A Sergio, Juan Fernando, Juan David, David, Germán al cuadrado, Yuri, gracias por el apoyo y su compañerismo. Fueron más de cuatro años trabajando a su lado y por supuesto aprendiendo de cada uno de ustedes. Gracias, Gracias, Gracias!

También agradezco a las personas que me encontré en las pasantías, a Victor, Luz, Simon, Sebas, Rafita, Álvaro, Peter, en DTU. Sin ustedes no hubiese sido posible aprender de Radio sobre Fibra. Álvaro, Rafa y Víctor, aprendí demasiado de ustedes! Para mí son mi ejemplo a seguir. Agradezco también a Angelique, Fabien, Karim y a Daniel Romero en Francia quienes me acogieron e hicieron más fácil mi estadía.

Por último agradezco al profe Ferney y a Jesús en la Universidad Pontificia Bolivariana, quienes me prestaron su laboratorio y me ayudaron con los últimos experimentos de este trabajo.

A todos muchas gracias!!!

Resumen

Las tecnologías 5G son sistemas de generación de servicios móviles configurados para cambiar la forma en que las personas, los dispositivos y las máquinas se conectan. La infraestructura 5G está definida como una red ubicua de banda ultra-ancha que soportará Internet en el futuro, dicha red representa una revolución en el campo de las telecomunicaciones. Permitirá eficientemente nuevos servicios ultra-confiables, rápidos y seguros, preservando la privacidad y acelerando los servicios críticos para todos y para cada cosa. Estas redes son la evolución del Internet de las cosas, en donde cada una de ellas es tratada como un objeto cognitivo formando sistemas cibernéticos (CPS). La "experiencia de inmersión total", enriquecida con "información de contexto" y "todo como un servicio" son los principales impulsores para una adopción masiva de los nuevos componentes de ésta tecnología y su aceptación del mercado [1].

Se espera que 5G sea aproximadamente 10 veces más rápido que 4G LTE. Por lo tanto, los desafíos técnicos que deben abordarse en el diseño del sistema 5G son muchos y sin precedentes. Actualmente hay varias actividades en todo el mundo para capturar las aplicaciones y los requisitos para 5G, algunas empresas proveedoras de servicio y fabricantes incluso ya han realizado pruebas para la implementación de dichas redes. Algunos de los principales requisitos que demandan estas redes se pueden resumir en: 100-1000 veces más capacidad del sistema, tasas de datos de usuario en el orden de Gbps en todas partes, latencia en el orden de 1 milisegundo, 10-100 veces mayor número de dispositivos conectados por área, 10 veces más duración de la batería para dispositivos. Estos requisitos transformarán dramáticamente la experiencia inalámbrica de un usuario en un sistema 5G al ofrecer conectividad generalizada rápida en cualquier momento, en cualquier lugar, a cualquier dispositivo [2].

Todo esto requiere un habilitador en el nuevo enfoque de las redes de acceso por radio, que podrían ser comunicaciones híbridas de fibra óptica y transmisiones inalámbricas vía radio. La fotónica por su parte ha sido reconocida por la Unión Europea como una Tecnología Clave Habilitadora (KET), una tecnología que permite un mercado que es muchas veces más grande que el mercado de la tecnología en sí. Las técnicas fotónicas combinadas con la generación de microondas en lo que se conoce en su término en inglés como microwave-photonics se han convertido en habilitadores clave para desbloquear futuras comunicaciones inalámbricas de banda ancha con tasas de datos de terabit a fin de soportar las tendencias actuales del tráfico de datos móviles [3].

El objetivo de esta tesis es concebir experimentalmente y validar enlaces de acceso híbridos de fibra óptica-radio, cuya latencia sea de 1 milisegundo con el fin de soportar Internet táctil, el cual es una aplicación de 5G, teniendo en cuenta los requisitos del sistema. Para ello, primero se realizó una investigación sobre la implementación de enlaces de datos con redes híbridas fibra óptica-radio en la banda de 75-110 GHz con baja latencia. Con esto, se analizaron los componentes de la comunicación híbrida fibra óptica-radio en la banda W. En segundo lugar, se realizaron mediciones de los retardos que se generan en cada uno de los elementos en el sistema híbrido de banda W, haciendo la estimación de la latencia general del sistema e identificando fuentes potenciales de demora en los sistemas híbridos de comunicación óptica-RF de alta velocidad de datos. La principal contribución de este trabajo fue el desarrollo de un procedimiento para medir la latencia utilizando radio definida por software (SDR), además de introducir estos sistemas en los enlaces híbridos fibra óptica-radio.

Una vez conocido como medir la latencia en un sistema híbrido de fibra óptica-radio, los siguientes objetivos que se desarrollaron fueron: probar un esquema de multiplexación apropiado, como la multiplexación por división de frecuencia ortogonal (OFDM) y la multiplexación por división de frecuencia generalizada (GFDM), para lograr una latencia más baja. A su vez, implementar Multiplexación por división de longitud de onda (WDM) para conocer la latencia y la confiabilidad en cuanto a tasa de error de bits variando la multiplexacion eléctrica y óptica.

Palabras clave: Latencia, Radio sobre Fibra, Banda W, Sistemas 5G, Internet Táctil, Radio definida por Software, Esquemas de multiplexación, Formatos de Modulación.

Abstract

5G technologies are systems that will set to change the way people, devices and machines connect. This generation of mobile services provide connection in just one click. The advanced 5G infrastructure, defined as “ubiquitous ultra-broadband network supporting future Internet”, represents a revolution in the telecommunications field. It will enable new secure and reliable services to everyone and everything with ultra-low latency. “Full Immersive Experience”, enriched by “Context Information” and “Anything as a Service” are the main drivers for a substantial adoption of the fifth generation networks [1].

The technical challenges that must be taken into account in the design of the 5G system are many and unprecedented. Therefore,5G is expected to be about 10 times faster than LTE-4G, in addition, it is projected that this network will have100-1000 times higher system capacity, user data rates in the order of Gbps everywhere, 10-100 higher number of connected devices per area, latency in the order of 1 millisecond, and 10 times longer battery life for devices. Due to all these technological changes, for years, researchers, suppliers and manufacturers around the world have studied this new network. In order to transform the user's wireless experience and be able to offer fast generalized connectivity anytime, anywhere, to any device.[2].

All this requires an enabler in the new approach of radio access networks, which could be hybrid optical Fiber-Wireless communications. “Photonics technology has been recognized by the European Union as a Key Enabling Technology (KET), which is a technology that enables a market, many times larger than the market of technology itself”. Photonic techniques have become key enablers to unlock future broadband wireless communications with terabit data rates in order to support the current trends of mobile data traffic[3].

The aim of this thesis is to conceive experimentally and validate 1 millisecond latency hybrid optical Fiber-Wireless access links support for tactile Internet taking into account the system requirements. For this purpose, first a review about the implementation of high-speed data links at 75-110 GHz band with low latency was made. Likewise, this work summarizes the components of hybrid optical Fiber-Wireless communication in W-Band. Second, measurements of the delay contribution from individual elements in the W -Band hybrid system were made. In addition, the main contribution was to develop a procedure for measuring latency physically using software defined radio (SDR) and

estimating the overall system latency. In this procedure, potential sources of delay can be identified in current high-data-rate hybrid optical-RF communication systems.

After knowing how to measure latency in a hybrid optical Fiber-Wireless system, the following objectives were developed: to test an appropriate multiplexing scheme such as Orthogonal Frequency Division Multiplexing (OFDM), and Generalized Frequency Division Multiplexing (GFDM), to achieve the lowest latency with improved performance; and to implement WDM (Wavelength Division Multiplexing) to achieve the required low latency.

Keywords: Latency, Radio over Fiber, W-Band, 5G system, Tactile Internet, Software Defined Radio, multiplexing schemes, Modulation formats.

Contents

Figure List

Table List

Symbols and abbreviations List

4G fourth generation (mobile network)
5G fifth generation (mobile network)
adc analog to digital converter
ber bit error rate
bpsk binary phase shift keying
bw bandwidth
bs Base station

co central office
cw continuous wave (un-modulated tone)
dmux de-multiplexer
e/o electrical to optical conversion
ecl external cavity laser
ed envelope detector
fec forward error correction
Fiwi Fiber-Wireless

fft fast Fourier transform
gmsk Gaussian minimum shift keying
gfdm Generalized frequency division multiplexing
if intermediate frequency
iot internet of things
isi inter symbol interference
ld laser diode
lna low noise amplifier
lo local oscillator
los line of sight
lpf low pass filter
mimo multiple-input multiple-output
mmw millimeter wave (frequency range)
mod modulator
mpa medium power amplifier
mux multiplexer
mwp microwave photonics
mzm Mach Zender Modulator
o/e optical to electrical conversion
ofdm orthogonal frequency division multiplexing
ook on-off keying
osc oscillator
pa power amplifier
pc polarization controller
pd photodiode
psk phase shift keying
qam quadrature amplitude modulation
qpsk quadrature phase shift keying (also: quaternary phase shift keying)
ran radio access network
rau radio access unit
rf radio frequency

RoF Radio over Fiber
rx receiver
sdr software-defined radio
se spectral efficiency (typically in [bit/s/Hz])
smf (standard) single mode fiber
snr signal to noise ratio
tx transmitter
wdm wavelength division multiplexing

Chapter 1

1. Thesis Overview

1.1. Background

Electronic and light wave communication systems have steadily developed over several generations to the point of currently being integral part of every sphere of our life. The wireless mobile communication technology, which is passing through its 3rd and 4th generation, provides mobile broadband Internet access for services such as IP telephony, gaming, video conferencing and cloud computing. Currently, we are in the age of Internet of things (IoT).

Considering its functionality and identity, it is reasonable to define the IoT as "things having identities and virtual personalities operating in smart spaces using intelligent interfaces to connect and communicate within social, environmental, and user contexts"[4].

A different definition, that puts the focus on the seamless integration, could be formulated as "interconnected objects having an active role in what might be called the Future Internet" [5]. Other authors[6] state that the Internet of Things does not have a singular definition. However, the main idea is that any device can be connected to other devices or humans.

In the near future, a major revolution in wireless internet technology awaits with the advent of the highly innovative concept of *Tactile Internet*, as the evolution of IoT, and the *5th generation* of mobile networks [7]. These technologies would revolve around real time human interaction with its immediate or remote environment through wireless steering and control of virtual and real objects. Tactile Internet is acclaimed by the world's leading telecom service providers and is envisioned to find novel applications on the solution of the complex challenges faced by our society in industry automation, transport systems, sports and lifelong learning, healthcare, energy (smartgrids), robotics and manufacturing, telepresence and education[8] [9]. In summary, things are going to be connected, but this connection has to be instantaneous with the lowest possible delay.

Alternatively, Fiber-Wireless communication is a key solution for satisfying the high transmission bandwidths and reliable mobility requirements of the modern society [10]. A Radio over Fiber system RoF or Fiber-Wireless system FiWi was experimentally demonstrated as early as in 1990 to take advantage of the low loss and broadband bandwidth of optical fibers [11]. RoF systems consist of heterogeneous networks formed by wireless and optical links [12], where one or multiple analogous carriers are transported into the fibers. RoF is widely used to provide access to wireless communications with a wide range of applications and coverage of locations, where wired media are not suitable [13].

Radio over Fiber networks have some advantages over other transmission systems. Among these advantages, it is possible to mention high quality and the fact that optical fiber supports up to 10 km or more distances, with minimal signal loss and degradation. The optical fiber works by transmitting light along a material made of dielectric glass. This provides a transmission medium without electromagnetic interference effects, which allows to transmit signals without unaltered in electrically noisy environments. Likewise, optical fiber is a secure medium that propagated light which makes it difficult to alter or there interferences of unwanted signals. Besides, low attenuation loss, large bandwidth, immunity to radio frequency interference, immunity to electromagnetic interference and easy installation and maintenance are other important benefits. It is easier to add new cell sites, upgrade technology, and accommodate multi-service signals within a single system for outdoor applications[14]. Multi-operator and multi-service operation are possible. Finally, RoF links are important for conventional indoor applications because a mobile service center has consistently driven the demand for interconnecting and distributing radio signals from a base station to the remote antenna units[15] [16].

With the blueprint for advanced concepts such as FiWi, Tactile Internet, and 5G mobile communication technology[17], the theoretical limits in the design requirements of an ideal communication system are being studied, such as infinite throughput, zero delay and no information distortion. It is important to analyze how to achieve the requirements of the new generation of networks and to study all their challenges, so that in the future it can be easy to deploy and start-up.

1.2. Motivation, Contributions and Thesis Structure

The appearance of new services has meant the unusual increase of requirement of bandwidth to satisfy the needs of users. The solutions of the TSP (Telecommunication Service provider) to satisfy this increase of the demand of traffic are diverse. Nowadays, it is possible to find different mechanisms to optimize the several types of existing networks. In the same way, the exigencies of quality of service in the telecommunication networks, as delays, loss of packages, throughput, grow more every day with the demand of the users.

This research recognizes the needs of the users in terms of the demands on high-speed transmission and a good quality of service. In this sense, RoF with its advantages seems to be an excellent option, since photonic technologies for wireless systems operating at 75-110 GHz support terabit aggregate capacities. This will change the landscape of high capacity communications with wireless connectivity. Furthermore, it is important to make a study of 5G technology for mobile wireless, because a good selection of the parameters could make a network more efficient and effective. Consequently, this research will study each of the components and their delay in the network in order to achieve a Radio over Fiber link with a lower or equal to 1 ms latency.

This project focuses on the needs of 5G networks and Tactile Internet. First, the study of the state of the art demonstrates that Radio-over-Fiber networks are a solution for future networks. Subsequently, the design of Radio-over-Fiber networks in W-Band (75-110 GHz) is made focused on how to measure and evidence latency according to the tactile Internet requirements. In other words, the main objective of this project is to demonstrate how the latency can be measured in a hybrid Fiber-Wireless link and how end-to-end latencies close to 1 ms are achieved by studying the different techniques of modulation and multiplexing (of both, the electrical and the optical signal).

This thesis experimentally researches hybrid optical fiber- wireless links on W-Band and 3.5GHz band, demonstrating its potential and possibly promoting their implementation, for mobile backhaul networks and for future networks of frontal haul, respectively. Likewise, this research includes a very important aspect for wireless technologies such as cognitive radio. In this sense, the integration of Software-Defined Radio (SDR) is studied and a procedure to measure latency through this technology was developed.

The research in this thesis also involves the multiplexing schemes and modulation formats. First, in the W-Band setup, some modulation formats of the electrical signal created with software defined radio were compared. Then, multiplexing schemes such as OFDM and GFDM were also compared into a 3.5GHz setup. The feasibility of both multiplexing schemes was considered into the front-haul 5G networks. Additionally, WDM was included into a 3.5GHz setup in order to analyze which combination has a better performance in end to end latency. Finally, some simulations in Optisystem and Matlab were made in order to verify the experimental results.

The results of this thesis are presented through this document in six chapters. In addition, in the following paragraphs, the main contributions of this thesis, which have already been mentioned, are framed within the structure of the thesis.

The First Chapter presents the general background of this work, showing the motivation, the main contribution of this doctoral work and the structure of the thesis. The Second Chapter is called “Hybrid Optical Fiber-Wireless Networks or Radio-over-Fiber Systems”. In this chapter, a mathematical and theoretical description of Radio-over-Fiber systems are presented. Additionally, it explains the reasons for working with mm-waves, specifically with W-Band frequencies, and 5th Generation of mobile networks, as well as the definition of Tactile Internet as a departure point for this research. The Third Chapter is entitled "Latency" and presents a review of the theories and an analysis of the state of the art, starting with the concepts of latency, how they have been measured and what types of latency have been measured in Radio-over-Fiber networks. Finally, a design of the procedure to measure latency in hybrid networks is presented.

The Fourth Chapter is called "Hybrid Fiber-Wireless system at W-Band with low latency". It presents all the setup of a W-Band Hybrid Fiber-Wireless system, from the design to the measurements of latency and reliability, and it analysis.

The Fifth Chapter is entitled "Multiplexing in Radio-over-Fiber system with low latency". It presents the different techniques for modulation and multiplexing in two experiments of Radio-over-Fiber network, measuring the latency and the bit error rate. An analysis of modulation and multiplexing techniques using the equipment presented is discussed. Finally, the conclusions, future work of the project, publications, related products and the respective bibliographical references are presented.

Chapter 2

2. Hybrid optical Fiber-Wireless networks or Radio-over-Fiber Systems

Hybrid communications systems have existed for many years. Previously, hybrid - coaxial systems for the analog television deployment and other types of telecommunications were used. Currently, the integration between optical fiber and wireless systems is considered a solution for access or last mile networks since they allow high transmission capabilities compared with radio systems themselves. The combination of fiber and wireless links allows the use of the entire fiber bandwidth through the flexibility, mobility and portability of wireless systems.

Radio over Fiber systems or Fiber Wireless (Fi-Wi) are considered key for solving the challenges of 5G networks, that is, a solution for different types of communication scenarios such as: (a) mobile front-/backhaul, (b) spanning obstacles for providing broadband access to rural areas, (c) short-range indoor wireless distribution, (d) building-to-building communication and (e) recovery and protection of fiber links, as evidenced in [18],[19],[20],[21]. This chapter presents a compilation of the main Radio-over-Fiber concepts, the techniques to make Fiber-Wireless links and its mathematics theory. In addition, the relation between Radio-over-Fiber and 5G, and Tactile Internet and W-Band is described.

2.1. Radio over Fiber System

In an RoF system, also called Fiber-Wireless system (Fi-Wi) [16], the objective is to carry the information through the optical fiber by modulating the light signal with a radio signal [22].

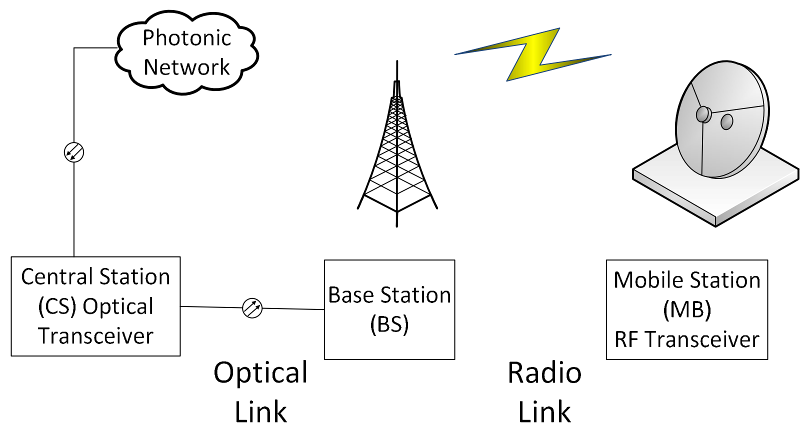

Fig. 2.1. Radio over Fiber components

Source: [15]

Basically, an RoF system is composed of a Central Station (CS) or Header and a Base Station (BS) (Figure 2.1). The RoF system processes the RF signal at the CS and uses fiber optics to distribute the RF signal to the BSs [23]. The CS is the gateway between the transport network and the BSs, while the BS handles the communication with the users. In Figure 2.2, the CS and the BS are shown in detail.

The CS is composed of two main blocks. The Transmission (Tx) Block has a Laser Diode (LD) and an optical modulator that modulates the output of the laser with the RF signal. The Reception (Rx) Block has a Photodiode (PD) that receives the optical signal and transforms it into an electrical signal, which is filtered using a Band Pass Filter (BPS) and then amplified. The BS has the same blocks, but it receives the signal from the optical fiber in the Rx Block and transmits the RF signal modulated using the Tx Block.

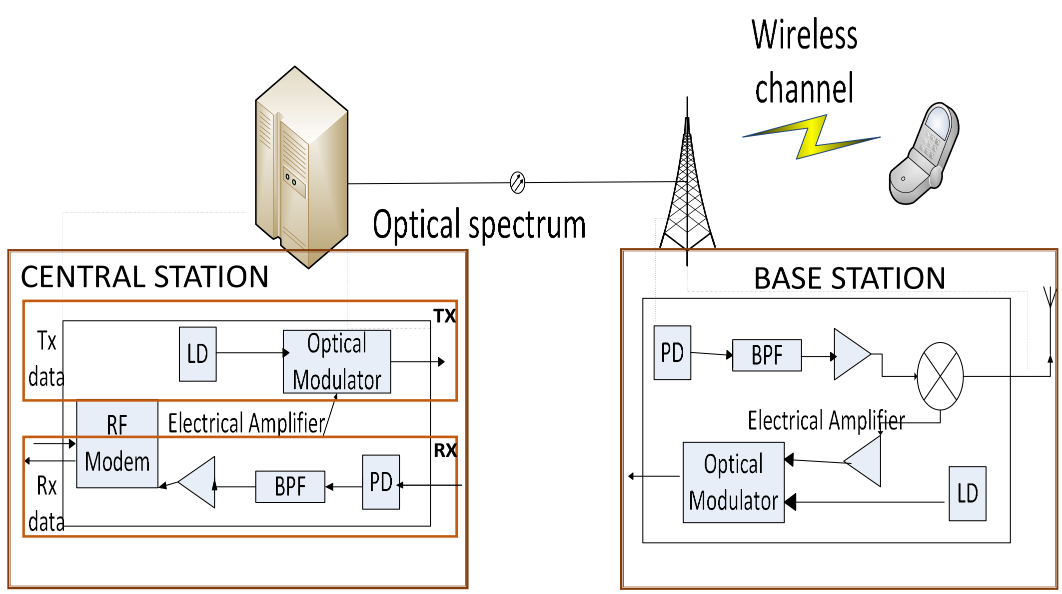

Fig 2.2. CS and BS components in an RoF system

Source: [24]

2.1.1. RoF Architectures

To implement an RoF system, there are several techniques. Three of them are presented in this section[25], [26], [18].

RF-Over-Fiber: The wireless signal or millimeter wave is carried directly on the fiber without translating the frequency into the remote BS. The wireless signal is externally modulated onto an optical carrier signal producing an Optical Double Sideband (ODSB). In this architecture, the modulated signal is generated at the CS in an RF band and transmitted in a straight line to the BSs by an External Optical Modulator (EOM). At each BS, the modulated signal is recovered by detecting the modulated optical signal with a PD and transmitting it to the mobile hosts (MH). For the uplink from an MH to the CS, the reverse process is made. The signals received at a BS are amplified and directly transmitted to the CS by modulating an optical signal from a LD by an EOM[25].

IF-Over-Fiber: In this technique, the wireless signals are converted to a lower intermediate frequency (IF) at the CS before being sent through the optical fiber. This technique significantly reduces chromatic dispersion [16]. In this architecture, the modulated signal is generated at the CS in an IF band and transmitted to the BSs by an EOM. At each BS, the modulated signal is recovered by detecting the modulated optical signal with a PD, upconverted to an RF band, and finally transmitted to the mobile hosts. Besides, the antenna BSs implemented for RoF system and incorporating IF-Over-Fiber transport requires additional electronic hardware such as a mm -wave frequency local oscillator for up- and down frequency conversion [26].

Baseband-Over-Fiber: In this scheme, the wireless baseband signal is transported on the fiber using digital electronic circuitry for processing the signal at the BS. It is similar to the previous one, with the difference that the circuitry for processing the signal and converting the information required in the BS is added. In this architecture, the modulated signal is generated at the CS in baseband and transmitted to the BSs by an EOM. At each BS, the modulated signal is recovered by detecting the modulated optical signal with a PD, upconverted to an RF band through an IF band or directly, and finally transmitted to the mobile hosts [18].

For IF-Over-Fiber and Baseband-Over-Fiber, the bandwidth required for optical modulation can be greatly reduced. However, additional hardware for up-converting it to RF band is required. In both schemes, the signals received at a BS are amplified and down-converted to an IF or a baseband frequency and transmitted to the CS by modulating an optical signal from an LD by using an EOM.

Digitized Radio over Fiber can be classified into Digitized RF-over-Fiber (DRFoF) and Digitized IF-over-Fiber (DIFoF), considering whether the radio signal is converted or not to an IF frequency. In this technique, the wireless signals are digitized before the optical transport in order to produce a sampled digital data stream in a serial format that can directly modulate the optical source. This has a relevant importance because the dynamic range of the optical link is independent of the fiber transmission distance until the received signal goes beyond the link sensitivity. The ADC/DAC technology is the enabling key for this scheme. Figure 2.3 shows the different techniques for implementing a Radio-over-Fiber system.

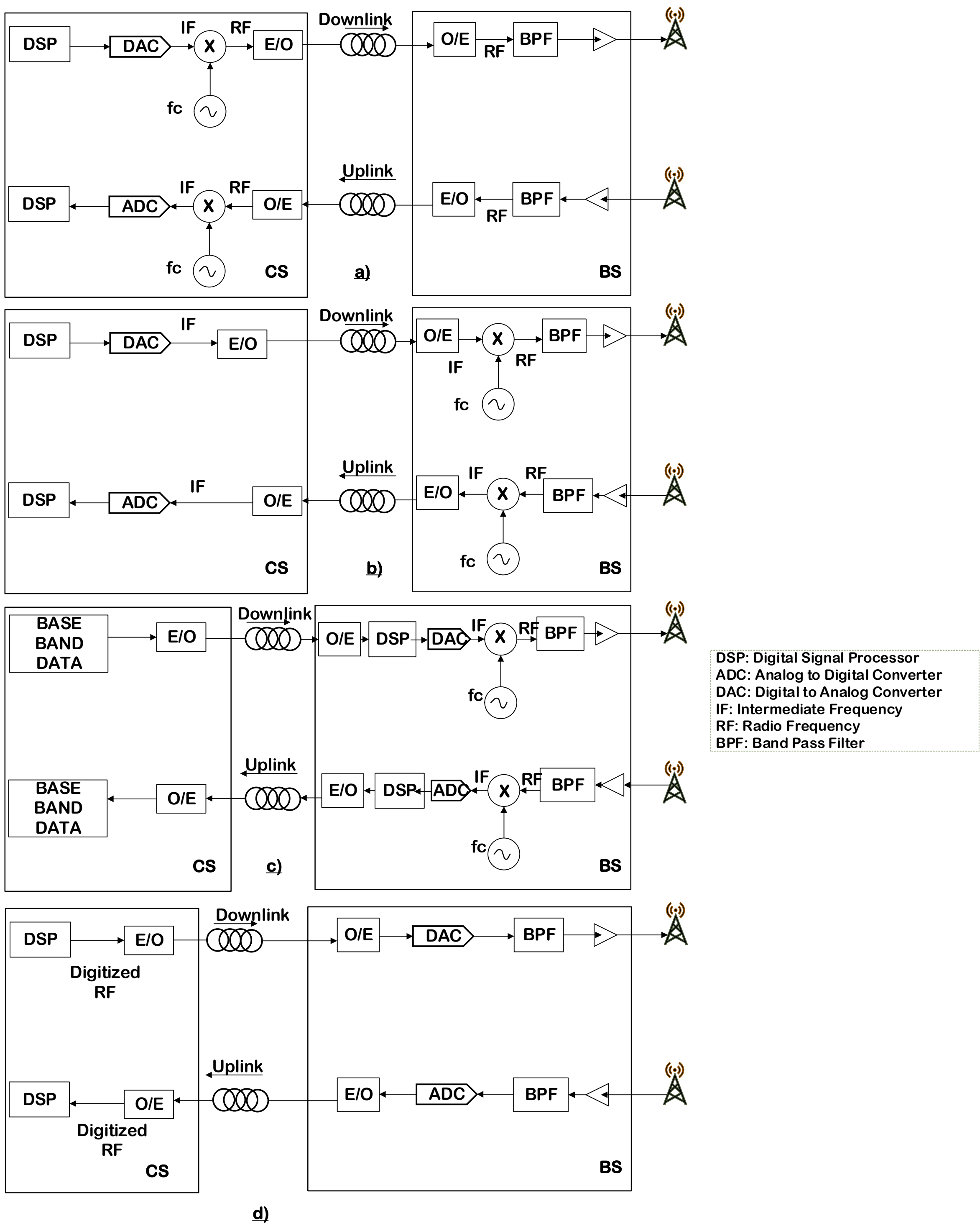

Fig. 2.3. RoF Schemes.
a) RF-over fiber, b) IF-over fiber, c) Base band-over fiber, d) Digitized RF-over fiber
Source:[27]

2.1.2. Techniques for generation of mm-waves in RoF

Figure 2.4. shows the classification of the main optical transmission or generation techniques for producing millimeter-waves for Radio over Fiber systems.

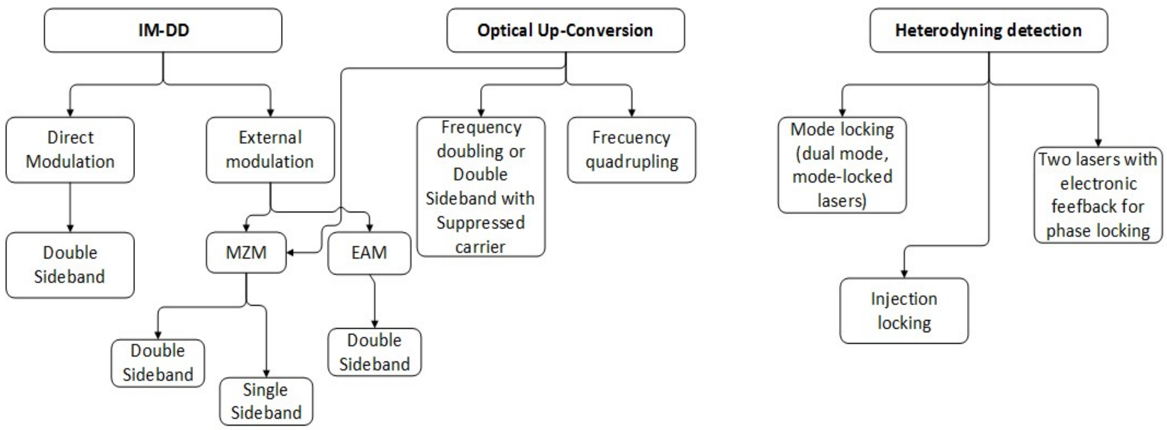

Fig. 2.4. Optical transmission techniques

Source: [26]

In general, there are several ways to generate and detect the signal in Radio-over-Fiber systems. Nonetheless, Fiber-Wireless modulation can be done either by directly modulating the optical source or by externally modulating the optical carrier after generation. These techniques can be used to modulate the intensity (optical power) or amplitude, frequency (doubling or quadrupling) and phase of the optical carrier. These techniques are called "intensity modulation" and "coherent modulation"[28]. The detection techniques may be implemented using an external modulator with envelope detection or using heterodyne detection. The associated detection processes are called 'direct detection' and 'coherent detection,' respectively. There are benefits and drawbacks of each of these approaches. Intensity modulation (and direct detection at the photodetector (IM/DD)) is the most widely used approach due to its simplicity[28].

In Table 2.1., some advantages and disadvantages of the generation of mm-wave for RoF techniques are presented.

Table 2.1. mm-waves RoF Generation Techniques

Techniques	*Advantages*	*Disadvantages*
Heterodyning detection	• No fiber dispersion effect • 100% intensity of modulation depth • High link gain • High carrier to noise ratio (CNR)	• Phase correlated optical carriers • More complex systems
External Modulation	• Simple configuration • DFB laser diode	• High Insertion loss • High RF return loss

	• Supports high frequency RF (MZM) signals	• Frequency chirping • Requires high drive voltage
Direct Modulation	• The simplest configuration • Low cost BS	• High RF return loss • WDM • Crosstalk
Optical Up Conversion	• No fiber dispersion effect • Direct IF modulation	• Requires mm-wave oscillator • Requires high conversion efficiency mixer • Requires additional cost

Source: [22][27]

2.1.3. Components of an RoF link

This section presents the main components of an RoF system, their performance and the equations that describe them. In addition, different figures of merit that affect a RoF link performance are described.

2.1.3.1. Laser Diode

A laser diode is an optical component that incorporates an optical gain medium in a resonant optical cavity to produce coherent light. In fiber optic communication systems, diode lasers are primarily used as transmitters. For short-reach links, they are directly modulated, whereas for longer reach links, they are used in conjunction with external modulation[29]. The limiting factors of a direct modulated laser are its modulation bandwidth, extinction ratio, chirp and linearity. For baseband data modulation, these parameters do not affect significantly the performance of a typical RoF link.

I n Fiber-Wireless applications there are two kinds of lasers that are commonly used: Distributed feedback and Fabry Perot lasers. Nevertheless, VCSEL lasers were used in some experiments of this project and, thus, are presented in this section.

Fabry - Perot laser (FP) [28]. This laser is an oscillator with a rectangular cuboid resonator that uses the reflection from the cavity ends for feedback. The linewidth of this laser is quite wide and may cause a little high distortion due to fiber dispersion. FP emits light in a few longitudinal modes, therefore, it is also susceptible to mode hopping and mode partition noise. These characteristics usually limit the FP to less demanding RoF links. Nonetheless, it is the most common laser diode, has low cost and is widely available [28].

Distributed feedback (DFB) laser [28]. The DFB laser has a resonator that is a periodic structure made with a phase shift in its middle. The positive optical feedback needed for resonance is obtained from distributed Bragg diffraction grating with optical gain within the gratings. Typically, single frequency operation is often easily achieved, since only one lasing mode is created. The DFB is a relatively low-cost single-mode laser, is more immune to fiber dispersion and sideband noise and is available for emission in different spectral regions, at least in the range from 800 nm to 2800 nm. In addition, it provides a high dynamic range and less distorted emission under direct modulation conditions. These lasers are widely used in Fiber-Wireless systems [28].

Vertical Cavity Surface Emitting Laser (VCSEL). This is a semiconductor laser that differs from other laser structures because it is a surface emitting device instead of an edge emitting device. VCSELs emit their energy in perpendicular paths with respect to semiconductor layers. They allow the long wavelength light emission with a reduced power consumption. Finally, they are relatively easy to manufacture, as well as the cheapest in the market.

2.1.4.1.1. Linearity and Nonlinearity

The nonlinearity is an inherent process in lasers because the region where the output light increases exponentially in the stimulated emission, which is often considered as a linear region, is in fact nonlinear. This nonlinear nature of the laser is an intrinsic problem in many analog applications, and also in Fiber-Wireless links[28].

For an ideal linear characteristic, the laser-diode input/output relationship is given as (1) [30],

$$P_{opt} = Z(I - I_{TH})$$
$$Z = \frac{hf}{e}\eta_L \qquad (1),$$

where I is the input current of the microwave signal including the DC bias; I_{TH} is the diode threshold current, Z is the "P-I" slope (i.e. the gradient of the output optical power vs. the input electrical current curve). Z is equivalent to the f (frequency in hertz) multiplied by h (Planck constant) and multiplied for η_L (laser quantum efficiency), which is all divided into e (electron charge). Finally, P_{opt} is the output optical power of the laser-diode.

In general, for the non-linear case, the input/output relationship can be written as (2) [29].

$$P_{opt} = a + b(I - I_{TH}) + c(I - I_{TH})^2 + d(I - I_{TH})^3 \qquad (2)$$

The terms a,b, c and d are constants. Likewise, two types of nonlinearities, statistic and dynamic, can be specified for lasers diodes in the time domain.

On the one hand, the statistic nonlinearity express the P-I curve as an exponential equation or third order polynomial by means of the next equation:

$$P_{opt}(t) = P_o[1 + ms(t) + a_2m^2s^2(t) + a_3m^3s^3(t) \qquad (3),$$

where $s(t)$ is the modulating signal current and m is the modulation depth. The optical modulation depth m is defined as the ratio of the peak optical power to the average optical power P_o . A lower m yields less nonlinear distortion. However, a lower m also reduces the RF sub-carrier power and signal-to-noise ratio. A higher modulation depth increases the saturation distortion and the probability of clipping. $P_{opt}(t)$ is the instantaneous optical power emitted from the laser . P_o, as previously mentioned, is the mean optical power. a_2, a_3 are the coefficients of the third-order laser transfer curve [28].

On the other hand, the dynamic nonlinearity is given by two differential equations [28] called laser rate equations, which specified the nonlinear electron-to-photon conversion process. This nonlinearity is important when there is an unexpected change in the modulating signal. In general, the nonlinearity of the laser limits the Spurious Free Dynamic Range (SFDR) of the RoF link and, therefore, it will limit the radio cell size[28].

2.1.4.1.2. *Relative Intensity Noise*

In an RoF System, the noise contribution has to be considered. The main noise of the Laser Diode is the Relative Intensity Noise (RIN). The RIN depends on the coherency of the light source. This noise relates the photon density fluctuation to the mean photon square density. It is defined in equation (4) [29],

$$\mathrm{RIN} = \frac{\langle \delta \mathrm{P(t)}^2 \rangle}{(\mathrm{P_0})^2} \qquad (4),$$

where the angular bracket terms correspond to averaged terms measured in a specific period of time. The term $\delta \mathrm{P(t)}^2$corresponds to the mean square of the assumed Gaussian noise distribution and $\mathrm{P_0}$ is the optical output power. The RIN units is dBc/Hz.

The RIN is often described in decibels or $10\, Log_{10}(\mathrm{RIN})$. For analog application, the next equation can be used to determine the maximum allowed RIN.

$$\mathrm{SNR} = \frac{\mathrm{m}^2}{2} \frac{\mathrm{P_0^2}}{\langle \delta \mathrm{P(t)}^2 \rangle} \qquad (5),$$

where $m = \frac{\mathrm{P_1}}{\mathrm{P_0}}$, $\mathrm{P_0}$ is the optical output power and $\mathrm{P_1}$ is the injected power, m is the Intensity Modulation index.

2.1.3.2. Modulation

Modulation is the process of adapting the signal by changing a property of a waveform in order to send it through the medium. In some cases RF signals are incompatible for direct transmission over the medium and, therefore, modulation techniques for the communication have to be used[31]. In RoF links, direct and external modulation can be used. In this project, only external modulation is used. For this reason, only this kind of modulation is described.

2.1.4.2.1. *External Intensity Modulation*

External intensity modulation uses an External Optical Modulator (EOM) to change the amplitude of the constant optical output that is driven through the laser source. External modulation is widely used, capable of providing high bandwidths and significantly better power budget, and alleviates issues such as laser chirp, saturation or clipping. Therefore, it is preferred in high-performance links.

There are two kinds of Electro Optical Modulators: the Mach Zehnder Modulator (MZM) and the Electro-Absorption Modulator (EAM).

Mach-Zehnder Modulator

The MZM is an interferometer: it has two arms and two 3-dB optical couplers. A constant optical wave emerging from the laser is divided equally by a splitter into two beams, which are guided in the two arms of the interferometer, and initially have zero phase difference. On one arm, an applied electrical field on the electrodes introduces a small change in the refractive index of the material in the modulator, therefore, the optical field in that arm is phase-shifted by $\Delta\phi$[28]. The beam in the other branch maintains its original state. At the output of the MZM, a second coupler allows the combination of the two mutually interfering waves and the phase-shift generates a differential delay [26].

The optical output power at the output of the MZM is given by

$$P_{out} = \frac{P_{in}}{2}[1 + cos(\Delta\phi(v))] \qquad (6),$$

where P_{in} and P_{out} are the optical powers at the input and at the output of the MZM, respectively, and $\Delta\phi$ is the phase difference between the two interfering beams.

The performance of the MZM is governed by factors such as bias voltage, impedance, optical loss, maximum input power the modulator can handle, bandwidth, linearity, and sensitivity to temperature and polarization. It is important to use the right bias of the MZM to minimize the nonlinearity and reduce the power in unwanted higher-order harmonics[28].

Usually, the MZM will produce a double-sideband spectrum. Nonetheless, it can be configured to generate single-sideband modulation. In addition, the MZM can be used for both digital and analog (RF) modulation[28].

The MZMs are the most used modulator because they have several advantages. First, the MZM is capable of handling a high input power up, hundreds of milliwatts of Constant Wave (CW) optical power without degradations. Second, this kind of modulators has low insertion loss. Third, it provides high bandwidth over hundreds of GHz [28].

Electro-Absorption Modulator

The Electro-Absorption Modulator (EAM) exploits the absorption spectrum of semiconductors. Biasing a semiconductor crystal (with a voltage V) can change its absorption coefficient α (cm^{-1}) and thus modulate the propagating optical signal.

An EAM can be configured as an RF-Optical modulator as well as a photodetector, thus, it is composed of an active semiconductor region sandwiched between a p-doped and an n-doped layer, forming a p-i-n structure. Indeed, the EAM works based on the principle known as the Franz-Keldysh effect. Consequently, the effective bandgap of a semiconductor decreases with the increasing electric field.

In practical EAMs, the active region is usually considered as a bulk quantum-confined structure or multiple quantum wells (MQWs). It provides the quantum-confined Stark effect which produces a stronger field-dependent absorption effect. An electric field applied perpendicularly to the active layer shifts the absorption edge to lower photon energies[32].

The transfer function of an electro-optical modulator is represented as[33]:

$$H_{mod} = \frac{P_{EOM}}{P_{in}} = \alpha cos^2\left[\frac{1}{2}\left(\frac{\pi V_{DC}}{V_{\pi DC}} + \frac{\pi V_{RF(t)}}{V_{\pi RF}} + \theta_{RF} + \theta_{DC}\right)\right] \quad (7),$$

where P_{EOM} represents the electro-optical modulator power, P_{in} represents the input power, α represents the insertion losses of the modulator, θ_{RF} represents the phase mistmatching between the optical and microwave signals, θ_{DC} represents the auto-polarization, V_{DC} and V_{DC} represent a DC and RF voltage, $V_{\pi DC}$ and $V_{\pi RF}$ represent the half-wave voltage DC and RF, respectively.

An EAM has a nonlinear transfer function with a strong dependence on input optical wavelength and power. This causes distortions and reduces the dynamic range of RoF links, therefore, it limits the link gain of an RF link and makes linearization difficult. The strongest advantage of EAM is its ability to be incorporated into the intrinsic region of the Positive-Intrinsic-Negative (PIN) diode. This structure can also act as a high speed photodetector giving a useful functional duality to the structure[32].

2.1.3.3. Optical Fiber

In RoF links, single mode and multimode fiber can be used, depending on the application. In either case, the optical signal undergoes a certain number of distortions due to the fiber geometry and the properties of the material that constitute the fiber. A single-mode fiber is the most used for Fi-Wi applications due to its low dispersion characteristics.

The effects on the optical signal can be divided into two classes: linear effects and non-linear effects. Brillouin diffusion and Raman diffusion belong to the non-linear effects and attenuation and chromatic dispersion belong to the linear effects.
The attenuation governs the power link budget and the dispersion influences the intersymbol interference (ISI). Nonetheless, the effect of chromatic dispersion is negligible for most practical RoF links [28].

A model that attempts to consider the major effects of fiber propagation is called a split step model [34]. In this model, the different effects were split over all the optical fiber in numerous small sections. Each small section acts independently and can be modeled by a number of digital filters in simulation software. The non-linear parameter acts as a multiplier value dependent on the injected laser power. The non-linear effects can be represented by N, which can be described as:

$$N^2 = \frac{2\pi n_2}{\lambda A_{eff}} P_{opt} L_D \quad (8),$$

where n_2 is the non-linear index coefficient, λ is the operating wavelength, A_{eff} is the effective area of the fiber, and L_D is the dispersion length.

Taking into account only the linear effects, a mathematical model of the single mode fiber transfer function can be expressed as [19][20]:

$$\begin{gathered} H(f) = |H(f)| e^{-j\alpha(f)} \\ \alpha = \pi^2 \beta_2 L = \frac{-\pi D L \lambda^2}{2C} \end{gathered} \quad (9),$$

where D represents the dispersion at the operating wavelength, λ represents the operating wavelength, L represents the length of the fiber, and f represents the frequency of the optical carrier and its sidebands.

2.1.3.4. Photodetector

In an RoF link, a photodetector is responsible for transforming an optical signal into an electrical one, but in most cases the signal is very weak. Therefore, an electronic amplification circuitry is needed to ensure that an optimized power signal-to-noise ratio (SNR) is obtained [35]. Then, the main function of the photodetector is to detect the RF modulated photonic signal with an expected level of SNR[28].

A photodetector works with a fundamental mechanism called optical absorption, which has basic requirements like sensitivity at the required wavelength, efficient conversion of photons to electrons, fast response time to operate at high frequencies, low noise, small size for efficient coupling to optical fiber, high reliability and low cost [28]. The most important concepts related to photodetector theory are: quantum efficiency, responsivity, bandwidth, detector technology, e.g. APD, PIN and receiver noise, which are explained below.

2.1.4.4.1. PIN and APD Technology

There are two types of detectors, called the Positive-Intrinsic-Negative (PIN) and the Avalanche Photodiode (APD). On the one hand, the latter has a self-multiplying mechanism that turns into an internal gain like an avalanche, as its name suggest. The disadvantage is the excessive noise that results from this mechanism. In addition, this kind of photodetector requires high bias voltage[28].

On the other hand, PIN photodiodes have an intrinsic semiconductor region sandwiched between a p-doped and an n-doped region. It works under a moderate reverse bias. Therefore, the active area increases and strengthens and may become the photocurrent. PIN detectors are robust, have low cost, small size and provide reasonable noise performance. Thus, PIN diodes are commonly used[28].

In any case, a relationship should exist between the photo detected current and the transmitted signal. The following equation shows the relationship between the photo detected current and the square of the transmitted signal envelope, being C a constant.

$$I(t) = C\left|\overline{E(t)}\right|^2 \qquad (10)$$

2.1.4.4.2. Quantum Efficiency and Bandwidth

On the one hand, the quantum efficiency of a photodetector (η) is the probability that an incident photon will produce an electron-hole pair. Equivalently, it is the ratio of the electron flux (out of the photodetector) to the photon flux (incident on the photodetector) [28]. In other words, quantum efficiency can be defined as the relationship between the number of absorbed photons and the number of emitted electrons. The quantum efficiency can be expressed as follow:

$$\eta = \frac{I_p/q}{P_{in}/h\nu} \qquad (11),$$

where I_p/q means electrons per second and $P_{in}/h\nu$ means photons per second.

On the other hand, the bandwidth of a photodetector is the speed of response to the variation in the incident optical power. High-bandwidth detectors have low quantum efficiency and responsivity. Therefore, the quantum efficiency and bandwidth of a conventional photodiode have inverse dependencies on the photon absorption layer density, that is, the 'transit time' of a carrier to cross the depletion layer rises with the density of the photo absorption layer, which limits the bandwidth. Otherwise, a higher density will enhance the photon absorption according to equation (12), improving the responsivity and quantum efficiency [28].

In conclusion, a high-speed detector with a large bandwidth can only handle 1 to 2 mA of photocurrent, which means that the bandwidth affects the responsivity and optical power density. At low frequencies, photodetectors have ideal responses regarding responsivity, power handling and linearity.

2.1.4.4.3. *Responsivity*

The responsivity of a photodetector is defined as the photocurrent produced per unit of incident optical power. In other words, it is the ratio of optical power incident on the device to the resulting current, measured in A/W. The photo detected current is given by

$$I_p = RP_{in} \qquad (12),$$

where I_p is the photocurrent, R is the responsivity and P_{in} is the incident power.

In this context, the responsivity can be expressed as[28]:

$$R = \eta q / h\upsilon = \eta\lambda / 1.24 \qquad (13),$$

where η is the quantum efficiency, and λ is the operating frequency. It can be observed that the responsivity of a photodiode increases with the wavelength until it reaches the cut-off wavelength[28].

The responsivity is related to the receiver sensitivity, thus, both are associated with the photo detected current. In this way, the receiver sensitivity in an RoF link can be defined as the minimum average optical power level that must arrive at the photodetector to achieve a desired SNR for a given bandwidth[28].

2.1.4.4.4. *Receiver Noise*

In general, in an optical receiver there are always a quantum, thermal, and dark current noise powers added to the signal. The dark current is defined as the current generated in a photodetector in the absence of any optical signal. With no incident light, there is a small leakage currently known as the dark current, which increases with the temperature and the reverse bias. As the incident light increases, more electrons and holes are generated and the reverse current increases linearly.

In an RoF system, the main noise contribution is given by the thermal and the shot noise of the photodetector. A mathematical model explained in [30] is utilized to evaluate the effect of noise resulting from the amplification process. The total noise received is calculated and superimposed over the ideal photodiode signal current. As mentioned previously, the noise in the photodiode includes quantum shot noise I_{sh} , dark current noise I_{dk} , and thermal noise I_{th} . The total current can be expressed as:

$$I_{total} = I_{sig} + \sqrt[2]{I_{noise}{}^2}$$

$$\sqrt[2]{I_{noise}{}^2} = I_{sh}^2 + I_{dk}^2 + I_{th}^2$$

$$I_{sh}^2 = 2qI_{sig}B$$
$$I_{dk}^2 = 2qI_{dk}B \qquad (14),$$
$$I_{th}^2 = 4K_B\frac{TB}{R}$$

where I_{sig} represents the photoelectric current and is the mean squared noise contributions from the photodiode. K_B is Boltzman constant, T is absolute temperature, R is the photodiode load resistor, and B represents the photodiode 3dB bandwidth. The thermal and the dark current noise are independent of the optical signal level. The quantum noise is proportional to the average value of the optical signal. The dark current noise is often too small and can be ignored[28].

It has been demonstrated that both shot noise and dark current noise contributions from the bulk material of the photodiode follow a Poisson process, which is random. For this reason, the mean squared of these noise sources is considered for the calculations [35].

2.1.3.5. Optical Amplifier

An Er-doped fiber amplifier (EDFA) is an optical amplifier used to enhance the signal level in an optical link, in addition EDFA is used in fiber-optic systems to compensate losses. The basic principle of EDFA consists of a singular doped fiber for example quartz glass fiber. A laser light is irradiated into this Er-doped fiber, in order to achieve an optical gain through a population inversion.

EFASs have a flat gain profile in the 1530-nm to 1570-nm region of the spectrum. Moreover, EDFAs allow signals to be regenerated without having to be converted back to electrical signals, therefore, systems are faster and more reliable. Signal gain of EDFA can be as high as 30 dB.

The mathematical expression for the EDFA output is given by

$$G_{EDFA}(dB) = 10\log\frac{P_{out}}{P_{in}} \qquad (15),$$

where P_{out} is the power output from the EDFA and , P_{in} is the power that enter to the EDFA. Gain of EDFA depends on the pump power as well as on the pump wavelength.

2.1.3.6. Spurious Free Dynamic Range (SFDR)

Spurious-Free Dynamic Range (SFDR)[36] [28] is defined as the range of input power levels from which the output signal just exceed the output noise floor and for which any distortion components remain buried below the noise floor. In other words, it is the range in the bandwidth of concern between the smallest signal that can be detected and the largest signal that can be introduced into a system without creating detectable distortions.

SFDR considers all sources of distortion, regardless of their origin, and is the best operating region in the theory. Then, mathematically SFDR can be expressed as:

$$SFDR = (inputlevel - Noisefloor) \quad (16)$$

A receiver Noise floor (in dBm) is given by

$$-174 + 10\log B_N + F \quad (17),$$

where B_N represents the receiver noise bandwidth in hertz and F is the receiver noise figure in dB. This noise is the lower limit of SFDR. The value of -174 (dBm/Hz) is a constant at 25°C which represent the Background Noise Level (BNL).

The input level depends on Third Order Intercept Point (IP3). Defining this parameter is possible to characterize a systems third order distortions to establish the SFDR. The best form to understand IP3 is considering two signals, S_1 (with a Frequency F_1) and S_2 (with a frequency F_2) , with the same amplitude and with a small difference in frequency between them. Then, harmonics at two times the corresponding frequency are generated. Third order spurs occur when the frequency corresponding to ($2F_1$ - F_2), and at ($2F_2$- F_1), are very close to F_1 and F_2. Third order spurs will increase 3 dB for every 1 dB increase in the fundamental frequency.

Figure 2.5., shows the point interception of IP3. In both curves the fundamental frequency’s output power vs. input power is graphed. The firs curve is with a grade of 1:1, until to reach the systems non-linear region. The second curve is a graphic with a grade of 3:1 in the linear region of the system. The Third Order Intercept point (IP3).occurs when the linear portions of these two graphics, are extended as the dotted line, then they are intercepted.

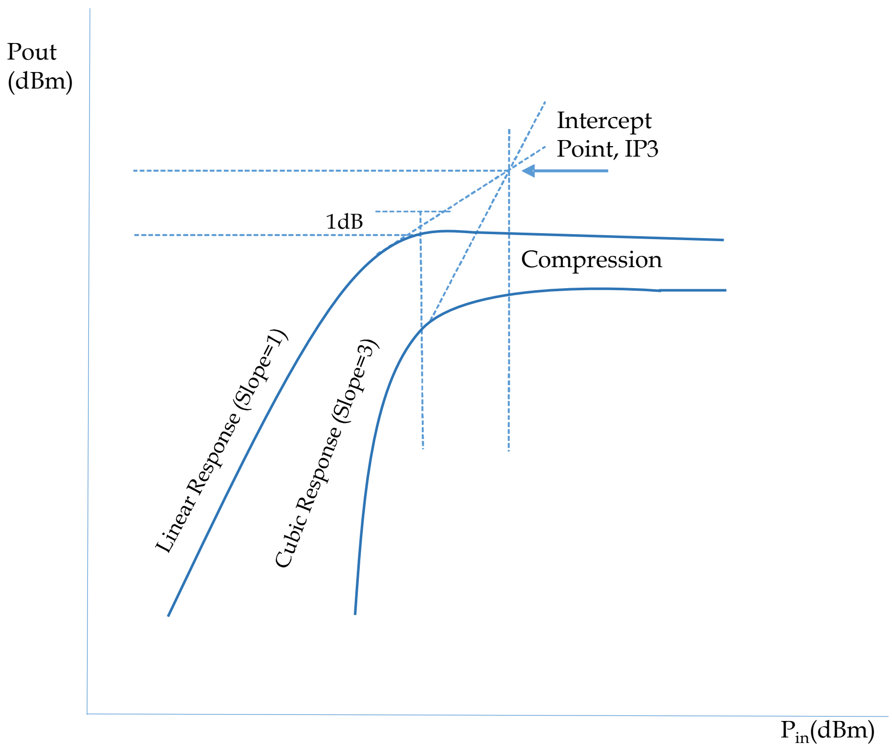

Fig. 2.5. Third Order Intercept Point IP3

Source:[37]

The IP3 can be used to predict the third order distortion that will appear in a system. Then the SFDR can be expressed as follow.

$$SFDR = \frac{2}{3}(IP_3 - Noisefloor) = \frac{2}{3}(IP_3 - (-174 + 10\log B_N + F) \quad (18)$$

2.1.3.7. The wireless channel

The wireless indoor propagation have special characteristics and can be especially difficult to model. The channel indoors varies considerably with the environment and depends on the kind of construction materials, the building structure, layout of rooms, antenna position, wall thickness, open-closed doors, among others. Far-field radiation also varies based on receiver locations and antenna types [38].

Since wireless communication is a fairly broad topic of study, in this section, only the most important wireless channel features for Fi-Wi links are described. Regarding RoF links, it is important to consider the application or use of these, thus, the main indoor propagation models are presented in a brief review. In addition, the most widely used models in terms of path losses, multi-path propagation and fading are described.

Some models describe indoor propagation. Some of the most commonly used are: Ericsson multiple breakpoint model, attenuation factor model, simple indoor path-loss model and ITU model for indoor attenuation. As this project was made within an indoor environment, thus, only this kind of propagation is described.

2.1.4.7.1. *Path- Loss Models*

In wireless channels, path-loss is the main factor in the analysis and design of the link budget. This component represents the attenuation of the radio wave as it propagates through space. It can be defined as the ratio of the effective transmitted power to the received power[28].

Path-loss are caused by many effects, such as free-space loss, refraction, diffraction, reflection, and absorption. In addition, path-loss takes into account the topography, if the environment is urban or rural, vegetation and foliage, humidity of the air, the distance between the transmitter and the receiver, and the height and location of antennas [28].

There are a lot of path-loss models that have been used in practice. The most common and easy model are the log-distance model and the Friis Model,

Log-distance Model

Log-distance model can be used for both indoors and outdoors propagation. The next equation describes the model[39].

$$PL = PL_0 + 10\gamma log_{10} \frac{d}{d_0} + X_g \qquad (19),$$

where PL is the path loss in dB, PL_0 is the path loss at the reference distance d_0 (dB), d is the length of the path, and d_0 is the reference distance to eliminate near-field effects. The factor γ is the path-loss exponent and X_g is a Gaussian-distributed random variable that reflects the fluctuation (dB) caused by flat fading[28]

Friis Model

Free space loss model - FSL, describes the attenuation between transmitter and receiver. For instance, is well-known as Friis transmission equation. In this model, the free-space power loss of an electromagnetic wave is proportional to the square of its carrier frequency.

$$path\ loss = \left(\frac{4\pi d f_c}{c}\right)^{\gamma} \qquad (20),$$

Here, d is the distance between the wireless receiver and the base station antenna, f_c is the carrier frequency, c is the speed of the light, y is the path-loss exponent, which can vary from 1,5 to 6 and is associated with the environment. For this experiment, as it has line of sight, this constant is 2. The next equation shows the path loss in dB.

$$path\ loss_{dB} = 10\ Log\left(\frac{4\pi d f_c}{c}\right)^2 \tag{21),}$$
$$= 20\ Log\left(\frac{4\pi d f_c}{c}\right) = 20\text{Log d(m)} + 20Log\ f_c(Hz) - 147.56$$

2.1.4.7.2. *ITU Indoor propagation model*

This model estimates the path loss within a room or a closed area inside a building confined by walls or other partitions. It is also known as the ITU model for indoor attenuation. In this model, the path-loss is determined as follows:

$$PL = 20logf_c + \gamma logd + P_f(n_f) - 28 \tag{22),}$$

where f_c is the carrier frequency of transmission (MHz), d is the distance (m), n_f is the number of floors between the transmitter and the receiver, and $P_f(n_f)$ is the floor-loss penetration factor.

2.1.4.7.3. *Attenuation factor model*

The attenuation factor model is given by free space loss added with attenuation factor. It incorporates a special path loss exponent and a floor attenuation factor to provide an estimate of indoor path loss. The model [40] is given in the following equation:

$$PL(d) = PL(d_0) + 20log_{10}\frac{d}{d_0} + \alpha d + A_f \tag{23),}$$

where α is the attenuation constant in dB/m and A_f is the attenuation factor for a given channel.

2.1.4.7.4. *Fading and Multipath propagation*

On the one hand, multipath propagation is a main issue in wireless communication. Multipath propagation occurs when radio waves take multiple paths, as its name suggests, and several of them reach the antenna causing a received signal that may has constructive and destructive interference and phase shifting, producing errors and affecting the quality of the communication. In addition, the signal received may vary depending on the bandwidth of the transmitted information and the delay spread [41].

On the other hand, fading is a propagation phenomenon whereby rapid fluctuations of the amplitudes, phases, or multipath delays of a radio wave signal happen in a time period. Fading depends on the moving relative speed of the mobile user, the multipath propagation, the speed of surrounding objects and the transmission bandwidth of the signal. Moreover, it can be classified in accordance with the relation between the signal and the channel parameters. Depending on the relative speed and the Doppler spread, it can be categorized as ‘fast fading’ or "slow fading.’ However, if fading depends on the signal parameters, it can be ‘flat fading’ or "frequency selective fading.’

Two other important concepts are related with fading: delay spread and coherence bandwidth. The coherence bandwidth is a statistical measure of the bandwidth over which the channel has equal gain and linear phase, thus, it can be considered flat. Therefore, the delay spread measures how the coherence bandwidth of the wireless channel is affected. The coherence bandwidth (B_C) and the root-mean-square delay spread (δ_{τ},) of the channel have an inverse relationship[42][43].

2.2. State of the art of Hybrid Fiber-Wireless systems

In this section, a compilation of Fiber-Wireless systems in W-Band is presented, considering the relevance of W-Band and its relation with emerging technologies such as 5G and tactile Internet.

2.2.1. W-Band Fiber-Wireless Systems

Currently, there are challenges to improve the capacity and reach of wideband communications. It has been shown that hybrid systems such as Radio over Fiber (RoF) overcome the linear and nonlinear distortions caused by signal degradations. This generates a remarkable improvement in hybrid links that lead to a significant reduction of dynamic range and receiver sensitivity and also to transmit higher bandwidths. This section presents the main works regarding transmission capacity and reduction of dynamic range for W-Band Fiber-Wireless system.

One of the measures that quantified the efforts in the design of RoF links is the Spurious-Free Dynamic Range (SFDR) with low noise figure. As previously mentioned, the SFDR is the ratio of the maximum signal component at the input to the strongest spurious signal in the output. This measurement is important because it is used to specify the performance of radio receivers.

Currently, the most studied analogue links are those based on IM-DD (Intensity Modulation- Direct Detection) using an MZM modulator biased in the linear regime [44], which can achieve 110 $dB.Hz^{-2/3}$ of SFDR. This configuration has some limitations, because the MZM has an intrinsic non-linear response. Additionally, when working at high RF frequencies, the optical fiber chromatic dispersion tolerance causes periodic power fading at the output of the photodetector. For this reason, various linearization techniques based on concatenated MZMs and predistortion have been proposed [11][44][45]. In spite of obtaining higher SFDR, up to 132 $dB.Hz^{-2/3}$, these experiments have narrow frequency band operation and require a precise bias control. All these technologies work at frequencies bellow 10 GHz [45] [46].

For high RF frequencies, a linearized IM-DD link at 18 GHz achieving an SFDR of 129 $dB.Hz^{-2/3}$ and 114 $dB.Hz^{-2/3}$ after photonic down conversion has been demonstrated[47]. PM-DD (Phase Modulation- Direct Detection) links present challenges in the phase tracking in order to recover the phase information. Nonetheless, they have been theoretically proven to offer higher linearity than un-linearized IM-DD links [48][49]. Photonic down conversion using PM-DD at 3 GHz and 10 GHz with 107 $dB.Hz^{-2/3}$ of

SFDR was also demonstrated. Linearization using dual wavelength PM has been proven to achieve an SFDR of 127 dB.Hz$^{-2/3}$ at 5 GHz. The theoretical analysis shows that it has a better performance than IM-DD links in terms of SFDR, noise figure and RF gain, but within a limited bandwidth [49]. However, the advances in [48][49][50][51][52][53] show that it is difficult to integrate in access networks because it involved matched receivers with short fiber lengths (below 1 km).

In recent researches, an RoF system using a quadrature-multiplexing technique is presented [54]. They achieved 102.8 dB.Hz $^{-2/3}$, improving by 2.7dB the intrinsic optical link. The system can support MIMO. In [55], an improved predistortion circuit for directly-modulated Radio over Fiber system was demonstrated, obtaining a 7.21% error vector magnitude performance improvement for 20 MHz 64QAM-OFDM at 2 GHz signal transmission over 10 km standard single mode fiber. This upgrading is useful for directly-modulated RoF systems in future 5G mobile networks. In [56], the authors tested the Spurious-Free Dynamic Range (SFDR) for a UWB Radio over Fiber (RoF) system using a polarization-dependent Electro-Absorption Modulator (EAM) that is linearized using mixed polarization. They achieved improvements of more than 9.5 dB.

In addition, Fiber-Wireless links allow a direct integration of the mobile front and back-haul with the optical distribution networks deployed. Hybrid links are today a solution to the high demand on increased bit rates that, nowadays, wireless networks do not have themselves. Taking into account the foregoing, another measure in RoF links is the generation of wireless signals exceeding 10 Gbps using photonic technologies [57]. With OFDM RF (Orthogonal Frequency-Division Multiplexing), generation and photonic up conversion [58][59] can achieve bit rates over 30 Gbps in the 60 GHz band, within the 7 GHz of available bandwidth. For gigabit generation beyond 100 GHz, 8 Gbps was achieved at 250 GHz by optical heterodyning [60].

Interestingly, most contributions in RoF links have focused on millimeter-waves because higher radio frequency bands can achieve higher data rates. The mm-wave band is a range of electromagnetic waves with frequencies between 30 GHz and 300 GHz, or the wavelength of one to ten millimeters in free space [61]. Until recently, this part of the spectrum has not been used because few electronic components could generate or receive mm-waves. Through advances in antennas and semiconductors, these frequencies are now ideally and affordably generated by the use of photonic technologies [62].

Regulatory agencies have been recently establishing the spectrum for emergent technologies as 5G. Most countries have set their position to harmonize in the near future the spectrum for 5G and launch two bands, 3.6-3.8 GHz and 26 GHz [63][64][65]. Nevertheless, the W-Band (75-110 GHz) has attracted increasing attention due to its potential for further expansion of the wireless capacity towards the threshold of 100 Gbps. In addition, the W-Band does not show any resonant absorption. Within its entire range, 1 dB/km absorption is hardly exceeded, even for high humidity levels[66].

According to Resolution 238 of the World Radio-communication Conference in 2015 (WRC-15), 66-76 GHz and 81-86 GHz bands were established as possible wireless bands communication in the future[67]. Until now no commercial project has yet been implemented in W-Band around the world. Nonetheless, in US the Federal Communications Commission (FCC) has opened the commercial use of spectra in the 71 GHz – 75.5 GHz, 81 GHz – 86 GHz, 92 GHz – 100 GHz, and 102 GHz – 109.5 GHz bands, which are recommended for high-speed wireless communications [66].

Regarding the experimental W-Band, OOK (On-Off Keying) wireless systems have been demonstrated to employ optical generation and electrical envelope detection at 10 Gbps [60] and 20 Gbps [68]. More spectral efficient links have been demonstrated using PSK modulation, up to 16 Gbps in the 70-80 GHz band [69] on a single-chip all-electrical transceiver. A 1.25 Gbps link was achieved at 105 GHz RF frequency using IF optical up-conversion [70]. The use of all-optical transmitter was reported in [71] using a DQPSK optical modulator, with up to 4.6 Gbps at 92 GHz RF frequency. Recently, a 20 Gbps W-Band wireless link has been demonstrated based on baseband generation and frequency quadrupling [72]. In [73], the reception used a broadband electrical mixer rather than photonic technologies and revealed that several challenges need to be overcome to reach longer transmission distances.

In general, with the development of hybrid Fiber-Wireless systems, a number of setups and several links has been reported, which offer transmissions of high Gbps data rates [74] [75]and applications RoF indoor, building-to-building, as well as mobile front haul and backhaul [76][77][78].

2.2.2. 5th Generation of mobile communications and Tactile Internet

5G technologies are the evolution of mobile communication networks; it is expected to be in use around 2020. The idea around 5G is a technology that integrates several techniques, scenarios and user cases rather than the invention of a new single radio access technology. However, there is not yet a unique definition for 5G [79].

Besides, 5G technologies are systems that will provide connection in just one click. The advanced 5G infrastructure represents a revolution in the field of telecommunications because it will be a ubiquitous broadband network that supports haptic internet. It will efficiently allow new services with low latency and ultra-reliable. “Full Immersive Experience”, enriched by “Context Information” and “Anything as a Service”, are the main drivers for a massive adoption of the new enabling technology components and market uptake [1].

5G will need extreme base station, unprecedented numbers of antennas, very high carrier frequencies with massive bandwidths, and device densities. However, unlike the previous four generations, it will also be highly integrative: it will connect spectrum together with LTE and Wi-Fi and any 5G air interface in order to provide a very good user experience and coverage. Given this, the core of the network will have to reach very high levels of flexibility and intelligence. In addition, spectrum regulation will have to be rethought and improved, and energy and cost efficiency will become even more critical considerations [80].Also, 5G Fi-Wi is expected to be about 6 times faster than 4G LTE. Some of the main requirements of 5G are: 10-100 higher number of connected devices per area, 100-1000 times higher system capacity, user data rates in the order of Gbps everywhere, latency in the order of 1 millisecond, 10 times longer battery life for devices [2].

On the other hand, Tactile Internet is the idea of a real-time Internet to be achieved through all round maximum improvement in the network latency. It starts from the process of generation of information, its access to a transmission network, its modulation and coding techniques and presentation to the end user, while maintaining desired metrics in QoS[81].

With the expansion of the Mobile Internet and the Internet of things, Tactile Internet requires significantly lower round trip delay times in the range of one millisecond. It is a more realistic internet because it takes into account the time of iteration between the senses of the human body and the machines. The instantaneous reaction of the Tactile Internet will enhance the way of communicating and will enable an unpredictable plurality of new applications, products, and services [82].

Some future applications of Tactile Internet described in [82], like education and lifelong learning, healthcare, personal safety zones, traffic in a smart city or energy, will have more instantaneous reaction times and will result in novel experiences for people that need and use this kind of applications. According to [83], the difference between 5G and Tactile internet is that 5G will keep its human-to-human (H2H) communications for conventional triple-play services (voice, video, data), focusing on the integration with other wireless technologies as WiFi and decentralization. In contrast, the Tactile Internet will be centered on human-to-machine (H2M) communications using tactile or haptic devices to its maximum advantage.

Photonics integrated with wireless networks enables Radio over Fiber links to generate some advantages over other transmission systems and, in the future, will enable 5G and Tactile Internet. Several works have demonstrated that microwave photonics is a key enabler to develop 5G [84]. In some works, researches have analyzed how Fiber-Wireless communication is a solution to 5G, taking into account the fundamentals of propagation characteristics, path loss, large-scale antenna arrays, coverage, and capacity [85] as well as all the aspects related to applications such as device-to-device communications, heterogeneous networks, and multimedia transmission[86]. In the same way, [87] described the transport network in terms of capacity, flexibility and costs. In [88], authors analyze the major relevant activities in the current standardization landscape of 5G and the potential impact on the Xhaul architecture. In conclusion, several works about Fiber-Wireless systems have been presented and worked with different setups, in different bands of the spectrum in order to achieve 5G and Tactile Internet [17][89][90].

Chapter 3

3. Latency

Nowadays, users of telecommunication services demand real-time services increasingly. For instance, to enable natural conversation, modern telephony is designed to ensure that voice is transmitted within 100 milliseconds. To allow a seamless video experience, modern TV sets have a minimum picture-refresh rate of 100 Hertz, translating into a maximum inter-picture latency of 10 milliseconds. In those applications, the natural reaction time sets time targets that technical specifications must achieve in the communication. Among the senses, the visual-tactile interaction between humans and technical systems is becoming more important, especially with the high penetration of the smartphones market. Thus, services are needed in real time and with the lowest delays[82][9].

Latency is defined as the time delay between the transmission and reception of a telecommunication signal in data transmission and computing systems [91]. Latency is often a critical element of subjective quality, thus, data latencies are often required to be short and guaranteed [80][92]. There are different kinds of latency in the literature [93], such as User Plane Latency (UP), Control Plane Latency (CP), End to End Latency, Round Trip Time, among others. Likewise, researchers have measured delays, round trip time[94], and transmission time interval [95], among others, according to each researching need.

This chapter collects information about the different kinds of latency and its components in a link and in a network. Besides, the state of the art about latency measurements is presented. Finally, a procedure to measure latency is presented as a contribution of this research. This chapter takes into account the procedure of my own publication in [8].

3.1. Latency in Radio over Fiber systems

In this section, first, the different concepts about latency are described, showing the difference between latency in a network and latency in a link. Then, the definition of latency chosen for this work is presented.

3.1.1. Latency concepts in literature

Generally, latency is associated with delay, some researchers define Latency as the new bandwidth due to its relevance. As mentioned previously, latency is the time delay between transmission and reception in a network[96], [97].

Figure 3.1 shows the different concepts of latency in the OSI model, such as control plane latency, user plane latency, transmission time interval, media delay, and round trip time, in relation with the end to end physical link latency, which is the concept that will be considered in the experiments of this thesis.

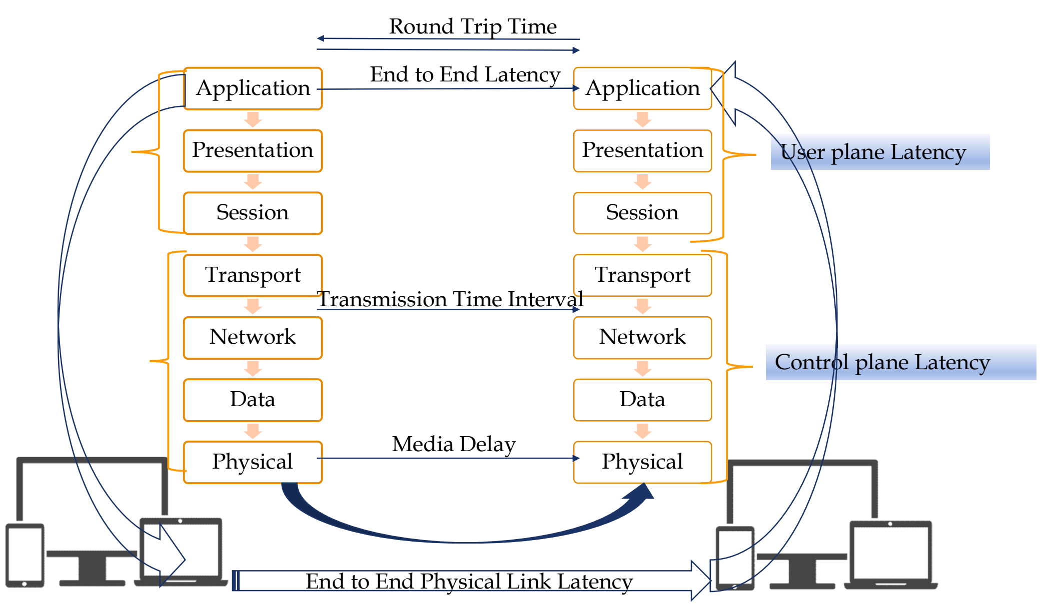

Fig. 3.1. Latency concepts into OSI Model

The first concept in literature split latency into two parts: the user plane latency and the control plane latency. On the one hand, the user plane latency is the delay when an application is exchanging data with a server. On the other hand, control plane latency, also called setup latency, is the latency in which a User Equipment (UE) can make a transition to a state where it can send or receive data[98].

User plane latency includes the time required for a bit to propagate over the link from one node to another. It also involves the time spent by a node to move forward all the bits of the packet onto the link. Control plane latency includes the time needed to process an incoming packet for packet forwarding. Finally, it takes into account the time that the packet needs to wait in the queue to be transmitted onto the link [99].

End to end latency is considered as the sum of all delays in the link. It is composed of four components: the processing delay, queuing delay, transmission delay and propagation delay, according to next equation[100].

$$L_n = d_p + d_q + d_t + d_{pr} \tag{24}$$

In the equation, L_n is the total nodal latency in a network. d_p is the propagation delay or the time it takes a packet to travel through the media considering the size packet and bandwidth channel. d_q is the queuing delay that depends on the contention, congestion and storage delays. d_t is the transmission delay that introduces the medium itself (optical fiber, wireless, or both of them). d_{pr} is the router and other processing delays, considering that each gateway node takes time to examine and possibly change the header in a packet.

The factors that influence those delays are: distance, packet size, data rate, computational complexity (communication & application) and congestion. In addition, the concept of latency can vary depending on the answers to the following questions: where exactly latency is being measured? In what application? Is it one-way or round-trip?.

There are other concepts of latency that have been measured in the literature, such as Round Trip Time RTT [101] and Transmission Timer Interval TTI [102]. The RTT is the time required by a packet to travel from the source to the destination and back again. The TTI is defined as the inter-arrival time of transport block sets and it is equal to the periodicity at which a transport block set is transferred by the physical layer onto the radio interface. They can be related to the previously mentioned through Figure 3.1.

On top of that, the found concepts of latency show that it is different when it is in a network or in a link, thus, it depends on the number of nodes that a network has. For instance, according to [103], in wireless networks appear two new concepts about latency which are: forwarding latency and queuing latency. The forwarding latency is determined by the number of hops that the packet has to pass through, while the queuing latency is determined by the channel contention.

Against to this, the end to end latency definition for a link does not take into account the number of nodes of the network. This concept is supported in the sum of the delays generated in a link from the physical to the application layers. Figure 3.1., also shows this concept.

3.1.2. Definition of Latency chosen of this work

In this research, the number of nodes or hops will not be considered. The reason is that the proposed RoF links and their respective measures only take into account the times between the central station, the base station and the end user. As it is a physical link, the concept of latency assumed must consider the time of codification, modulation, multiplexing and sending of the data packets (t_a *signal alignment delay*). Moreover, this concept contemplates the propagation time through the medium (t_p *propagation delay*) and the digital processing time that the physical signals need to be converted and presented to the end user from one point of the link to the other (t_{dsp} *digital signal processing delay*). For this work the next expression shows the End to End Latency definition selected.

$$End\ to\ End\ Latency_{link} = t_a + t_p + t_{dsp} \tag{25}$$

In this latency concept, the size of the packet introduces delay, since a larger packet will take longer to be received and returned than a smaller one. In addition, the technique of modulation and multiplexing becomes important because the best selection of these schemes can generate more or less delay, which could be significant in a network with several nodes.

3.2. State of the art

In terms of latency, some works [104] [105] described comparisons or improvements in mobile networks, such as High Speed Packet Access HSPA, 3G and LTE. The results showed that optimizations of the LTE scheduling, resource allocation policies and TTI reduction have improved the latency substantially. For example, TTI in EDGE is 20 ms, WCDMA brings TTI to 10 ms, while in HSDPA it is brought to 2 ms. In [106], authors described one of the critical parameters for latency. They exposed that the remaining time for round trip time propagation between the Remote Radio Head (RRH) and the Base Band Unit (BBU) is only 700 µs for LTE and 400 µs for LTE-Advanced. After implementation, authors explain that LTE reduces the latency from call setup to idle latency in aprox. 360 ms compared to an HSPA system, where signaling is carried on HSPA channels [98]. In [107], they achieved 1.2 ms time of latency.

Other researchers have already been working on how to achieve low latency. In[108], the authors show that they can achieve short Time Division Duplexing (TDD) latency with physical RTT in the order of < 1.5 ms, including synchronization, scheduling signaling and actual data transmission with acknowledgement. Meanwhile, Fettweit affirmed that a Generalized Frequency Division Multiplexing (GFDM) well configured by LTE can reduce the latency in a factor of 15; and when a GFDM configuration is proposed to allow the coexistence of 5G and 4G signals, the latency of the 5G signaling can be 10 times smaller than the current LTE system [109].

In [110], the authors explained that they used a flexible, customizable Field Programmable Gate Array (FPGA) platform to develop a proof-of-concept GFDM testbed for experimental research. They showed alternative waveforms to OFDM for the next networks generation like Generalized Frequency Division Multiplexing (GFDM), Universal Filtered Multi-Carrier (UFMC), Biorthogonal Frequency Division Multiplexing (BFDM), and Filter-Bank Multi-Carrier (FBMC). They also mentioned that for suitable low latency in Tactile Internet applications, high efficiency must be achieved with short burst transmissions. Thus, they tested different schemes to generate the signal.

Other papers show that they also used FPGA to make a hardware testbed for measuring latency, like in [111] . They made a transceiver based on Xilinx Virtex 5 FPGA which can achieve a latency with sub-nanosecond precision. Similarly in [112], the fiber latency measurement is based on the idea of using the FPGA carry logic as precision time digital converter plus clock counter.

Other authors have been using testbeds to measure latency. In [113], they built an LTE experimental testbed using Open Air Interface (OAI) for LTE systems. As well as, in [114] a low-cost test bed using "smart small factor pluggable" in-line probes is presented. They used LTE signals that are generated by a software base station (Amari LTE-100). They also used Ettus N210 USRP to de-packet, decode, up-convert to RF and transmit over the air the signal.

In [115], the objective is to avoid the overhead of active or probing measurements and to perform passive measurements solely by using information available in the data transmitted and received by the applications. Therefore, they exploit and analyze the properties of various network, transport and application protocols like ICMP, IP, TCP or NTP to calculate latencies and the bandwidth used/available in the network.

As shown before, one important aspect of this research is to find a procedure to measure time transmission in each part of the link. Latency can be measured through hardware using FPGA [116] [117] [111], a Network performance tester[118] or Ettus Universal Software Radio Peripheral USRP+GNU Radio [119]. A commonly used metric to characterize U-plane latency is the PING delay, i.e. the delay of a UE sending a PING to the first IP node in the network and receiving the PING reply [120]. Likewise, delay can be measured through different testbeds [121].

Table 3.1., summarizes some researches, especially those about the techniques that have been employed to measure latency, their approach and measurement reached.

Table 3.1. Latency Summary

Tittle/ Year	**Approach**	**Measurement reached**
5G new radio and ultra-low latency application: A PHY implementation perspective[122]**/2016**	Authors used an SDR signal processing platform to implement a 5G system at physical (PHY) and medium access layers (MAC).	Authors achieved delays between 1 and 2 ms.
Switched Ethernet Front haul Architecture for Cloud-Radio Access Networks [114]**/2016**	Authors used a hardware testbed with LTE signals generated by a software base station. Authors sent different Ethernet frame lengths. They measured an estimated delay for the front-haul obtained through Precision Time Protocol (PTP) time-stamping, as well as the interframe delays and transport block retransmissions.	They did not show a measurement of end to end latency.

Design and FPGA Implementation of High-Speed, Fixed-Latency Serial Transceivers [111]**/2014**	Authors proposed a fixed-latency serial transceiver based on the dynamic phase-shift and changeable delay-tune technologies. This kind of implementation can be applied to measure latency in a high-speed link.	Authors implemented a 2.5 Gbps serial link and they obtained a solution with sub-nanosecond accuracy. They did not show an end to end latency measurement.
OPMDC: Architecture Design and Implementation of a New Optical Pyramid Data Center Network[107]**/2015**	Authors built an optical pyramid data center prototype with 7 switching optical nodes and 3 tiers. They also designed a wavelength scheduling algorithm, called source and destination relay and aggregation (SDRA). Authors sent a large video file via python-based TCP socket, from the source server (S) to the destination server (D).	They got end to end latency of 1.232 ms and 1.72 ms, respectively.
Latency Analysis in GNU Radio/USRP-based Software Radio Platforms [123]**/2013**	Authors identified different types of delays in the Software Defined Radio platforms and estimated the time of these delays. They calculated the round-trip time between two SDR systems using TUN/TAP components with GNU Radio tunnel program. Finally, they proposed a method called hwlatency to measure the latency in hardware side. Authors sent 400 ICMP packets using standard Linux PING command through TUN TAP application.	The total packet size was 2 kB. The Tx latency was equal to RTT/4 = 6.125ms. The ΔHardware was about 0.61ms, and the GNU Radio latency was at least 0.256ms.
A Comparison Between One-way Delays in Operating HSPA and LTE Networks[104]**/2012**	Authors carried out delay-measurements in an HSPA and an LTE network. The HSPA network operates in Frequency Division Duplex (FDD) Dual-Cell (DC) mode, with bandwidth of 10MHz. For LTE, the bandwidth is 20MHz, operating in FDD as well. Both networks belong to the same mobile operator and are publicly accessible. Their approach is assessing one-way delay. Authors tested different applications for LTE and HSPA network.	For LTE (up/down), they got: Online Gaming (31 / 13 ms), M2M (30 / 10 ms) and VoIP (30 / 15 ms). For HSPA (up/down), the same applications were obtained with (12 / 17 ms), (10 / 16 ms) and (35 / 16 ms), respectively.
Latency Analysis of 3G Network [124]**/2012**	Authors tested the delay of each part of the 3G Network, including the delay of the UE, and the access and core networks, in a real network in Austria. They sniffed IP Packets at each link in the network and time stamped them, in order to determine all the delay experienced by a single packet.	Authors got one-way delay of 30 ms for HSPA network and 20 ms for LTE network.

A Study on Ultra Low-Latency Mobile Networks[105]**/2008**	Authors developed a testbed using LogicBench, which is a platform suitable for emulating and prototyping a system.	Authors got end-to-end latency per IP packet of 10 ms. The IP packet and Layer-2-frame lengths were 1,200 bytes and 200 bytes, respectively.
An Experimental Study of Network Performance Impact of Increased Latency in Software Defined Radio [125]**/2008**	Authors implemented two short-range wireless physical layer standards, common in sensor networks, using USRP to measure latency. The first physical layer uses a simple FSK modulation scheme, and the second one is the physical layer of IEEE 802.15.4 and uses O-QPSK modulation.	Authors got 22.5 ms and 26.5 ms RTT.
State of Mobile Networks in USA[126]**/2017**	In this report, an End-to-end RTT latency is reported based on: 5,928,296,946 measurements and 237,213 devices, over different locations across USA.	Authors reported that latency in 3G Mobile telephone networks is between 134-204 ms and in 4G mobile networks is between 58-70 ms.
QoS requirements for Multimedia Services[127]**/2008**	In this paper, authors established the requirements for current applications in terms of latency.	They published that some applications took between 100 and 200 ms of latency.

3.3. Procedure to measure latency

The time delay can be measured using Hardware with a FPGA [116], [128]or a Network performance tester [118] or using Ettus USRP+GNU Radio [119]. Likewise, delay can be measured through different test beds [121] or doing Ping [120]. In order to establish a procedure to measure latency, in this work, USRP+GNU Radio were used. This section presents a description of the hardware and software used and of the procedure itself, as well as its corresponding validation.

3.3.1. GNU Radio + USRP

First of all, the functioning of GNU Radio and USRP is presented. The use of SDR allows to have a universal and flexible radio platform to receive and transmit, which can be tuned in different bandwidths according to the hardware used. Using SDR, the band can be programed and a determined multiplexing and modulation technique can be used.

SDR is a skillful system to adjust and vary radio environment (cognitive radio), while supporting multiple standards with a field-programmable gate-array (FPGA) [129][130].

GNU Radio is an open source SDR framework, for designing software-based Digital Signal Processing (DSP) radio systems. Its structure consists of a python-based GUI with connected processing blocks that perform operations on the signals and create flow graphs. Most of GNU Radio applications are written in Python. Python commands are used to control and modify all the USRP's software-defined parameters, such as transmit power, gain, frequency, antenna selection, etc. GNU Radio provides blocks for packet encoder and decoder, as well as modulation and demodulation of the radio frequency signal. In addition, GNU Radio is installed on a hardware platform called Universal Software Radio Peripheral (USRP) developed by Ettus Research. There are different kinds of USRP.

In this work, two types were used: the N210 and B205. On one hand, the USRP N210 has a WBX daughterboard, which is a transceiver with frequency range from 50 MHz to 2.2 GHz. The system consists of a motherboard with Xilinx Spartan XC3SD3400A FPGA and 2 pairs of DACs and ADCs[131].The connection to the PC is done by Ethernet interface.

On the other hand, the USRP model B205 consists of a programmable Xilinx Spartan-6 XC6SLX150 FPGA with RF coverage ranging from 70 MHz to 6 GHz. The USRP B205 is powered by a USB 3.0 connection for streaming data to the host computer. In appendix A is shown a datasheet of both of them. (USRP N210 and USRP NB205)

3.3.2. Latency Measurements using SDR

Once it was established the SDR that would be used. The procedure to measure latency is based on the definition of throughput. In this way, GNU Radio has a block called probe rate that measures the traffic throughput. It is important to mention that Network throughput is the measure of how much data a network carries in a specific period of time [132], [31]. The following expression shows a general definition of throughput.

$$T = \frac{S}{L} \qquad (26),$$

where S is the size of the packet and L is the period of time. If the data size is known in each point, the end to end time can be measured, because the different times corresponding to each delay point of the latency concept can be known.

Then, the points of probe rate block that are going to be measured in the flow graph of GNU Radio are established as shown in the Figure 3.2.

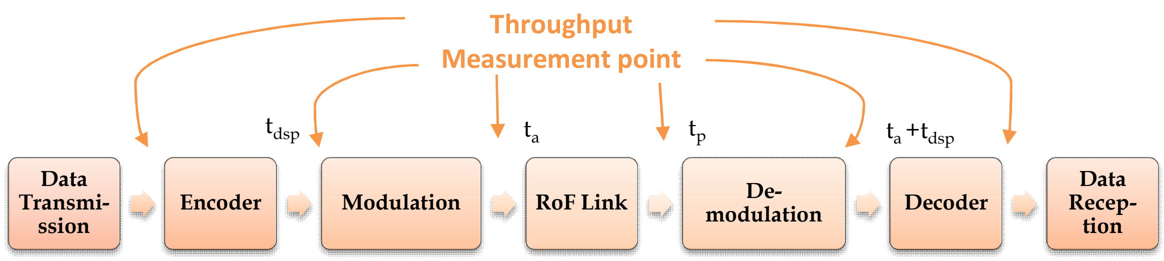

Fig. 3.2. Block Diagram of GNU Radio

In this project, the external throughput measurements are ignored because they are not significant. In addition, as mentioned before, each throughput measurement point placed in the flow graph represent each delay in the definition of latency of the 3.1.2 section.

The time shown after the encoder represents t_{dsp} *digital signal processing delay* in the transmission. This delay in the reception is included into the time measured before the demodulation block. This measurement includes the sum of t_a *signal alignment delay* in the reception and t_{dsp} *digital signal processing delay* also in the reception. The time after the modulation block in the transmission represents t_a *signal alignment delay.* Finally the time measured after RoF Link represents the t_p *propagation delay.* When using multiplexing schemes, another throughput measurement point is added. Nonetheless, this measurement is part of the signal alignment delay.

This means that the concept of End to End latency of this thesis takes into account different delays, and each point of measurement must be well established in the flow graph, according to the experiment. The next expression shows how to calculate end to end latency.

$$L_{end\ to\ end} = \sum_{i=1}^{x} \frac{S_i}{T_i} \qquad (27),$$

where Si and Ti are the size of the packet and the probe rate throughput measure in each point of the flow graph in GNU Radio. The sum of all points of measurement gives the end-to-end latency, which is measured starting from the generation in the central office, crossing through a base station until reaching the end user.

One of the fundamental points in this procedure is to know the size of the package in each measurement point. To know the size in each point, Linux terminal was used with a block of GNU radio called file sink. The block file sink prints in a file the data that have been transmitted at that point and Linux terminal is used to visualize the packet. Knowing that each packet has a preamble, header, payload and CRC value, the length of each one of the components mentioned is established by the block encoder at the transmission and decoder at the reception. Therefore, the packet encoder makes 64 Bytes packets and sends the frame to the modulation block.

To know the throughput measure in each point, a message debug block in the flow graph is used to print the measure.

The next figure shows the GNU Radio flow graph where the blocks mentioned are displayed. Only one example is presented because chapters 4 and 5 will further describe them as well as each of the elements used in the experiments of this work.

a)Transmission

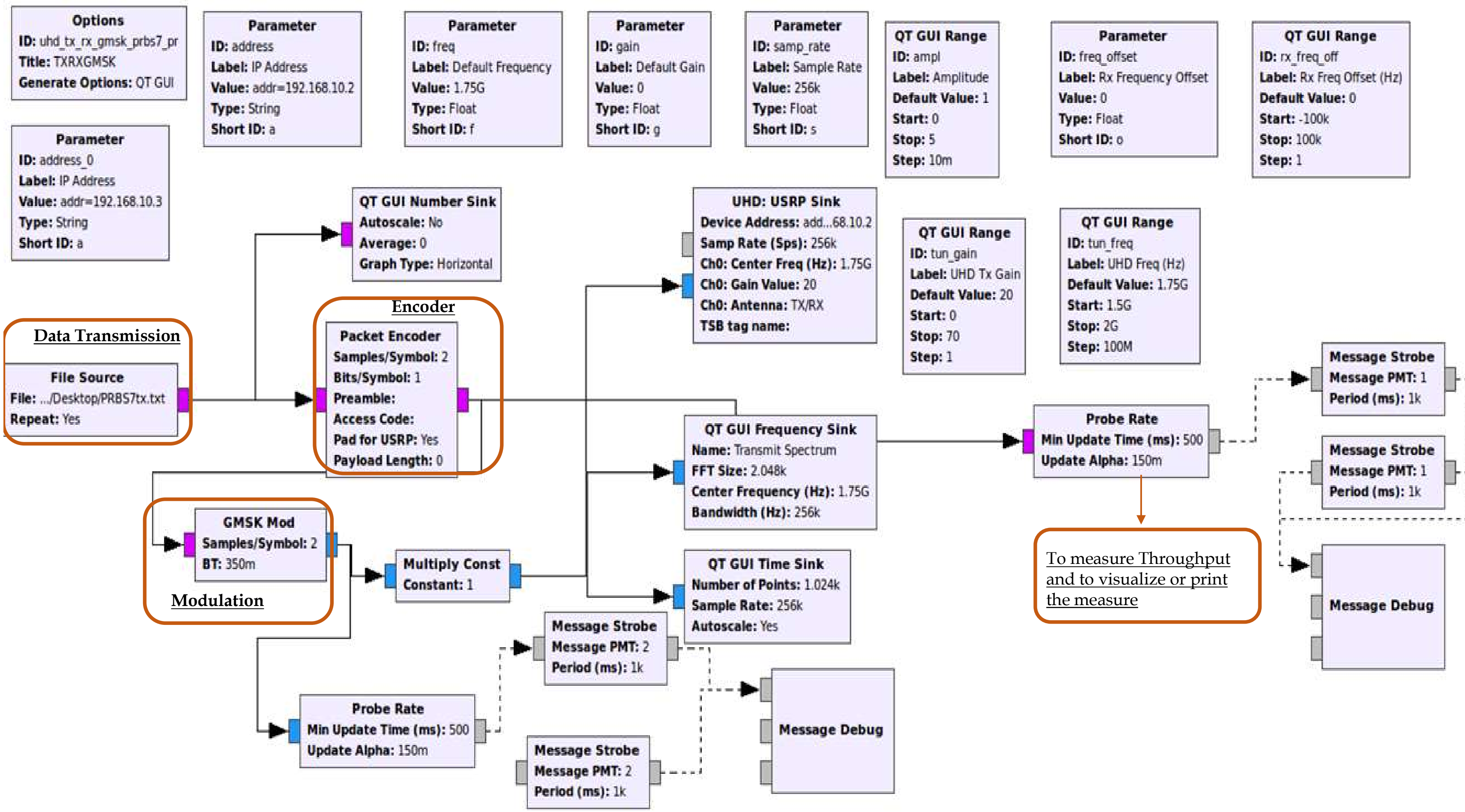

Fig. 3.3. GNU Radio Flow Graph. a) Transmission

b)Reception

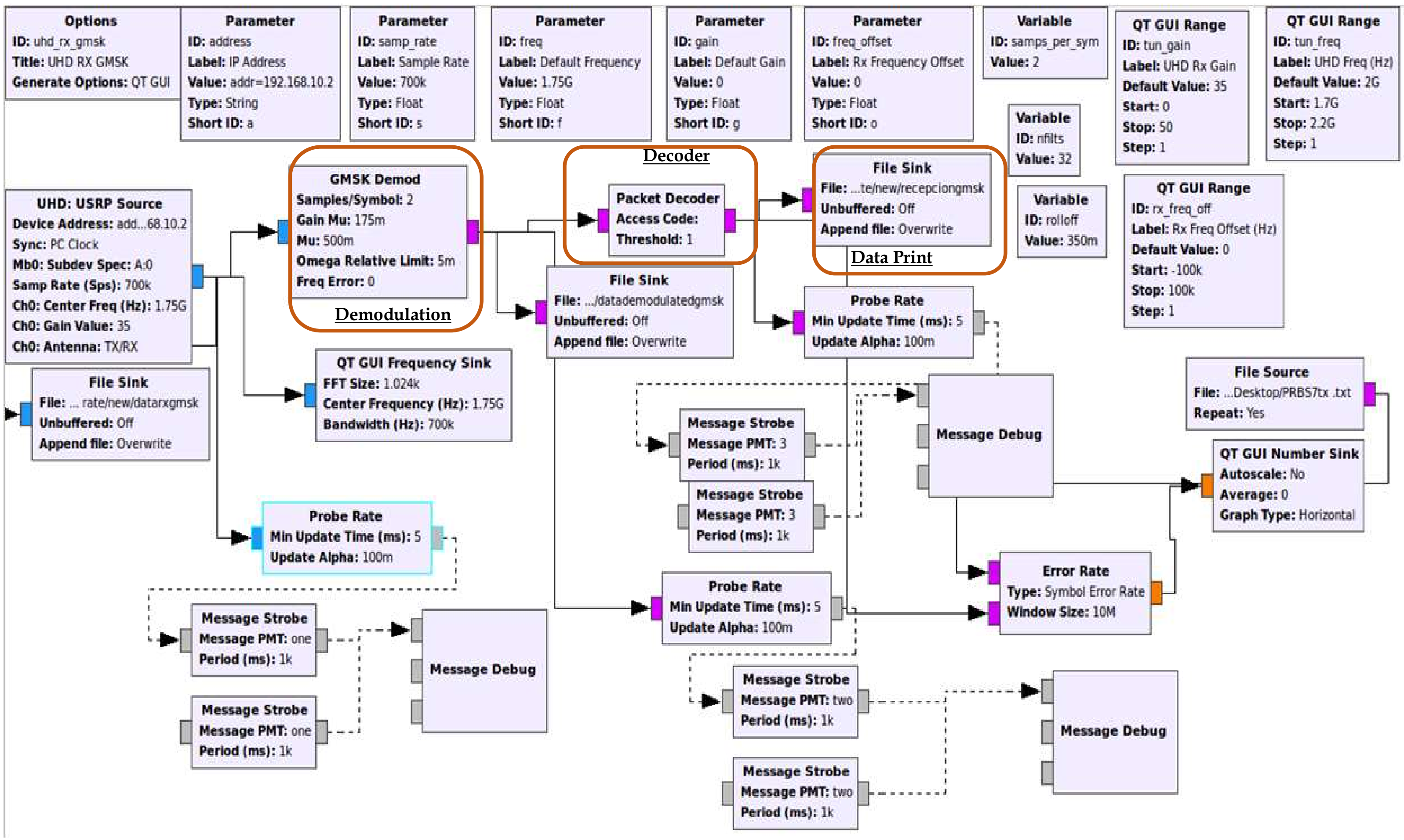

Fig. 3.3. GNU Radio Flow Graph. b) Reception

3.3.3. Validation of the procedure

In this work, different experiments were made and described in the next chapters. Nonetheless, a block diagram in GNU Radio, as shown in Figure 3.2., and GNU Radio flow graph of Figure 3.3., were established to validate the procedure for measuring latency using SDR.

A data file containing a $2^n - 1$ pseudorandom bit sequence (PRBS7) is sent on average 500 times to a packet encoder. The packet encoder makes 64 Bytes packets and sends the frame to modulation block, as mentioned previously. In the modulation block, parameters such as sampling frequency and number of bits per symbol are established.

Three data rates of 200, 500 and 700 kbps were used. This data rates were considered for the subsequent PING validation. After the modulation block, the data stream is sent through USRP to the Fiber-Wireless link as described in the next chapter. At the reception, data are received through USRP, demodulated and decoded. Then, a file sink is used to print the PRBS7 sequence to a file.

In order to validate this procedure, a tunnel utility in GNU Radio was used, which establishes a gateway between the transmitting and receiving USRP. The application creates a virtual Ethernet interface by opening the TUN/TAP modules, which is integrated in Linux kernel allowing tunnel IP traffic through the SDR system. The MAC address of the virtual Ethernet interface is auto-generated, but the IP address was set manually. A total of 400 ICMP packets were sent using standard Linux PING command. The tunnel technique is an option that involves the configuration of TUN/TAP interfaces and some knowledge of Linux networking to establish the bridge between the two USRP, and to adjust appropriately the parameters for the communication between them.

End to end Latency was taken as the average of the round-trip time divided into two. There were no changes in the setup used. Therefore, for the validation of the procedure PING was launched, using TUN/TAP interfaces between the transmission and the reception part.

Figure 3.4 displays the latency with the procedure described in comparison to PING measurements in the same setup.

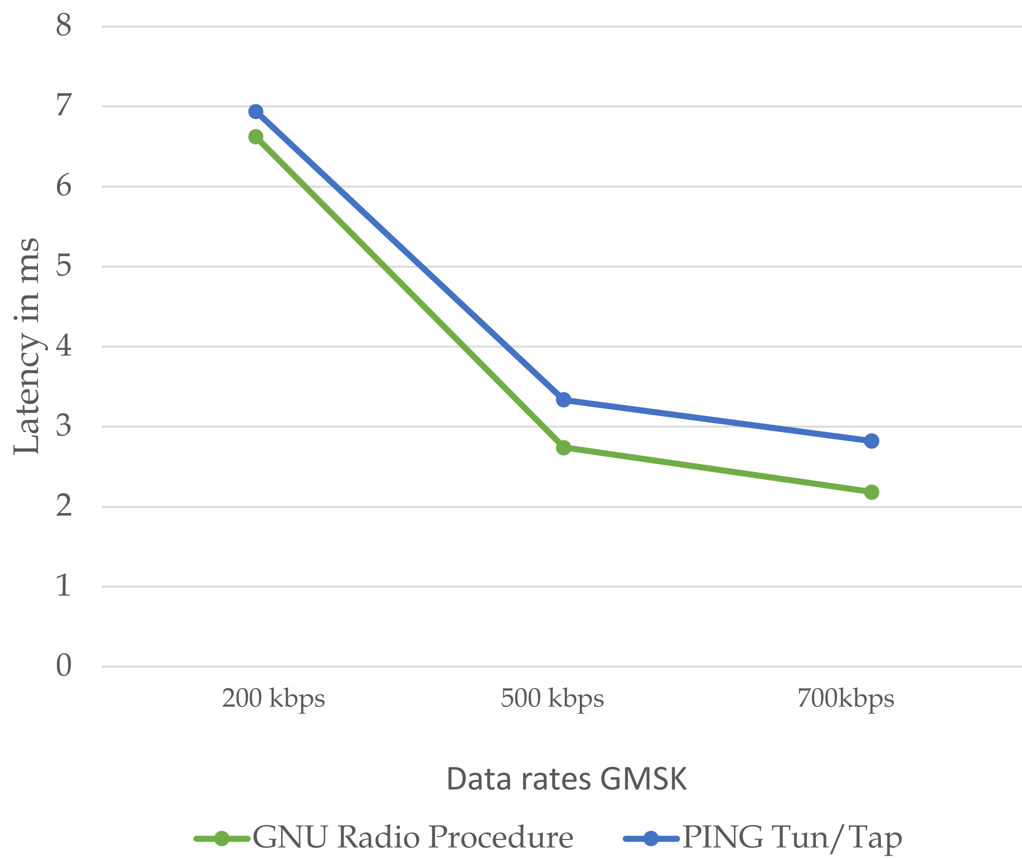

Fig. 3.4. Latency comparison between GNU Radio procedure and PING Tun/Tap

To validate how much the measures of the PING vary with respect to the measurements taken with the block Probe Rate of GNU Radio, a simple statistical analysis is made using the measure of variance. The variance formula is used to calculate the difference between a forecast and the actual result. The variance can be expressed as a percentage or as an integer. In this case, percentage is used and the value in ms obtained with GNU Radio with the value obtained by Ping Tun/Tap for each data rate.

The next equation shows how to calculate the percentage of variation.

$$PV = \frac{x_1 - x_0}{x_0} \quad \%, \qquad (28),$$

where x_0 is the value of PIN Tun/Tap and x_1 is the GNU Radio value in ms.

The percentage of variation for each data rate is calculated and then, an average is made to obtain the final result. The percentage of variation of the procedure presented is on average 14% with respect to the tunneled ping over tun/tap interfaces.

The acceptable percentage of variation level is depended on the spirit of the research. It is different in each field. For instance in [133] they measured the variation, and presented an allowable limit of error in Clinical Chemistry Quality Control also there are measurements of variations in the agriculture and researchers established a range of these. Basically a percentage of variation <10 is very good, 10-20 is good, 20-30 is acceptable, and CV>30 is not acceptable.

In the absence of measurements that compare procedures to measure latency, and establish the same range of the other fields. It can be said that the results indicate that there is no great variation, thus it is possible to take this method to make other experiments.

Finally, the use of software defined radio makes the implementation feasible and easy because it is a graphic environment. In addition, Tun/tap is an option that implies having more knowledge of kernel. With this, it is necessary to establish the bridge between the two USRP and to adjust appropriately the parameters for the communication between them.

Chapter 4

4. Hybrid Fiber-Wireless system at W-Band with low latency

In this section, first an experiment of Radio over Fiber in W-Band (75-110 GHz) is described; as well as, the equations that describe the system. Second, the results obtained in terms of bit error rate and latency are displayed, and finally the analysis of the system results in W-Band is shown.

First of all, it is important to mention that it was used W-Band as previously mentioned because W-Band (75-110GHz) is a key enabler of 5G Technology and Tactile Internet. In addition this band will be used for further expansion of the wireless capacity towards the threshold of 100 Gbps, then it will be possible to obtain high capacity in systems working at this frequency.

This experiment had three objectives. The first one, was to develop a procedure to measure latency and apply this procedure to measure latency in Radio over Fiber system. This procedure and its validation was described in section 3. The second objective involved two scenarios in order to compare only RF transmission with RoF transmission, this was very important because is suitable to show the performance of hybrid optical fiber-wireless communication and the reasons why this system support 5G and Tactile Internet. The last objective consisted of compare different RF modulation in terms of latency and Bit error Rate. This chapters takes into account the papers published in [8] and [134]

4.1. Experimental Setup

This experiment was developed in the laboratory of the Technical University of Denmark. As mentioned in section 2, there are different techniques to generate mm waves in Radio over Fiber system, for this experiment it was selected direct modulation with an external MZM, because of the RF signal generated. Specifically, it was launched at 86 GHz. A selfoptical heterodyning and envelope detection was implemented for the down link in the physical layer at W-Band [135], in order to obtain less errors in the system.

In general, a RoF link is composed of three stages: central office, base station and wireless or mobile receiver. In the central office, the optical signal is modulated with the radio frequency signal. The millimeter wave signal generated from the separation of the two optical tones is transported through an optical fiber to the base station. In the base station, the optical signal is turned to the electrical domain, amplified and transmitted to the free space. Finally, in the wireless or mobile receiver, the signal is amplified and adapted to the final user. Next sections will be describe each stage of the Radio over Fiber Link.

Figure 4.1., shows the experimental setup.

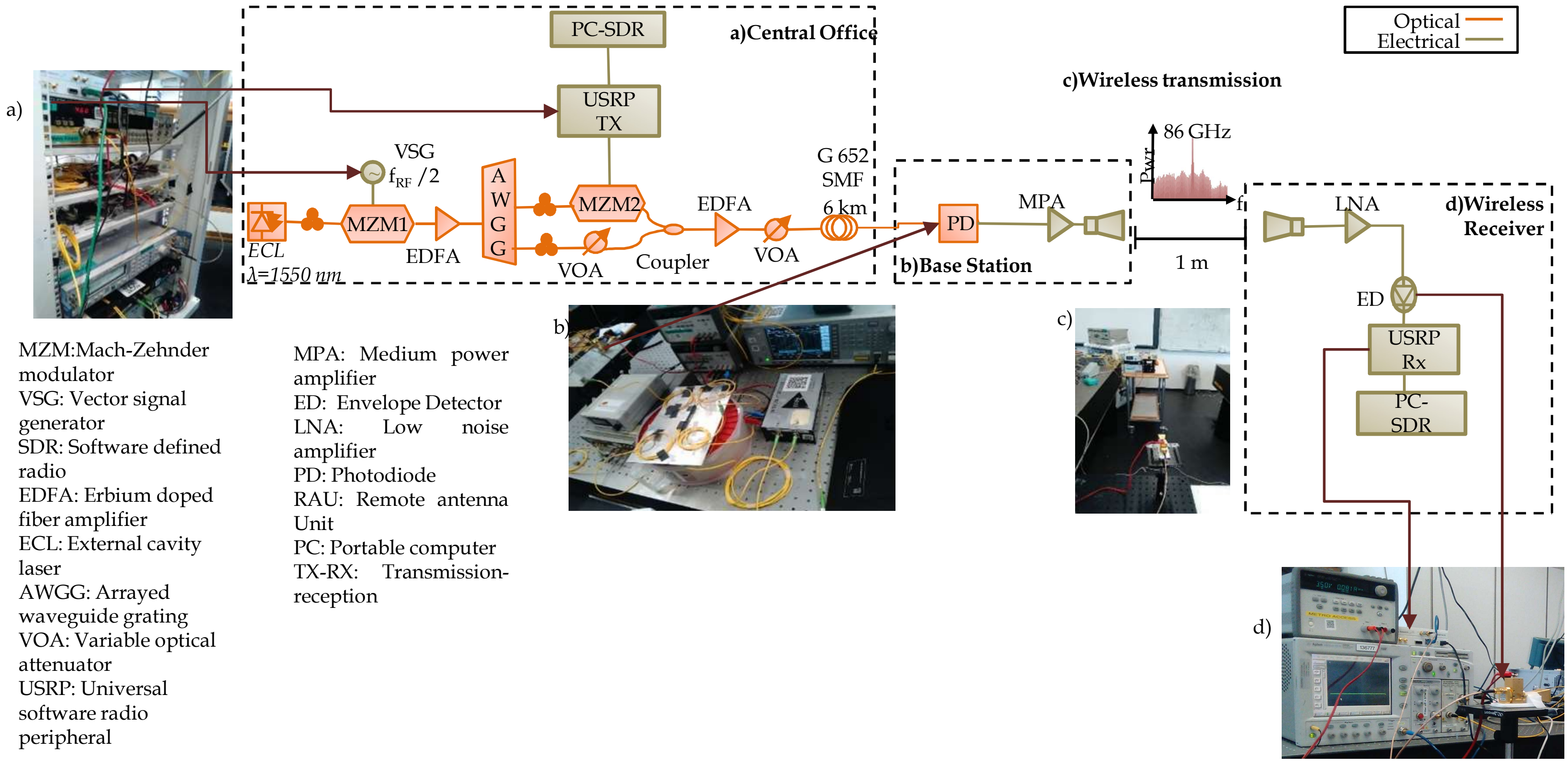

Fig. 4.1. W-Band Radio over Fiber Experimental Setup

4.1.1. Central Office

In the central office, the output of a 1550 nm External Cavity Laser (ECL), with an output power of 12.43 dBm (measured), is used as input to a Mach-Zehnder modulator (MZM1).

The equation that describes the laser signal is given by the next equation:

$$E_{in}(t) = E_0 e^{j\omega_0 t} \quad (29),$$

where E_0 and ω_0 are the optical field amplitude and angular frequency of the input optical carrier, respectively. The Emcore ECL was connected by Ethernet to a computer, where the power (16 dBm), the grid (500L), the channel (1) were programmed and by means of the software it was switched on or off.

The performance of the mach-zehnder modulator is given by different factors, such as bandwidth, impedance, optical loss and maximum input power. The modulator can handle linearity, sensitivity to temperature, applied voltage and polarization. In this experiment, a polarization controller was required following the laser, in order to match the polarization state of the modulator and thus maximize the output optical power.

As the modulator is driven with a pure sinusoidal tone of $f_{RF}/2 = 43$ GHz and 6 dBm of power, generated by a vector signal generator (VSG), the second harmonic of this tone is obtained at the output of the MZM1. Otherwise, the signal from the VSG can be written as

$$v(t) = v_{RF} cos(2\pi f_c t) \quad (30),$$

where f_c is the frequency of the RF signal and it was configured as $f_{RF}/2$ at 43 GHz, as referenced above.

Through the intensity modulation and stablishing 4.4V of Vπ in the MZM1. The MZM1 is configured at the minimum level of DC to obtain Double Side Band (DSB).Therefore, at the output of the MZM1 there are two optical signals with a separation of $f_{RF} = 86$ GHz, where $f_{RF} = |f_a - f_b|$ and $f_b, f_a = f_0 \pm f_{RF}/2$, respectively. f_0 is the frequency of the laser launched at 191,531 THz.

An erbium doped fiber amplifier (EDFA) is used to amplify the signal 22 dB with a noise figure (NF) of 5.8 dB, and an arrayed waveguide grating (AWGG) separates the two optical lines to enable the modulation of one of them by means of a second MZM2. The output of the EDFA is not a linear function of the input power.

The signal at the output of the EDFA is shown in Figure 4.2.

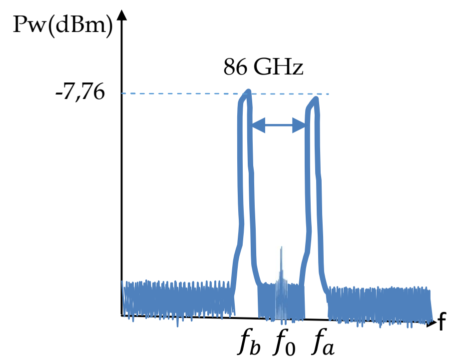

Fig. 4.2. EDFA Output in the W-Band Experimental Setup

The data signal to modulate the second MZM2 is generated by a USRP transceiver through GNU Radio software defined radio. One of the two optical signals is modulated with the data signal. In GNU Radio, the frequency of the data signal was configured at 1700 MHz.

The output of the MZM2 can be written as

$$E_{MZM2}(t) = E_0 e^{j\omega_0 t}\left(1 + e^{j\pi v(t)/v_\pi}\right) \quad (31),$$

where v_π is the half-wave voltage needed to achieve a differential phase shift of π between the two beams. This v_π in MZM2 was set at 5.2V. In this case the data signal has a very low frequency compared with the optical tone. Then, the output of the MZM2 is still the same tone with its respective harmonics.

The other optical tone is connected to a variable optical attenuator (VOA) to set equal power in both the unmodulated and modulated optical signals. An optical coupler combines them and a second EDFA amplifies the signal by 9.5 dB. A second VOA are employed to set the launch power into the 6 km SMF.

4.1.2. Base Station

After fiber transmission in the base station, a high-speed broadband photodiode (PD) (Finisar XPDV4120R) with a 3-dB bandwidth of 90 GHz converts the optical signal to the electrical domain, where the signal is boosted by a 12 dB medium power amplifier (MPA) before wireless transmission over 100 cm. A pair of horn antennas is used for wireless transmission, each one with 24 dB gain.

4.1.3. Wireless Transmission

The experimental setup was developed in the laboratory of the Photonics Department of the Technical University of Denmark, as aforementioned, which means indoor propagation. As the experimental setup was made in free space, it had a line of sight, i.e. no obstacles at either of the nodes.

In order to analyze the wireless channel, it is important to take into account the characterization of the wireless channel, because it is significant to the definition and development of the digital signal processing required for their compensation or mitigation. In theory, Friis Model indicates that the path loss of the present experiment must be:

$$path\ loss_{dB} = 10\ Log\left(\frac{4\pi d f_{RF}}{c}\right)^2 = 71.13\ dB \quad (32),$$

where f_{RF} is 86 GHz. The distance between transmitting and receiving antennas was of 1 meter.

Figure 4.3., shows the power in each point of the base station and wireless receiver in this experiment. At the wireless channel, we took the previously mentioned theoretical value given by Friis Model, because in [136], Rommel et al., from the same laboratory of DTU in 2016, did an experimental setup where they characterized the wireless channel of W-Band Radio over Fiber link and they conclude that Friis model is a good approximation to characterize the wireless channel.

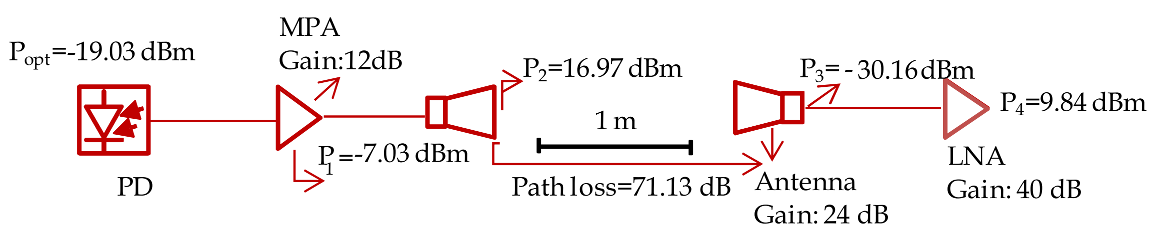

Fig. 4.3. Power Analysis

In addition in [136], they developed a similar setup and established that the manifestation of the fading channel with the former is mainly due to the distance between the antennas, the given environment and the resulting attenuation, while the small scale fading is described by a number of characteristics including the frequency response of the channel and its comparison with the signal spectrum in order to determine if the fading is frequency-selective or not. In figures 2and 3 of [136], they show the received power over distance(between 50cm and 400cm) and frequency(between 75 and 110 GHZ), showing the aggregated effect of path loss, shadowing and small-scale fading and comparing with the predictions based on the Friis transmission equation. The measurement of path loss in the current experiment at 86GHz and 100 cm, and our received power shown in figure 4.3., fits with those by Rommel et al.

4.1.4. Wireless Receiver

Finally, at the wireless receiver, the transmitted signal is amplified by a 40-dB low noise amplifier (LNA). A Schottky diode-based W-Band envelope detector (ED) with an input power of 18 dBm is used to down-convert the data signal to the original intermediate frequency (IF) generated by the USRP. The IF signal is sent to the receiver USRP and a PC software defined radio application (GNU Radio) is used to demodulate, storage and analyze the transmitted signals.

4.2. Results and Analysis of W-Band RoF system

In this first experiment at W-Band, we made three important analyses as mentioned in the introduction of the chapter. First, we developed a procedure to measure latency in the laboratory for this kind of experiments, using GNU Radio a kind of Software Defined Radio. Therefore, we introduce this technology into the photonics field. The time obtained or measured was verified with a PING validation, as explained in chapter 3.

The other two analysis took into account BER and Latency measurements in order to compare back to back against RoF scenario and compare RF modulation formats in terms of BER and Latency in the RoF link. Therefore, in this section the results of each of these objectives will be shown.

4.2.1. Latency Analysis between Back to Back Scenario and RoF Link.

In order to compare the time difference between Back-to-Back Software Defined Radio system (BtB SDR) and the hybrid Fiber-Wireless system, two scenarios were analyzed. Figure 4.4., show Back to Back scenario, which means it was only tested in two USRP with the wireless RF transmission. The W-Band Radio over Fiber setup was showed in Figure 4.1., and described in last section.

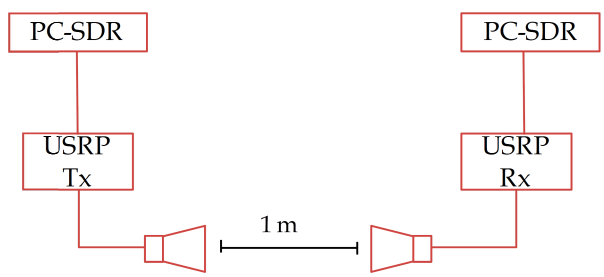

Fig. 4.4. Back to Back(BtB)Scenario

After determining and having the procedure to measure latency, it was important to establish whether in terms of latency there was a lot of difference between the hybrid Fiber-Wireless system and only the radio system. With the radio (RF) system, the operating frequency is limited by the USRP used (1700 MHz for this experiment), while in the Radio over Fiber system, the frequency was 86GHz, which indicates that the hybrid system can reach a higher capacity.

Latency measurements were made to compare the two systems, modulating one, two, three and four bits and using modulation in amplitude, frequency and phase of the electrical signal. Then, different RF modulation blocks as Gaussian Minimum Shift Keying-GMSK, Differential Quadrature Phase Shift Keying-DQPSK, Eight Phase Shift

Keying-8PSK, and Sixteen Quadrature Amplitude Modulation-QAM16 were used. These modulation schemes were used since we wanted to cover different modulated bits and different types of modulation.

In addition, it was possible to obtain the delay times of each process both in an RF system and in a Radio over Fiber system and were compared for the RoF setup. Figure 4.5., shows the real time achieved back-to-back in the wireless scenario against latency measurements of W-Band Radio over Fiber link.

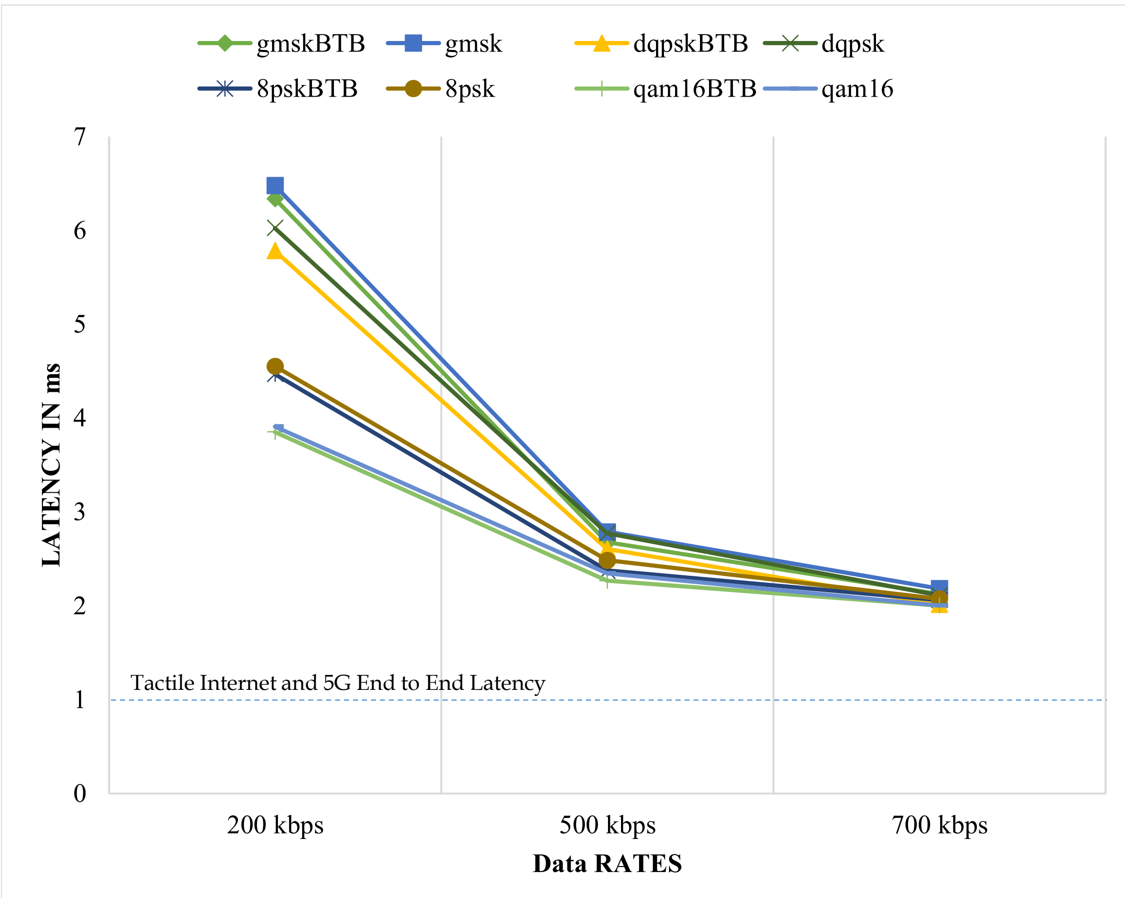

Fig. 4.5. Real time latency measurements Back to Back wireless scenario vs. W-Band Radio over Fiber link for different modulation techniques

The signal alignment delay was evaluated, and it was compared on average for both scenarios. Results show that the difference between Back-to-Back latency measurements and Radio-over-Fiber link is around 100 µs on average. This means that the difference between both scenarios is narrow compared with the benefits of the transmission capacity of Fiber optic-Wireless system explained at the beginning.

Table 4.1., shows an example of the measurements obtained, in this case it is shown for a GMSK Back to Back measurement. W-band setup tables' results of this experiment, following this example, are found in the last appendix of this document. It is important to

clarify that these measurements were made using the procedure to measure latency, therefore, the values take into account the throughput in different points as well as the packet size. Each packet size was extracted from kernel console.

Table 4.1. Latency Measurements

Transmission Throughput measured		**Reception Throughput measured**		**Delay in ms in the Transmission**	**Delay in ms in the Reception**	**End To End Latency**
1	36542,3	1	548365	1,751394959	1,400527021	6,113981045
2	789402	2	230648	1,297184451	1,664874614	
1	51165,9	1	439817	1,250833074	1,746180798	5,941500727
2	848804	2	220933	1,206403363	1,738083491	
1	37261,2	1	439463	1,717604371	1,747587396	6,747175928
2	666940	2	219854	1,535370498	1,746613662	
1	40240,1	1	440338	1,590453304	1,744114748	6,841238302
2	580534	2	220338	1,763893243	1,742777006	
1	42938,7	1	440732	1,490496918	1,742555567	6,261304846
2	793018	2	2,21E+05	1,291269555	1,736982807	
1	44016	1	442751	1,454016721	1,734609295	6,347645049
2	718300	2	221526	1,425588194	1,733430839	
1	31485,2	1	489654	2,032701079	1,56845446	7,405202564
2	505990	2	215695	2,02375541	1,780291615	
1	49176,5	1	545557	1,301434628	1,40773558	5,795831401
2	765110	2	219643	1,338369646	1,748291546	
1	57303,4	1	449915	1,116862176	1,706989098	5,934220439
2	7,36E+05	2	223272	1,390493856	1,719875309	
1	50145,1	1	438421	1,276296188	1,751740907	5,970669149
2	857577	2	219608	1,194061874	1,74857018	**6,335876945**

Taking into account the block diagram shown in figures 3.2 and 3.3, the numbers 1 and 2 represent the measure of the probe rate block in both transmitter and receiver. The adjacent cell of each number is the throughput measurement that prints GNU Radio. The delay of the transmission and reception is calculated taking into account the definition of throughput as explained in chapter 2. This measure is multiplied by a thousand, because is required to be given in milliseconds. For each data rate, ten tests were performed and the time taken as end-to-end latency is the average of these tests. All the results of this kind of table were summarized previously in Figure 4.4.

4.2.2. Latency and BER Analysis between different RF modulation in W-Band Radio over Fiber link.

Finally, once made a procedure to measure latency and measured it in a hybrid fiber optic-wireless system, it is important to analyze if the system is reliable by analyzing the errors presented in the scheme. We used an offline DSP through Matlab to evaluate the Bit Error Rate for both different modulation formats and also the Radio over Fiber scenario proposed.

Regarding latency measurements, as mentioned in section 3.1 and 3.2, the concept of end-to-end latency of this work considers the sum of three delays. The first delay considers the time of codification, modulation, multiplexing and sending of the data packets (t_a *signal alignment delay*). In this case, it depends on the message size. Our message is a pseudo-random binary sequence (PRBS7) sent repeatedly through GNU Radio. In addition, the SDR was in charge of making packages of 64 bytes as mentioned before. This time is the same for both scenarios (Back to Back and Radio over Fiber setup), and changes according to the modulation format because the size of the packet changes with the modulation scheme.

The second one is the propagation delay (t_p *propagation delay*), which is the time through the medium. In this case, only the time through the fiber was measured. The propagation time through 6 km of single mode optical fiber was 29.38 μs theoretical against 28.5 μs in practice. This theoretical value is obtained taking into account the length of the fiber multiplied by the refractive index and divided by the speed of light.

The third delay is the digital processing time that the physical signals need to be converted and presented to the end user from Central Office to point Wireless Receiver (t_{dsp} *digital signal processing delay*). In this experiment, it depends on the USRP N210 and comprises the WBX daughterboard and the FPGA motherboard. This delay also takes into account the queuing time, which depends on the USRP buffers size and interrupt coalescence (Interrupt coalescence refers to the amount of traffic that a network interface will receive) at the Network Interface Card NIC layer parameter. The value of the buffer size of the USRP was set by default, in that order, the buffer size was adjusted by itself to the data rate to which it was being transmitted and the data size.

Subsequently, the different modulation formats were compared on the W-Band RoF setup. Three data rates were considered (200, 500 and 700 kbs). It was not possible to increase this data rate because of the USRP used. Figure 4.6., shows the real time W-Band RoF latency measurements with the modulation techniques mentioned and the three different data rates. Each line represent each modulation format measured in those three data rates.

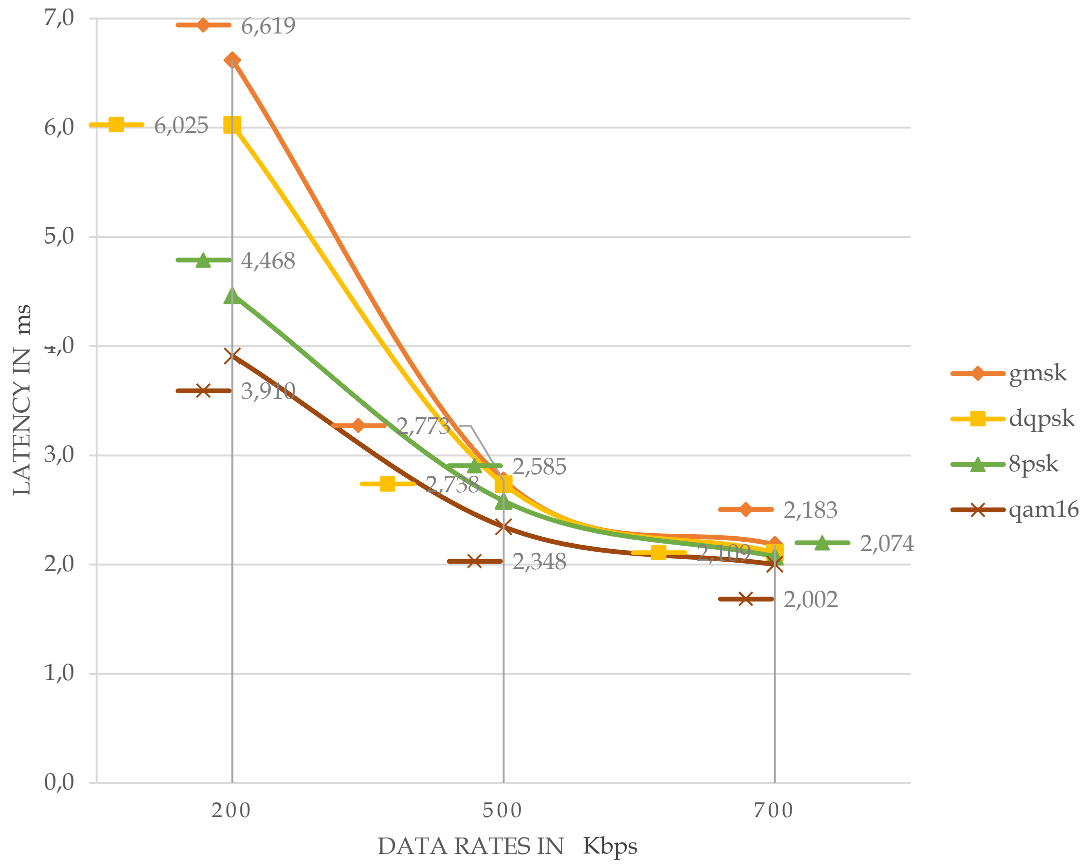

Fig.4.6. Real time W-Band RoF latency measurements for different modulation formats and data rates

As the modulation format advances in terms of number of bits per symbol processed and the data rate is high, the latency is lower. We reached an end to end latency of about 2 ms using software defined radio. If the data rate is high, an end to end latency of 1 ms required by 5G networks can be achieved, as will be demonstrated in the next chapter.

As mentioned, to compute the BERs and to synchronize the transmitted and received signal stored Matlab was used as an offline digital processing (DSP) method. Through the mix of three functions (such as repmat, finddelay and circshift), the synchronization of the transmitted and received signal was performed and by means of the simple definition of BER which indicates that the Bit Error Rate is the number of error bits, divided into the total number of bits that have been received in a given period of time. In Appendix B there is the Matlab code used for the offline processing of the signal. Figure 4.7., describes the BER measurements for different modulation formats and data rates analyzed.

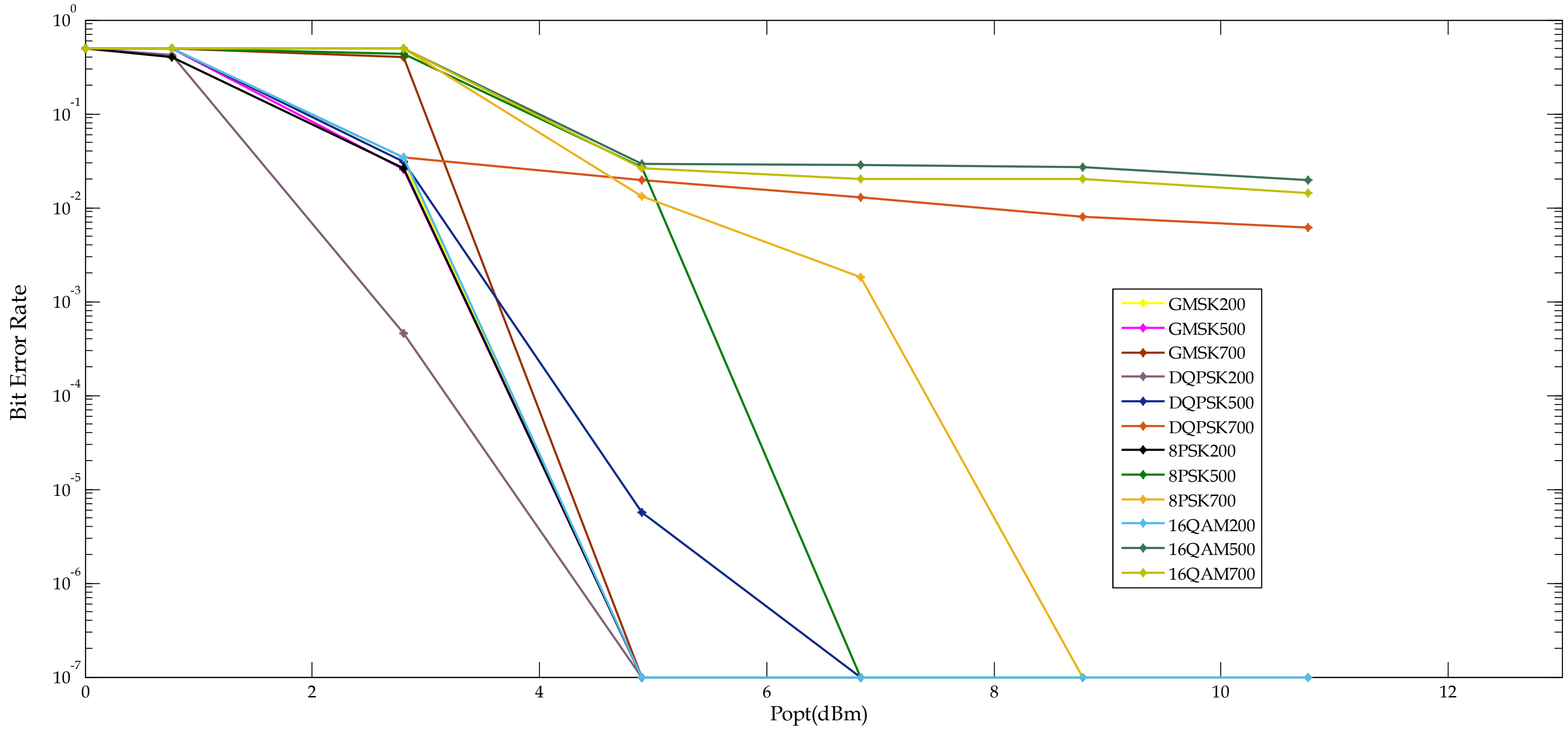

Fig. 4.7. BER measurements vs the optical power on the PD of the transmitter

Regarding figure 4.7., it is important to mention that the values of the optical power in the PD are normalized. Results of this evaluation show that modulation schemes with less processed bits per symbol achieved error free data. For a power in the PD of 5 dBm, it can be seen that acceptable bit error rates are obtained for the modulations which 1,2 or 3 bits are modulated. Moreover, when the optical power on the PD of the transmitter is weak, the USRP at the reception is not able to store all transmitted data. When the modulation format order is high with respect to the number of processed bits per symbol, less PRBS arrived complete.

The final result of this experiment demonstrates that hybrid fiber optic-wireless networks at W-band fulfill the requirements of the Tactile Internet, as well as the key performance indicators of 5G. In this experiment, data (PRBS) was sent, through the described configuration. Likewise, small amounts of data are continuously and repeatedly sent, demonstrating that this configuration can be used in applications such as automation and machine control in industrial, health, education and sensor applications. In this sense, it is verified that hybrid networks mixed with SDR are feasible due to their low latency and reliability shown in this chapter.

Chapter 5

5. Multiplexing and Modulation in a Radio over Fiber System with low latency

Currently, RoF systems support the current trends of mobile data traffic expected in 5G networks [137], [138]. As discussed above, Radio-over-Fiber systems (RoF) or Fiber-Wireless (Fi-Wi) take advantage of the low loss and the broadband bandwidth of the optical fibers [139] and have become key enablers to unlock future broadband wireless communications with multigigabit data rates [140], [141], [142], [143].

In addition, it was verified that the latency measured in a Radio over Fiber system and mixed with SDR systems fits the requirements of the 5G networks. It is worth mentioning that two major factors that determine the way a signal is transported through the channel in a telecommunication system are modulation and multiplexing techniques. Due to their importance, we proceed to study these two parameters.

Two experiments are carried out in another band proposed for 5G, in this case, the 3.5 GHz band. According to different agents of the telecommunication sector [144], [145], 5G will use the 3.5 GHz International Mobile Telecommunication (IMT) range between 3.3 GHz and 3.8 GHz to keep up with coverage demands and the growing use of data. The 3.5 GHz band is one of the first frequencies identified in the World Radio Communication Conference WRC-15 with a harmonized IMT spectrum as part of its allocation for the mobile service for consumers and businesses [146], [147].

The first experiment was made to compare OFDM and GFDM, taking into account that LTE and 4G systems use OFDM in their networks for developing the Internet of Things (IoT). On the other hand, WPON is a technique that has been quite used because it allows the multiplexing of a lot of optical signals, which means more number of users thanks to bandwidth. Therefore, the second experiment was made to measure latency in WDM'PON systems.

In this chapter, first we are going to present a small context about the modulation and multiplexing techniques that were analyzed throughout work. Then, the experiment that compares OFDM and GFDM is presented. Finally the experiment that includes WDM into a SDR-RoF system with it respective simulation is shown. This chapter takes into account the results published in [148], [149] and [150]

5.1. Modulation Techniques

As mentioned above, one of the major factors of the communication between two points is the modulation format. In Fiber-Wireless systems, the analog RF carrier is modulated by a data signal, which is a discrete signal. There are different modulation techniques, where either the amplitude, the phase or the frequency (or the combination of these) is changed in order to adapt the signal to the medium. Similarly, the modulation number (M) varies according to the modulation symbols, which depend on the number of modulated bits.

All the above techniques have advantages and disadvantages, in this work, the modulation techniques (GMSK, PSK and QAM) are evaluated for a Radio over Fiber system to see their influence in the measurements of latency.

5.1.1. Phase Shift Keying - PSK

Phase Shift Keying (PSK) is a digital modulation technique that transmits data by modulating the phase of a reference RF signal. This means handling a carrier phase in accordance with the transmitted bit stream. The general expression for PSK is [151]:

$$S_i(t) = \begin{cases} \sin(2\pi f t) & for\ bit\ 1 \\ \sin(2\pi f t + \pi) & for\ bit\ 0 \end{cases} \qquad (33),$$

where f is the carrier frequency.

There are a few PSK techniques commonly used: Binary PSK (BPSK), which uses two symbols M=2; Quadrature PSK (QPSK), which uses 4 symbols M=4; Differential PSK (DPSK); Differential QPSK (DQPSK); and Offset QPSK (OQPSK). Phase Shift Keying modulation uses a finite number of phase angles based on the modulating digits [152]. In BPSK, as mentioned previously, M=2 means that the phase varies between 2 values according to the bit emitted. In QPSK, M=4 means that the phase can take one out of four possible values. QPSK is the simplest form of QAM, as shown in the next section. QPSK can be used to maintain the bit rate of BPSK, but with half the bandwidth needed, or to double the bit rate compared to a BPSK system, maintaining the same bandwidth of the signal [28]. The difference is that QPSK has more robust transmitters and receivers than BPSK. QPSK is used in the IS-9 wireless network.

PSK (BPSK, QPSK) is coherent, which means that the demodulator is designed for the set of symbols used by the modulator. Likewise, it determines the phase of the received signal and maps it back to the original symbol, recovering the original data. Then, the receiver tracks the phase by means of a phase locked-loop circuit that compares the phase of the received signal with a reference signal generated locally. In RoF links, phase distortions may arise, hence PSK is sensitive to them [152].

DPSK (DPSK, DQPSK) is a non-coherent technique. In this format, the demodulator defines the changes in the phase of the received signal rather than the phase itself. Thus, DPSK can be simpler to implement than ordinary PSK, as no copy of the reference signal in the demodulator is needed to determine the exact phase of the received signal [28].

5.1.2. Gaussian Minimum Shift Keying - GMSK

There are two methods to generate the Gaussian Minimum Shift Keying (GMSK). The most used is based on the filtering of the MSK modulation by means of a Gaussian filter to avoid the abrupt changes of the phase that occur in the MSK modulation [153].

In this modulation, filtering converts each modulating data that occupies a time period (T) in baseband, in a response where each symbol occupies several periods, depending on the product bandwidth–time (BT) of the filter. This means that the RF bandwidth is controlled by the Gaussian low pass-filter. Since this pulse conformation does not change, the path model of the GMSK phase can be detected coherently as an MSK signal. In addition, GMSK allows efficient class C non-linear amplifiers to be used. GMSK was implemented in GSM mobile system, for this reason in this work was taken into account.

A block diagram that describe this kind of modulation is given by Figure 5.1.

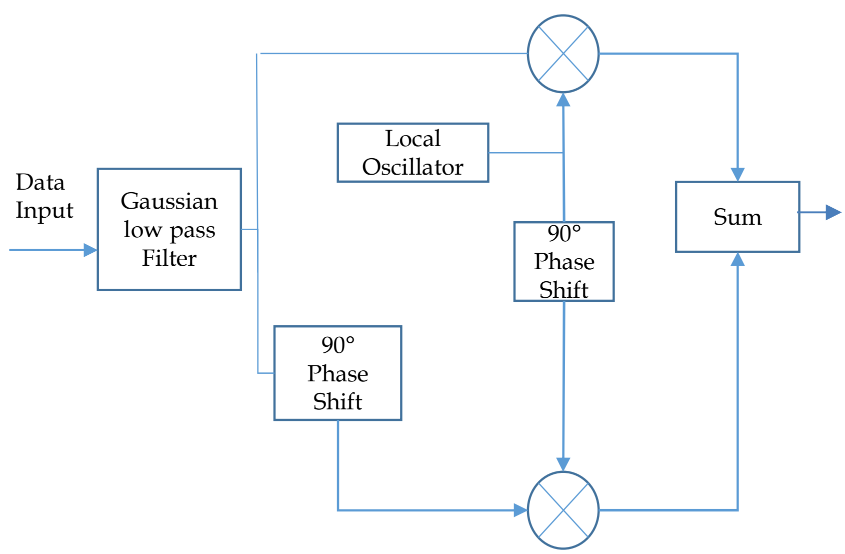

Fig. 5.1. GMSK Block Diagram
Source:[153]

5.1.3. Quadrature Amplitude Modulation - QAM

Quadrature Amplitude Modulation (QAM) can be considered as a combination of both PSK and Amplitude Shift Keying (ASK), as well as an extension of QPSK[151]. In QAM, the amplitudes of both the in-phase (I) and quadrature phase (Q) components of the RF carrier are changed according to the modulating symbols. It can be said that QAM modulates the RF carrier in amplitude and phase. QAM is widely used in wireless communications. The most common QAM schemes are 16-QAM, 32-QAM and 64 QAM[28].

The M-QAM signal can be written as follows[151]:

$$S_i(t) = b_{i.I}(t).cos(w_c t) - b_{i.Q}(t).sin(w_c t), \qquad i = 1,2,\ldots, \mathrm{M} \qquad (34),$$

The first term of the equation represents $I_i(t)$ and the second one represents $Q_i(t)$. $M = 2^k$ represents the modulation cardinality, k is the number of bits per symbol, $b_{i.Q}(t)$ and $b_{i.I}(t)$ are the $\sqrt{M} - level$ amplitude modulated baseband signals corresponding to the Q and I channel.

The signal in QAM can be represented as a combination of the in-phase and quadrature components. Nonetheless, the constellation points are distributed over the whole area of the constellation diagram instead of over the circle, like in PSK. Other QAM schemes use more values for the amplitudes [151]. Therefore, a better channel SNR is required for the successful transmission of high- level QAM signals.

5.2. Multiplexing Schemes

Multi-carrier systems use multiplexing topologies with a set of carriers in certain bandwidths of the frequency spectrum to transmit information. These multi-carrier schemes can be characterized according to their orthogonality. All frequency carriers are used simultaneously creating a time signal that is a juxtaposition of each of these individual signals.

There are many multiplexing techniques, however, one of the most implemented for the current commercial mobile networks is OFDM. In this section, OFDM will be explained in general, as well as GFDM, which is another technique that is beginning to be studied and used by advanced LTE systems.

5.2.1. OFDM

In OFDM, the signal is launched at baseband, which consists of a set of orthogonal sub-carriers that are a multiple of an original carrier. Each one is carrying a lower-rate stream encoded on digital modulation formats by taking the inverse Fast Fourier transform (IFFT) of phase-shift keyed (PSK) or quadrature amplitude modulated (QAM) sub symbols[154].

The objective in OFDM is to multiplex a data stream over time by assigning it a portion of the available bandwidth in the spectrum [150]. This scheme is characterized by some advantages compared to modulations traditionally used in previous mobile phone standards. The main advantages of this multiplexing scheme are high transmission rate, spectral efficiency and low intersymbol interference (ISI) [155].

Figure 5.2., shows a block diagram system. In the transmitter, the system input is a data stream or a sequence of coding bits. Then, the mapping is performed in a digital constellation that assigns a symbol, usually BPSK, QAM or QPSK, to the incoming bit sequence.

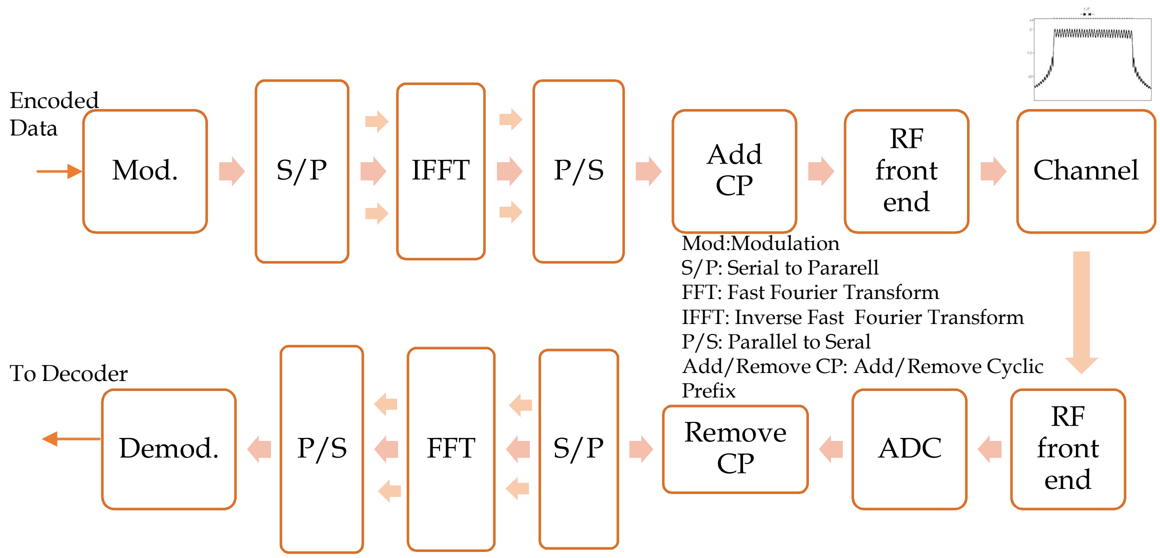

Fig. 5.2. OFDM Block Diagram
Source:[156]

The serial data symbols are then converted to parallel data symbols, which are driven to the Inverse Fast Fourier Transform (IFFT) block to obtain the time domain OFDM symbols. The function of IFFT block is to transform the aligned symbols into the corresponding subcarrier frequencies at the same time, taking N samples of each subcarrier and superimposing them with the others to form a new symbol, called the OFDM symbol. Time domain samples can be written as [157]:

$$x(n) = IFFT\{X(k)\} = \sum_{k=0}^{N-1} X(k)e^{j2\pi nk/N} \qquad 0 \leq n \leq N-1 \tag{35}$$

where $X(k)$is the transmitted symbol on the kth subcarrier and N is the number of subcarriers. Then, the OFDM symbols go to a parallel to serial scheme in order to be sequential in time. Afterward, the transmitter has the function of adding a cyclic prefix (also known as guard interval) to the OFDM symbol. This addition is done to avoid residual Inter-Symbol Interference (ISI) from the previous OFDM symbols. Finally, in the DAC block, baseband digital signal is converted to analog signal through the Digital-to-Analog Converter (DAC). Up-conversion to RF is an important part of the OFDM architecture, particularly, because this conversion places the spectrum of the OFDM signal around a center frequency. The RF frontend up-converts the signal to the RF frequencies using mixers, amplifies it using Power Amplifiers (PAs), and transmits the signal through antennas. In most cases, the channel is wireless, though it is also common to find Radio over Fiber links.

At the receiver, it performs the reverse process of the transmitter blocks. Conversion to baseband implies the inverse process to the conversion to RF, and includes the complementary blocks as an ADC, a receiver oscillator (with a system mostly based on a Phase Local Loop) and a low-or band-pass noise rejection filter. The Analog-to-Digital Converter (ADC) digitizes the analog signal and re-samples it. After frequency and time synchronization (which are not displayed in the figure for simplicity), Cyclic Prefix (CP) is removed. Then, a correct demultiplexing is required, since in case of mismatches in time, the symbols will recover with errors. In the parallel serial block, the OFDM symbols are aligned for the application of the Discrete Fourier Transform (DFT), which converts these samples to frequency domain. Finally, symbols are demodulated, de-interleaved, and decoded to obtain the transmitted information bits.

A basic baseband model of the received symbols in frequency domain can be written as [158]

$$Y(k) = H(k).X(k) + W(k) \tag{36}$$,

where $Y(k)$ is the received symbol on the kth subcarrier, $H(k)$ is the frequency response of the channel on the same subcarrier, and $W(k)$is the additive noise plus interference sample.

Finally it is important to mention that OFDM systems provide an efficient use of bandwidth, however have a high out-of-band emission originated from the side lobes of the modulated subcarriers. Therefore, it needs an out-of-band reduction method. It is important to clarify that any emission outside the frequency range separated from the assigned frequency of the emission in less than 250% of the necessary bandwidth of the emission will be considered an OOB emission [159].

5.2.2. GFDM

GFDM is a symbol-based multicarrier multiplexing technique that uses circular filtering in order to keep the signal well confined in time and frequency domains. It works using low out-of-band (OOB) emission [160]. Circular filtering implies a circular convolution[161].

In addition, GFDM employs a single Cyclic Prefix (CP) for several time-slots, increasing the spectral efficiency. GFDM can transmit multiple symbols, at different time slots, per each sub-carrier[162].

In GFDM, each subcarrier is pulse-shaped by a filter impulse response with S representing the number of samples, S= RT, where R denotes the number of samples per period and T is the number of periods of the filter. GFDM has advantages such as signal compact in time and low complexity signal processing. Figure 5.3., shows a GFDM block diagram of a basic transceiver.

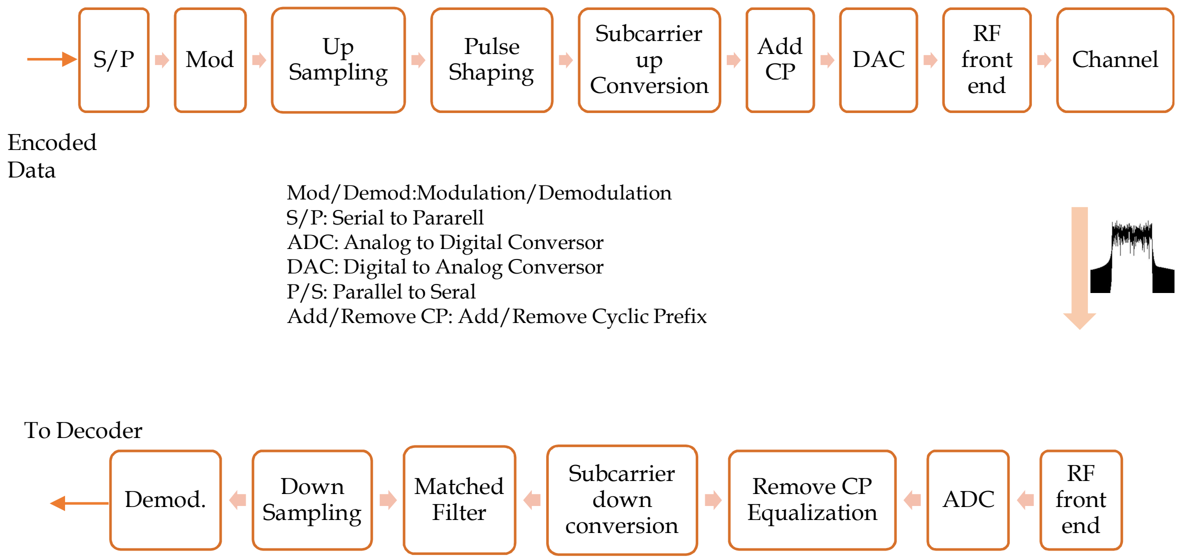

Fig. 5.3. GFDM Block Diagram

Source:[163]

First, a data source provides the coded data that feed the S/P block (series to parallel) and these data are arranged on K subcarriers that carry M each of the sub-symbols, resulting in a total of parallel MK subflows. The binary data is mapped into complex valued using QAM modulation or QPSK. The complex data symbols $d_k[m]$, m= 0,1,2…M − 1 are up-sampled by a factor N, resulting in [164]:

$$d_k^N[n] = \sum_{m=0}^{M-1} d_k\,[m]\delta[n - mN], \qquad n = 0, \ldots\ldots, NM - 1 \tag{37}$$

where $\delta[n - mN]$ is the Dirac fuction. It can be observed that $d_k^N[n = mN] = d_k[m]$ and $d_k^N[n \neq mN] = 0$.

Then, a pulse shaping filter $g[n],\ n = 0, \ldots, LN - 1,$ which is a circular filter with a length L ≤ M, is applied to the sequence $d_k^N[n]$.The filter is selected with a periodicity n mod MN in order to facilitate tail biting at the transmitter. The tail biting is a technique which is used to shorten the cyclic prefix in order to prevent overlapping of subsequent symbols and compensate for filtering tails[165].

The GFDM transmit sequence can be written as follows:

$$x[n] = \sum_{m=0}^{M-1} \sum_{k=0}^{K-1} d_{m,k}\, g[n - mN] e^{j\frac{2\pi kn}{N}} \tag{38}$$

where N is the upsampling factor that is necessary to pulse shape each of the subcarriers, respectively. Then, $d_{m,k}$ are the complex valued data symbols, delayed by mN in time and shifted by $k\frac{1}{N}$ in frequency domain, where $\frac{1}{N}$ is the subcarrier spacing.

The data block transmit signal is added to the CP cyclic prefix and it is passed to the digital-to-analog converter and sent over the channel.

At the receiver, first it is necessary an analog-to-digital conversion, thus, the received signal is denoted as y[n]. Then, it is passed to equalization and the CP block is removed. One way of reconstructing the data is to design the receiver such, $\widehat{y_k}$[n], which denotes the subcarrier received signal, obtained after digital down conversion . After convolving with the receiver matched filter g[n], the signal is down-sampling and demodulated,

5.3. Data Signal multiplexing - OFDM and GFDM Experiment

On the one hand, this experiment was configured in 3.5 GHz, since C band (RF band) will be one band of 5G mobile commercial networks [166], [167]. On the other hand, taking into account that Radio over Fiber system will be a key enabler of 5G networks, we configured a Fiber-Wireless system including OFDM and GFDM as multiplexing schemes, because there are no studies or comparisons of these multiplexing schemes in RoF system, even if OFDM and GFDM have been widely studied in recent years [168], [162].

This section presents a comparison between two important multiplexing systems for 5G such as OFDM and GFDM, regarding latency and bit error rate in Radio over Fiber systems. It is important to mention that low-latency and high reliability will be key performance indicators for future networks.

In the next paragraphs, first, the experimental setup and the parameters defined for the experiment are described, second, the results and analysis regarding the measurements of latency and bit error rate are shown.

5.3.1. Radio over Fiber setup including OFDM and GFDM

An experimental setup C-band (RF) Fiber-Wireless system was developed, including SDR as in the previous experiment in W-Band. Similarly, the same procedures were used to measure latency and BER. The radio-frequency signal was multiplexed using OFDM and GFDM for each experiment, using GNU Radio.

To perform the physical process of generating the modulated and multiplexed signal, two USRP N210 were used, one for the transmitter and another one for the receiver with a single channel established for transmission and reception (in USRP N210 it is possible to establish one channel to transmit and other channel to receive). Table 5.1., presents the parameters of each one of the formats used. Note that both multiplexing schemes have the same modulation technique, FFT size and sample rate. The active subcarriers and cyclic prefix in OFDM are less than GFDM, to reduce the number and size of guard bands in OFDM and to try to reduce out-of-band emissions.

Table 5.1. Flow Graph Parameters

Parameter	*OFDM Value*	*GFDM Value*
FFT Size	128	128
Bits per Symbol	2	2
Modulation Technique	QPSK	QPSK
Cyclic Prefix	32	64
Sample Rate	1Msps	1Msps
Active Subcarriers	88	110
Frequency	3.5GHz	3.5GHz

For both multiplexing schemes, we also run in GNU Radio a set of benchmarks of GitHub[169] with some modifications. Appendix C shows the print screen of the GNU Radio flow graph of each multiplexing technique. We adapted the benchmarks to the parameters of our setup and added some blocks to measure latency.

Regarding latency, it is important to mention that we included another measurement point, as shown in Figure 5.4. This extra measurement point is added to signal alignment delay, because it is part of the processes of the data signal.

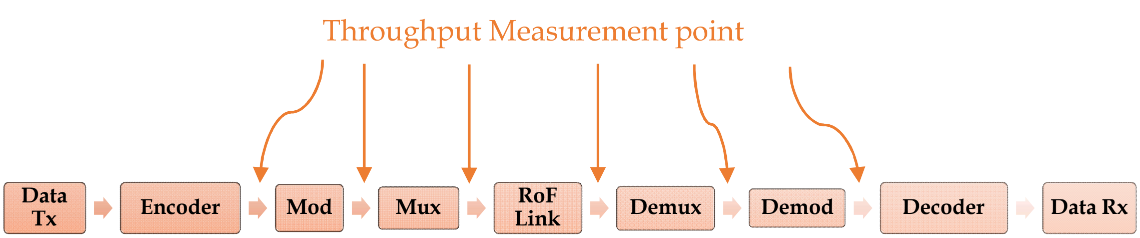

Fig. 5.4. Block Diagram of GNU Radio

Figure 5.5, (a) and (b), shows the block diagram and some pictures of the experimental setup, respectively, taking into account the incorporation of the hybrid system Fiber-wireless. In a central office, a VCSEL was used at 1550 nm wavelength to generate the optical signal. This signal was amplified with an Erbium Doped Fiber Amplifier, to obtain an output of 6.56 dBm. The EDFA output was modulated by an intensity Mach-Zender modulator (MZM) with the data signal generated by a USRP at 3.5 GHz of frequency.

a)

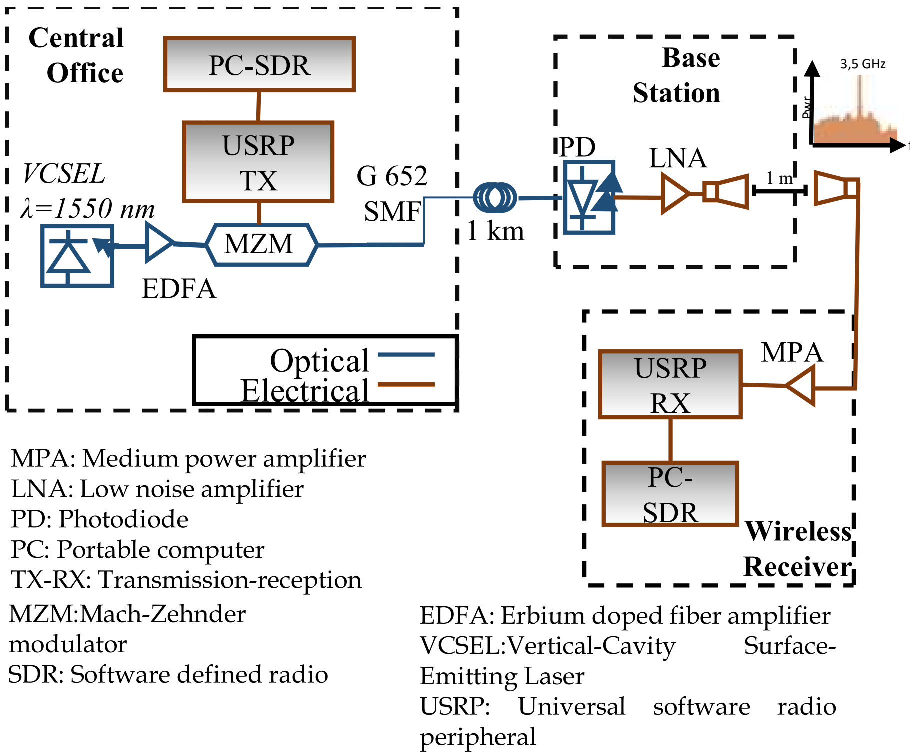

b)

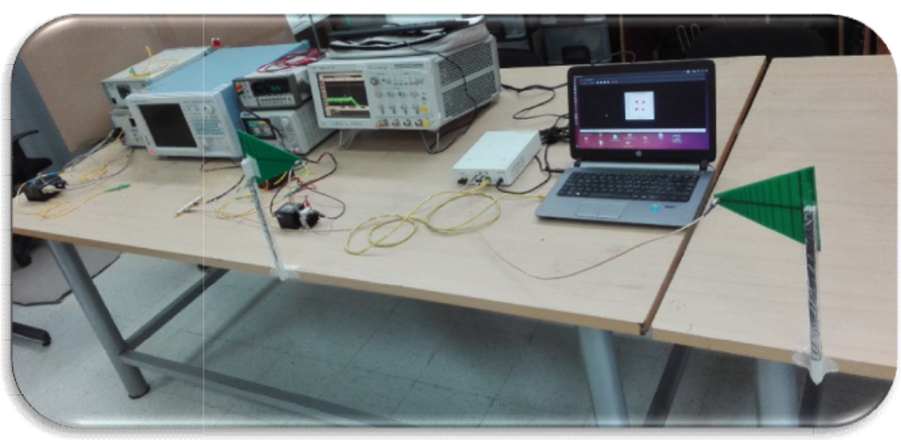

Fig. 5.5. Experimental Setup OFDM-GFDM RoF Link:
a) Block Diagram, b) Picture of the experimental setup

Although the electrical signal could be modulated directly, we used an optical external modulator because direct modulation causes an undesirable wavelength chirp, which origins a higher chromatic dispersion. Thus, the bit error rate could be greater, and the research was looking for an ultra-reliable system that fit with the key performance indicators of Tactile Internet or 5G networks.

After 1 km of optical fiber in the base station, a photodetector converts the optical signal to an electrical one, which is amplified 30 dB by a low noise amplifier. This signal is transmitted and received by a pair of log periodic directional antennas, with 5-6dBi Gain. Once the signal is received by the antenna, after 1 meter of wireless transmission, it is amplified by a medium power amplifier. Then, it is demodulated, decoded and de-multiplexed by another USRP through GNU Radio.

5.3.2. Comparison between OFDM and GFDM

As mentioned above, the data signal was multiplexed using OFDM and GFDM by means of GNU Radio and then it was driven to a MZM modulator in order to be transmitted through the Radio over Fiber Link described in last section. In the GNU Radio flow graph at the transmission, a PRBS7 sequence data file was sent repetitively. Then, in the receptor flow graph, the data information sent was stored in a file.

Figure 5.6 shows the RF spectrum and the constellation diagram per each multiplexing scheme. Both graphics were taken using software GNU Radio. Figure 5.6. a) displays the constellation diagram, at the left OFDM and at the right GFDM. In both schemes the signal is displayed as a two-dimensional xy-plane scatter diagrams in the complex plane at symbol sampling instants. Each symbol is set as a different combination of amplitude and phase of the carrier, thus each symbol is represented by a point on the constellation diagram. The collection of points of GFDM seems to be more robust than the OFDM one, nonetheless, this is because the points of the constellation GFDM are more dispersed than those of OFDM.

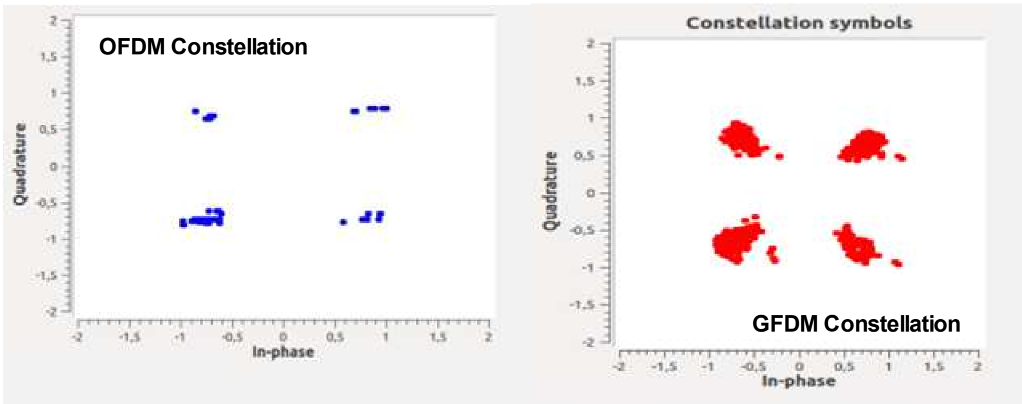

a) Constellation OFDM and GFDM

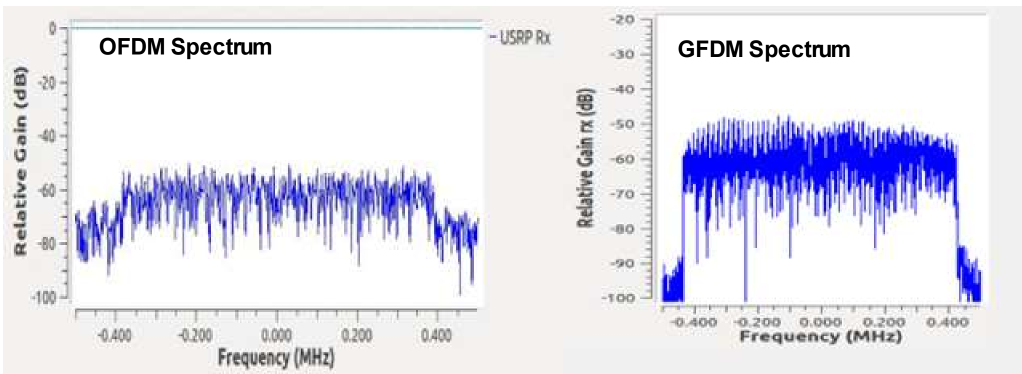

b) OFDM and GFDM Spectrum

Fig. 5.6. OFDM-GFDM RoF Link.
a) Constellations of OFDM and GFDM, b) Spectrum of OFDM and GFDM

In Figure 5.6. b) the GFDM spectrum in the reception USRP is at the right and the OFDM spectrum is at the left. The amplitude of both multiplexing spectra is similar and the spectrum corresponds to the theory of each scheme. The bandwidth is in accordance with the sample rate stablished in the flow graph of GNU Radio.

Once the transmission and reception with both multiplexing techniques have been tested, we proceed to measure the latency and the Bit Error Rate. To measure the BER, Digital Signal Processing (DSP) was used by means of Matlab, with the code of Appendix B. As in the previous experiment through Matlab, the synchronization of the signal was made and the bit error rate was calculated using the stored transmission and reception files.

The Bit Error Rate measurement is displayed in Figure 5.7., the comparison between OFDM and GFDM is presented. Red squares are the measurements of bit error rate for OFDM. Dark blue diamonds represent the measurements of GFDM. The horizontal axis denotes the optical power received in the photo detector. Vertical axis represents Bit Error Rate value. Results show that OFDM at the same condition of data rate and FFT size is slightly better than GFDM. Both techniques are suitable concerning bit error rate, because with a good optical power, Bit error Rates of 1x10-6 were achieved.

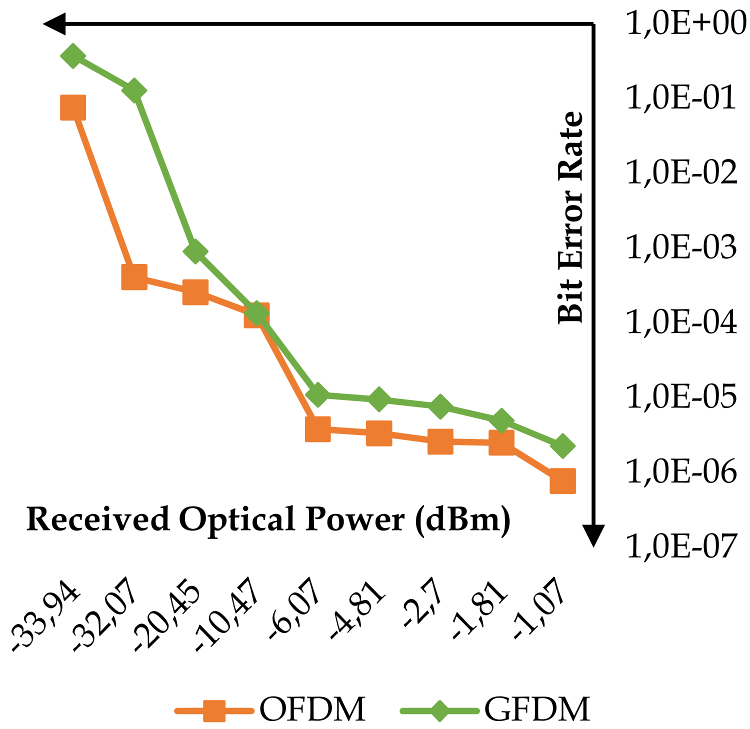

Fig. 5.7. Bit Error Rate against PD Power

Table 5.2 is obtained by comparing the bit error with other researches of OFDM and GFDM. In general, our measurements of Bit Error Rate for both multiplexing schemes were among the measurements of the other studies and from the power of -10.4 dBm the two multiplexing schemes have an acceptable BER.

Table 5.2. Bit Error Rate Comparison

Paper	*BER OFDM Value*	*BER GFDM Value*
100 Gbit/s hybrid optical Fiber-Wireless link in the W-Band (75–110 GHz)[76]	3.2×10−4	--
Bit Error Rate analysis of Generalized Frequency Division Multiplexing with weighted-type fractional Fourier transform precoding[170]	--	1×10−5
Bit Error Rate analysis of a MIMO-Generalized Frequency Division Multiplexing scheme for 5th generation of cellular systems[171]	1×10−4	1×10−3

GFDM Performance in terms of BER, PAPR and OOB and comparison to OFDM system[161]	1×10−3	1×10−2
Bit Error Rate Performance of Generalized Frequency Division Multiplexing [172]	1×10−4	1×10−3
KPIs (Key Performance Indicators) at the ITU level[173]	1×10−5	

Regarding latency measurements, we used the same procedure presented previously. Then, it was possible to know the instant delay by means of the throughput in GNU Radio. In both multiplexing schemes, three measurement points were placed in the transmission, as well as in the reception, as shown in Figure 5.3. The sum of all the measurements is the end to end latency.

In order to verify that adding all the Fiber-Wireless system does not affect considerably the end to end latency, the first measurements were made only using USRP transmitting and receiving, which means only wireless system (Back to Back scenario). Figure 5.8., presents the comparison between OFDM and GFDM Latency. Blue line denotes GFDM measurements and red line represents OFDM measurements.

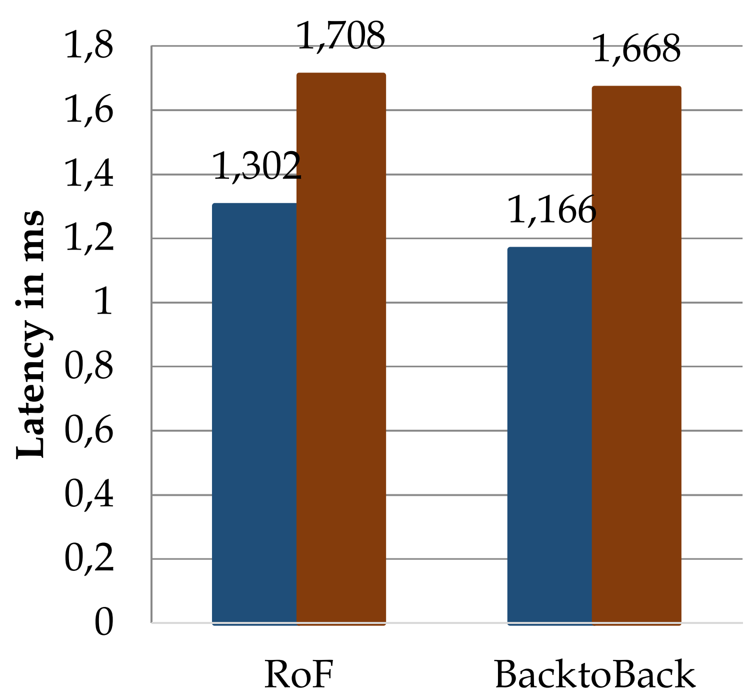

Fig. 5.8. OFDM and GFDM Latency measurements in ms

On the one hand, results show that only aprox 0.5 ms takes to implement Fiber-Wireless system. In addition, in both scenarios, the latency for GFDM is lower than in OFDM. The reason is that in OFDM, signals have one CP per symbol, which certainly causes long latency and low efficiency. On the other hand, taking into account a scenario with several nodes, like a mobile network, GFDM evidence a good performance regarding latency because 1.30 ms is into the key performance indicators of 5G networks, also considering that our setup only permits 1 Mbps.

In Figure 5.9., a synthesis chart is depicted. To obtain this figure, 1 to 10 scale was quantified. The lowest value is 1 and 10 corresponds to the highest value or the best measurement. For latency, the value of 10 is given to 1 ms because this value is the key performance of 5G networks[174]. In this way, the value that is the closest to 10 has the best latency. For the Bit Error Rate, the value of 10 is given to a BER of 1E-9, which is an acceptable value for the new generation networks according to the ITU and G series standards[175]. Consequently, the values closest to 10 represent the lowest Bit Error Rate, that is, the best communication.

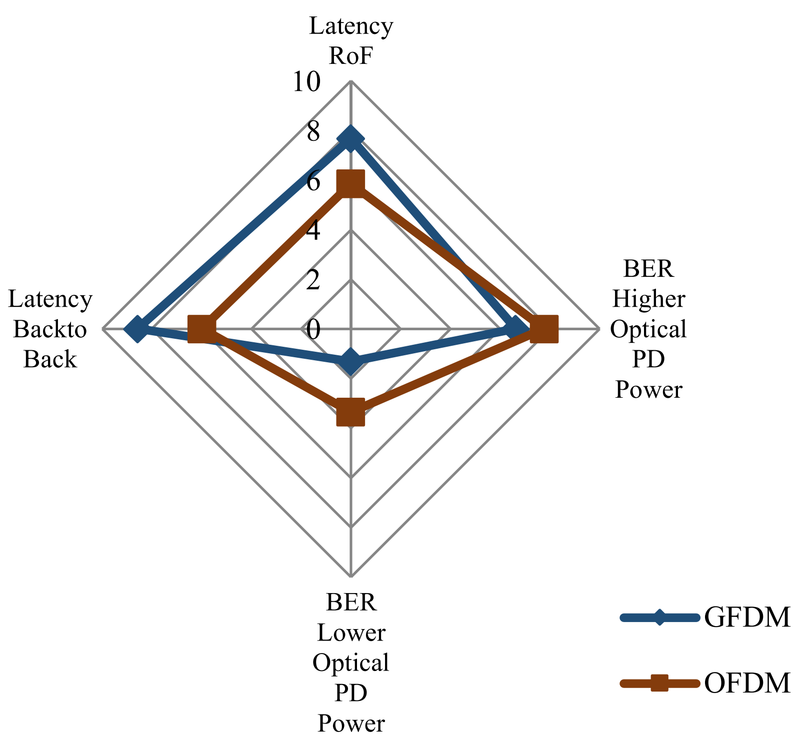

Fig. 5.9. OFDM and GFDM Performance

Regarding the performance about Bit Error Rate and Latency, GFDM is a remarkable option compared with OFDM. It could be observed that GFDM is slightly better in end-to-end latency and has a very similar performance in terms of BER. The number of guard subcarriers used in OFDM is reduced, as mentioned, since GFDM uses the lower OOB emissions.

For 5G applications on a Radio over Fiber system at C band, GFDM is suitable to be deployed. GFDM presents a good performance and reliability regarding bit error rate and for low latency applications. In addition, GFDM has a similar structure to OFDM and needs one extra module of the entire scheme.

5.4. Wavelength Division Multiplexing WDM in a Radio over Fiber System

In the WDM-PON technology, a number of optical carriers are multiplexed into a single optical Fiber through different wavelengths [176]. Each wavelength used in the network is allocated for a specific user, i.e. each wavelength is dedicated to a particular user from the Optical Line Terminal (OLT) to the remote node. Thus, many channels can be transmitted through the same fiber without interference. This method is often used to increase the capacity of existing fiber optic systems.

Generally, the separation between channels is given by standard G694.1 of the International Telecommunications Union (ITU) [177]. This indicates that for any given wavelength λ and corresponding frequency f, the spacing Δf must be 100 GHz, which means a separation of approximately 0.8-nm. Commercially available systems today can multiplex up to 128 individual wavelengths at 2.5 Gb/s or 32 individual wavelengths at 10 Gb/s. WDM is being widely deployed by several telecommunications companies, because it is a cost-effective alternative to set more fibers [178].

The combination of RoF with WDM-PON has many benefits aligned with the requirements of 5G networks [179]. WDM in RoF has the advantages of higher bandwidth, higher data rate, greater capacity and high security [180]. In WDM-PON, the splitters in the remote node are replaced by a multiplexer device and a demultiplexer in the Optical Distribute Network (ODN). Those networks do not have the splitter loss, thus they can transmit data through longer distances [181].

In this section, an experimental setup of a Fi-Wi WDM-PON system using SDR in the 3.5 GHz band is presented, in order to demonstrate low latency and reliable communication for future 5G networks. It is important to mention that using SDR, the band can be programmed and a determined multiplexing and modulation technique can be used [182].

5.4.1. WDM-PON RoF Experimental Setup

For this experiment, an RoF WDM-PON link was implemented in a 3.5 GHz band. This band was selected for its future use in commercial 5G networks. This setup uses an USRP developed by Ettus Research™ [183] for the RF generation. The model B205 was used, which consists of a programmable Xilinx Spartan-6 XC6SLX150 FPGA with RF coverage ranging from 70 MHz to 6 GHz. In the computer a GNU Radio software is placed.

In the experimental setup, a tunable Distributed Feedback Laser (DFB) with two outputs was used as input for two Mach-Zehnder modulators (MZM). The outputs were at 1558.17 nm and 1559.79 nm, with an output power of 12.99 dBm each. A polarization controller (PC) was placed at each output of the DFB, to maintain the polarization and obtain the maximum power of each laser output. The modulator was driven with an RF signal of 3.5 GHz that carries the data and is generated by a USRP transceiver through GNU Radio Software Defined Radio. This data signal modulated the laser signal in each MZM, which generated a modulated optical signal for each branch. Figure 5.10 shows the experimental setup and a picture of it.

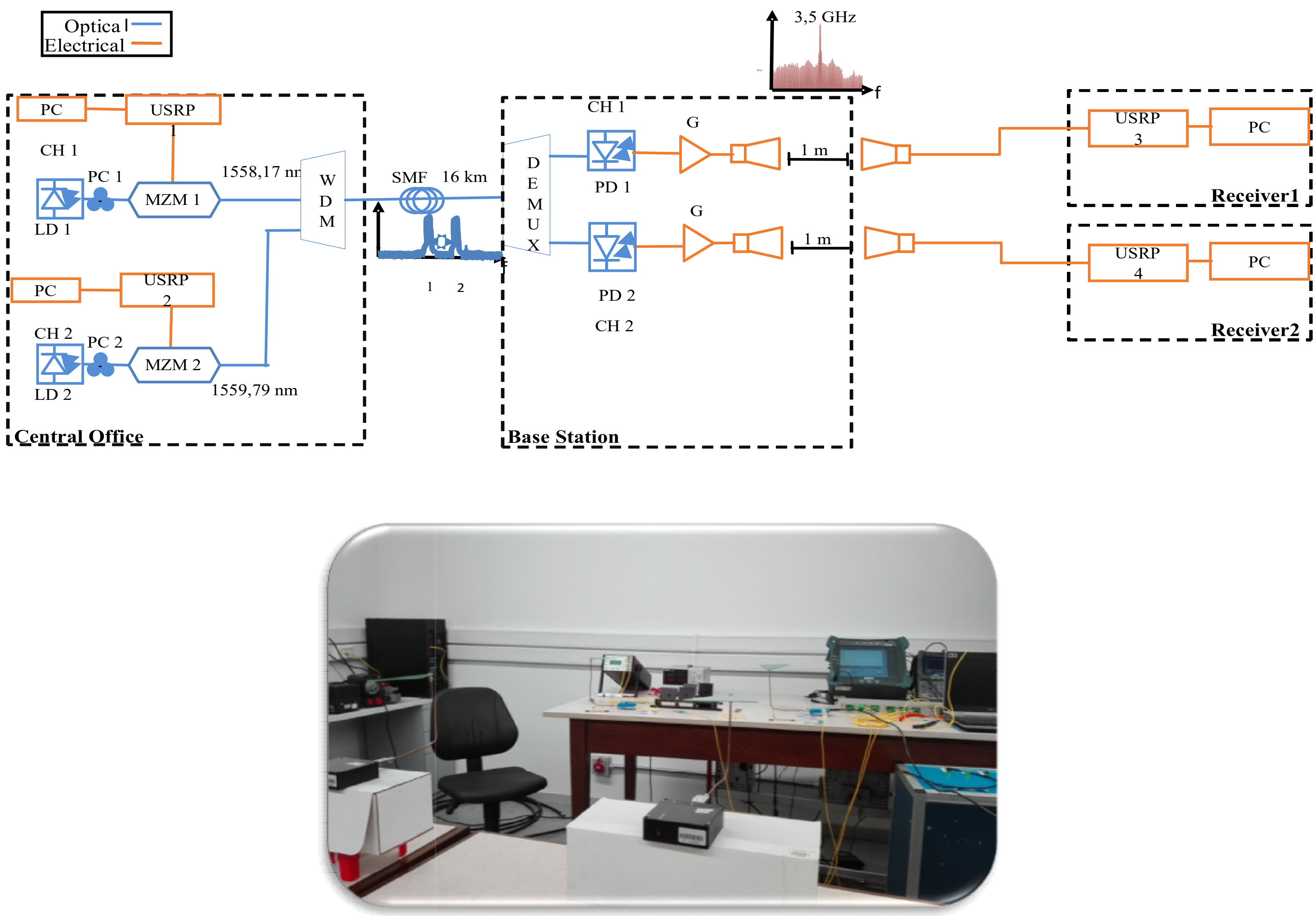

Fig. 5.10. Hybrid Wireless Optical Fiber WDM-PON Link:

In this experiment, two channels were used as a probe of concept, but it could be escalated to more channels, according to the number of Optical Network Users (ONU) of the network. Each signal from the MZMs was connected to a different channel of a Wavelength Division Multiplexing (WDM) device Padtec MDDC21041ST1. Then, the optical output line was joined to 16 km of Single Mode Optical Fiber (SMF). After the fiber, a demultiplexing device splits each signal simulating an Optical Distributed Network (ODN). The outputs, one for each channel, are linked to a high speed photodiode (PD). The photodiode converts the optical signal to the electrical domain, where the signal is boosted by a 30 dB electrical amplifier (PA) before wireless transmission over a distance of 1m.

A pair of LP09650 850 MHz to 6.5 GHz Log Periodic PCB directional antennae for each channel, at 5 dBi gain each, was used for the wireless transmission. At the receiver, the transmitted signal was amplified by a 20 dB fixed gain that was programmed by the USRP through GNU Radio. The RF signal was sent to a receiver USRP and to a PC SDR application to demodulate, storage and analyze the transmitted signals. As in the last experiments, Offline Digital Signal Processing (DSP) through Matlab was also used to measure the reliability in terms of BERs, and the procedure developed and shown before was used to measure the latency.

In the central office, we modulated the optical signal coming from the laser with a radio frequency signal that had the information packets and we sent each optical signal to the multiplexer. A pseudo-random binary sequence (PRBS7) was sent repeatedly through GNU Radio, which was in charge of making packages of 64 kB, codify and modulate the RF signal. We used Gaussian Modulation Shift Keying (GMSK) and Quadrature Phase Shift Keying (QPSK) to modulate the data signal at 1 Mbps and 2 Mbps. Two samples per symbol were fixed to obtain those data rates. In addition, we modified some parameters in the USRP, such as sample rate, gain, frequency and antenna selection. Table 5.3 presents the parameters established in the USRP.

Table 5.3. USRP Parameters

Parameter		Value
GMSK	Gain	35
	Sample Rate	2MSps- 4 MSps
QPSK	Gain Tx	35
	Sample Rate	2MSps- 1 MSps
Frequency		3.5 GHz
Antenna Selection		Transmission: Tx/Rx Port
		Reception: Rx Port

In the Base Station, after 16 km of optical fiber, we demultiplexed the signal and adapted it to the wireless media. At the end user, the signal was decodified, demodulated and data information was visualized using SDR. The USRP, by means of its FPGA, ADC and DAC, process the signal and adapt it again, so that the end user understands it through

GNU Radio. On average, 20.000 PRBS7 were received. Matlab, as mentioned before, is used to synchronize and quantify the BER in each channel.

5.4.2. Analysis of WDM-PON RoF links

Once the setup was configured, latency and BER were measured with the same procedures, since they are significant aspects in 5G networks. In this experiment, we evaluate if latencies required in Tactile Internet are achieved with optical multiplexing.

Figure 5.11., shows the latency in each channel with each modulation in two different data rates. It is important to remember the concept of end-to-end latency defined in this thesis, which is the sum of four components such as propagation time, transmission time, queuing time and processing delay [31].

a)

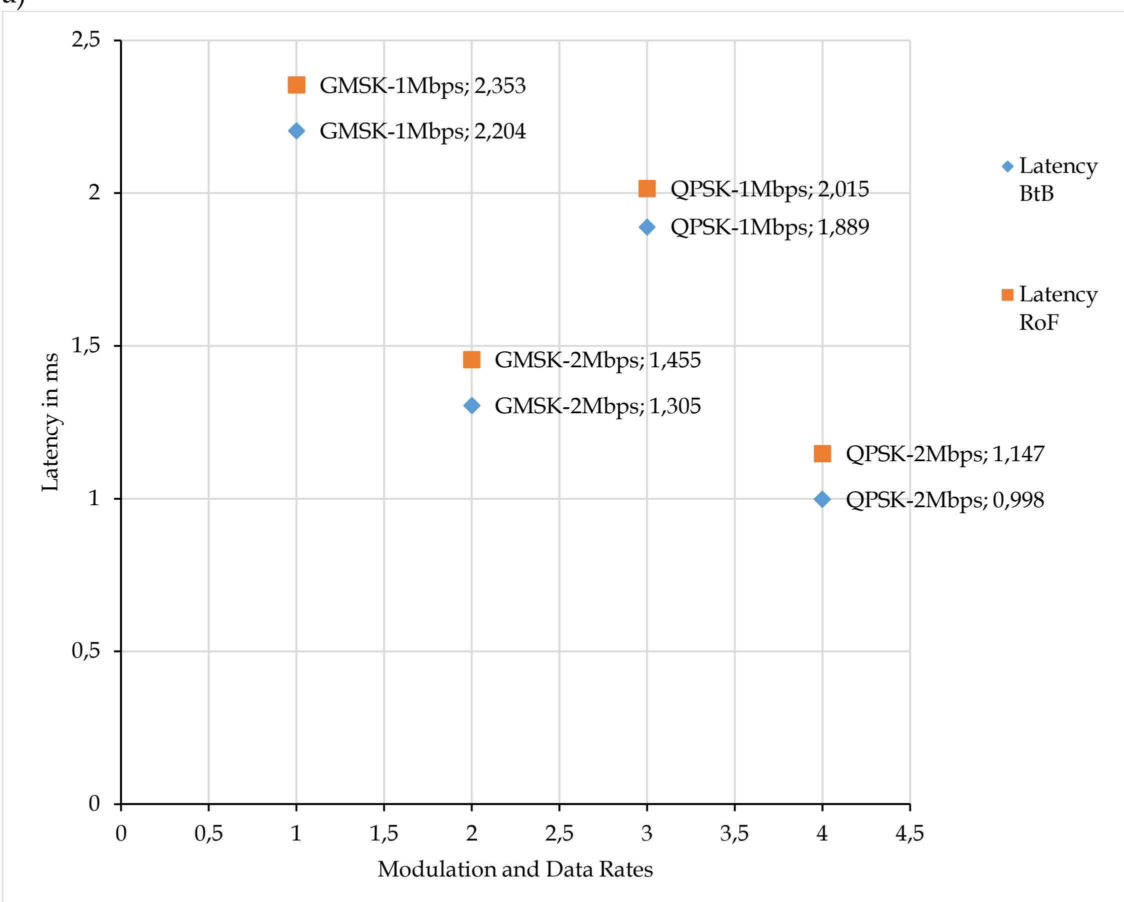

b)

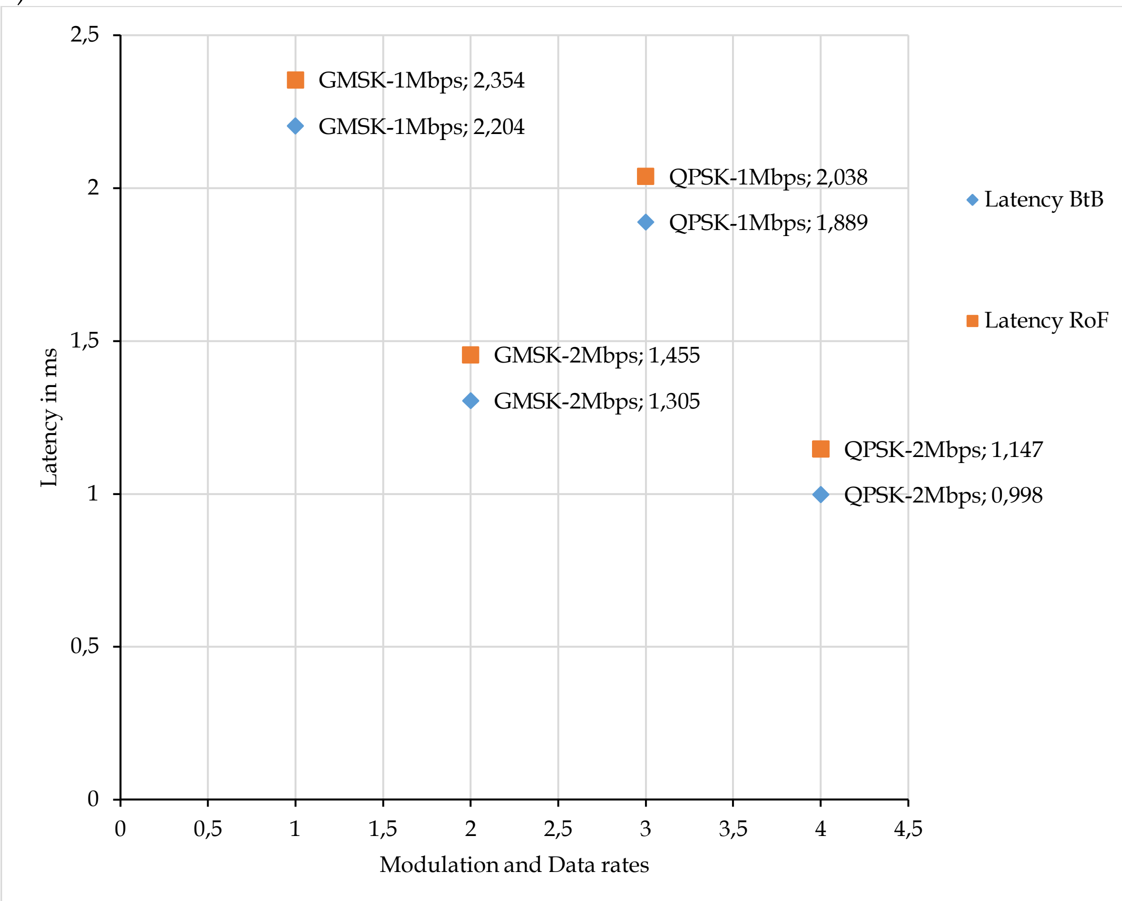

Fig. 5.11. Latency analysis WDM-PON RoF Link:
a) Channel 1, b) Channel 2

The X axis represents the modulation and the data rate. The Y axis describes the end to end latency in milliseconds. We present two measurements. The red diamonds represent the value measured only with the USRPs communicating each other by radio, separated by 1 meter of distance, which is back-to-back measurement. The orange squares represent the measurements performed taking into account all the setup described in the precedent section. In terms of latency, we achieved a minimum value of 1.14 ms for both channels with a QPSK modulation. The difference between both channels is in the order of ns. 1.14 ms, which fits with the requirements of the key performance indicators of 5G. Therefore, we demonstrated that WDM mixed with RoF and SDR is an optimal candidate that can be implemented in 5G networks.

In addition, the results show that the difference between back-to- back latency measurements and the Radio-over-fiber link is around 149 µs on average, where 78 microseconds belong to the transmission for the 16 km of optical fiber. Taking into account that the fiber used was 1550 nm single-mode, standard G652 with a refractive index of 1.4679. Equation 39 shows how can be calculated in theory the transmission time

Tx_{time}. In practice this time was measured sending a single tone and comparing the time between transmitted signal and received signal.

$$Tx_{time} = (distance * RI)/C \qquad (39),$$

where C is the speed of light ($3*10^8$ m/s) and RI is the Refractive Index (1.4679).

We showed also, that adding a WDM system does not affect significantly the latency and is very useful in terms of capacity and number of users connected to the network. The results indicate that we configured a low latency communication WDM-PON RoF for 5G networks.

Additionally, another requirement of 5G networks is the reliability communication to connect people and devices anywhere at any time. A well-known metric to measure reliability is the Bit Error Rate. WDM-PON Radio-over-fiber systems must have a bit error rate of 10E-09 on average, according to [184], [185].

Figure 5.12., shows the bit error rate for each modulation in each channel. The measurements were performed only for the bit error rate with the highest data rate achieved by the USRPs, which is the worst case in the experiment. As mentioned before, the bit error rate, as well as the total numbers of PRBS received in each channel, were measured using Matlab.

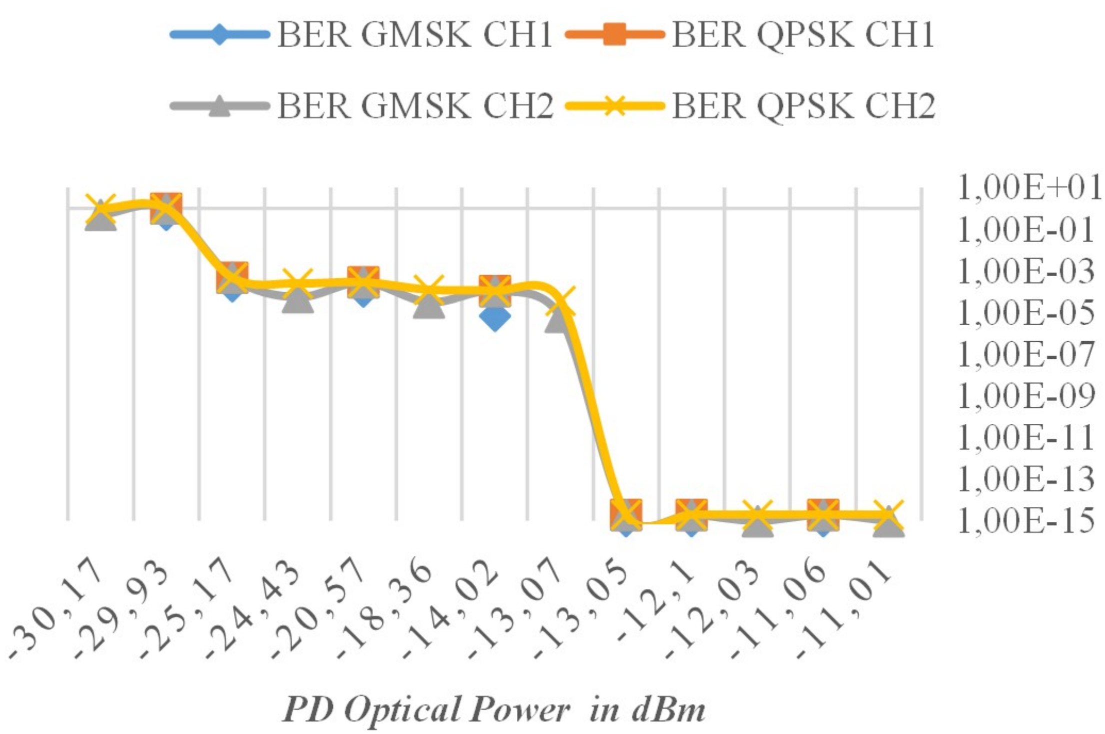

Fig. 5.12. Bit error Rate vs Photodiode Optical Power: a) Channel 1, b) Channel 2

The results of the DSP evaluation show that the modulation schemes with less processed bits per symbol have less errors than more advanced modulation schemes. In addition, when the optical power on the PD of the transmitter was over -13 dBm, we obtained error free in both modulation schemes. Then, both modulations techniques resulted in acceptable bit error rates from these optical power. When the modulation technique is high respect to the number of processed bits per symbol, less PRBS arrive completely.

As main conclusion, we demonstrated a WDM-PON Radio-over-fiber system using SDR with low latency and reliable. We took into account the requirements in terms of capacity, reliability, and we proved a system in the laboratory for Tactile Internet and 5G networks, which has high feasibility. We mixed several components such as those previously mentioned: Radio-over-fiber, WDM and SDR, in order to have a system devised for 5G networks.

Regarding latency, an important aspect to display is that it is an experiment where physical latency is being measured in real time. The value of latency obtained fitted in the requirements of the 5G networks. This means a breakthrough in the field because future networks demand this demonstrated type of communications.

5.4.3. WDM RoF Simulation

The simulations regarding WDM were made in Optisystem. These simulations were done to have other results in terms of system reliability in WDM RoF. For this reason, an analog system to that configured in section 5.4. was simulated. It is important to mention that this kind of software only allows to observe the behavior regarding Bit Error Rate, therefore it was not possible to simulate or measure the latency with this tool.

Figure 5.13., shows the setup configured in Optisystem, it has the same conditions used for building the experimental setup. Therefore, the system consists of two branches, where each one comprises a laser CW with the same wavelength and power as in the laboratory experiment. The output of this laser is modulated with an electrical signal, which has the same data rate and frequency as in the experiment in the laboratory. Through an MZM, both signals, optical and electrical, are modulated. The output of the two MZMs are launched to a WDM multiplexer. Then, the multiplexer output goes to 16 km of optical fiber simulating a WDM-PON system like the one developed experimentally. This signal is amplified and demultiplexed. Finally, each of the channels are driven to a photodetector. The photodected signal is used with the input signal to measure the BER.

Figure 5.14., displays the eye pattern of the two branches. It is important to mention that the system simulated is limited to only the optical part. For both BER analyzers, BER is 1.606E-18 for one branch and in the other branch is 1.528 E-21. Results show that both channels have a very good performance regarding BER.

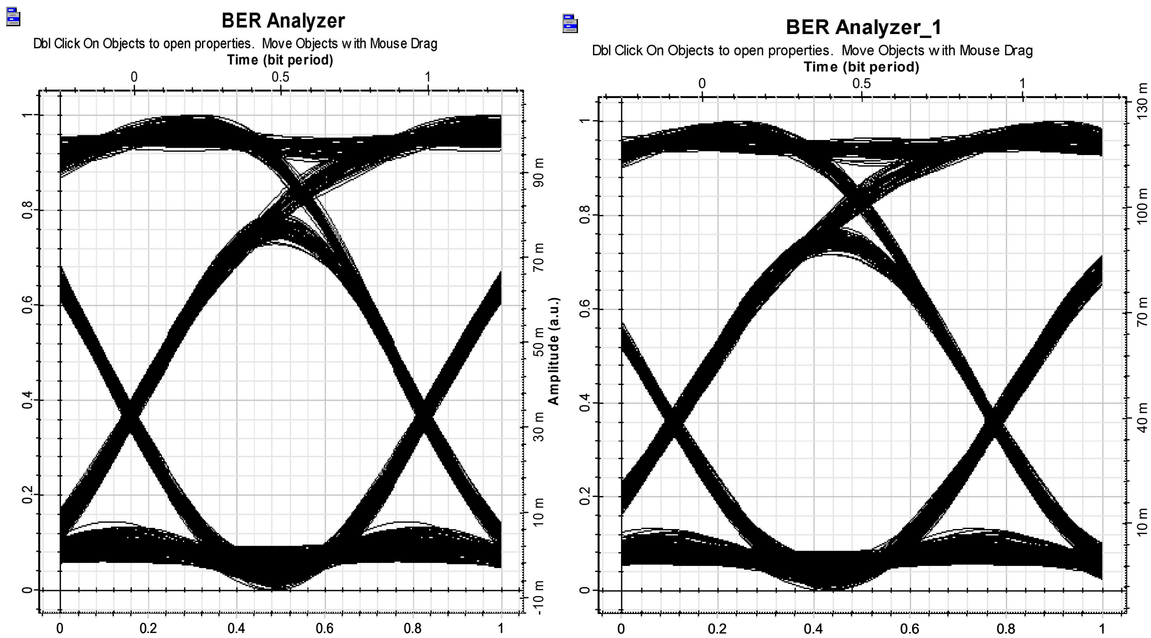

Fig. 5.14. BER WDM Eye Pattern

In order to simulate a real scheme with more than two users including WDM. New schemes were simulated in Optisystem which contemplates 20 kilometers of fiber and the use from two to sixteen channels in the multiplexer. In this way, we would have from 2 to 16 users in the WDM-PON network. For those system, the separation between channels were 0.81 nm, that is, 200 GHz, as shown in Figure 5.15 for 8 outputs of the multiplexer. It is important to mention that those systems were made taking into account the real wavelength data that the WDM equipment used in the previous experiment had.

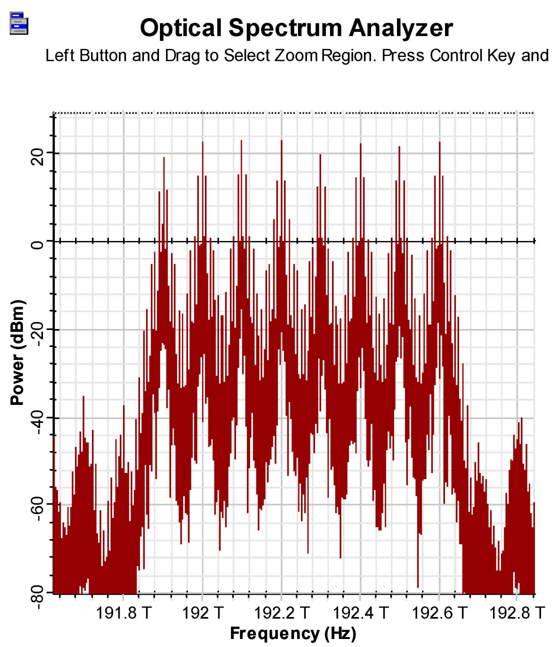

Fig. 5.15. WDM RoF Optical Spectrum

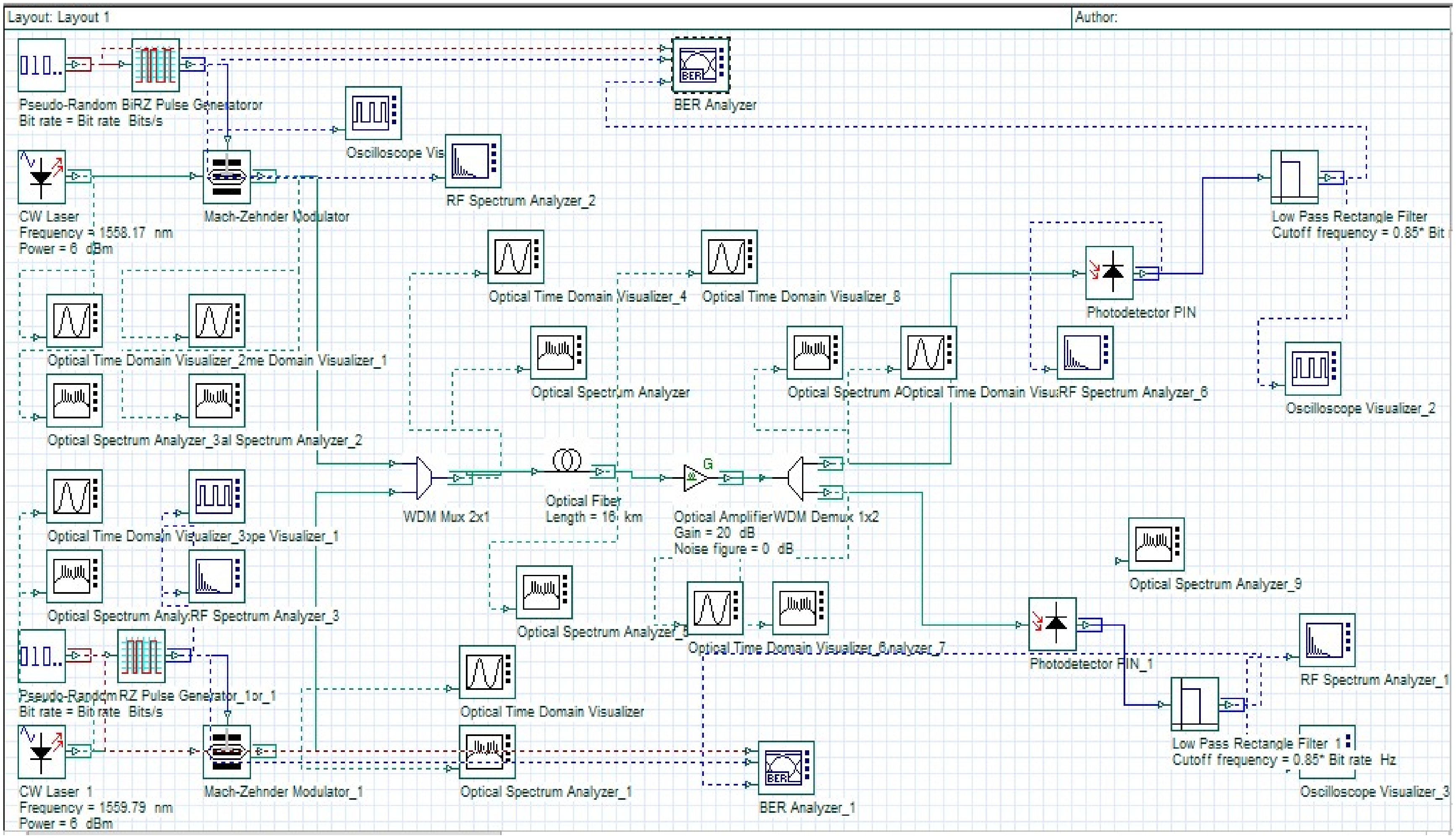

Fig. 5.13. WDM RoF with 2 users simulation

The optical power of the lasers is the same, 6 dBm for each laser by channel, in each channel the modulation of the electrical signal employed was On-Off keying. Figure 5.16 shows a screenshot of WDM*8 Optisystem simulation as an example of the simulations made in optisystem, it is important to mention that it was used the same configuration for two, four, six, eight and sixteen users. Finally Figure 5.17., shows the worse eye patterns for each system (WDM*2 outputs, WDM*4 outputs, WDM*6 outputs, WDM*8 outputs and WDM*16 outputs). The results describe that even transmitting through all the eight channels and increasing the distance of the optical fiber, the bit error rate is approximately 1*E-11 for all the systems from two to eight outputs, which means that this kind of system allows more users with a reasonable BER. Nonetheless, when the system has 16 outputs, the worse BER is 1E0, which means that this system it is not suitable for 16 users. Finally, Figure 5.18., shows the BER for the worse case in each system varying the number of output of the multiplexer.

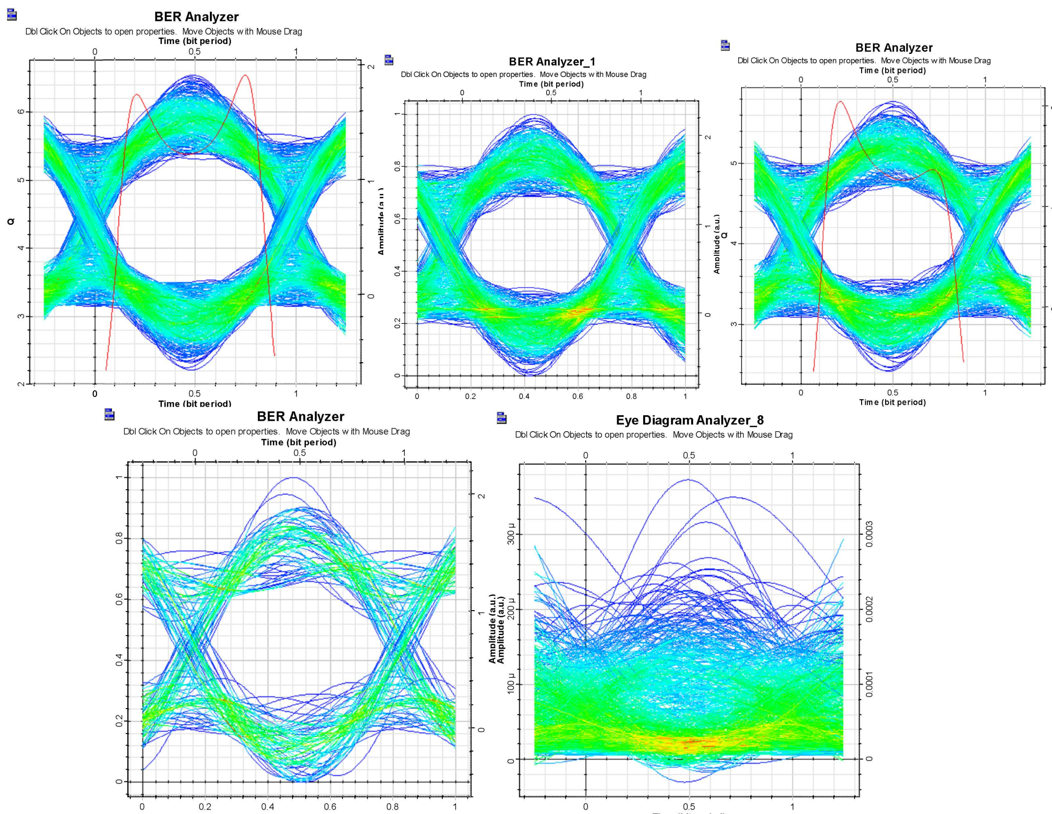

Fig. 5.17. BER WDM RoF Eye pattern from 2 to 16 output

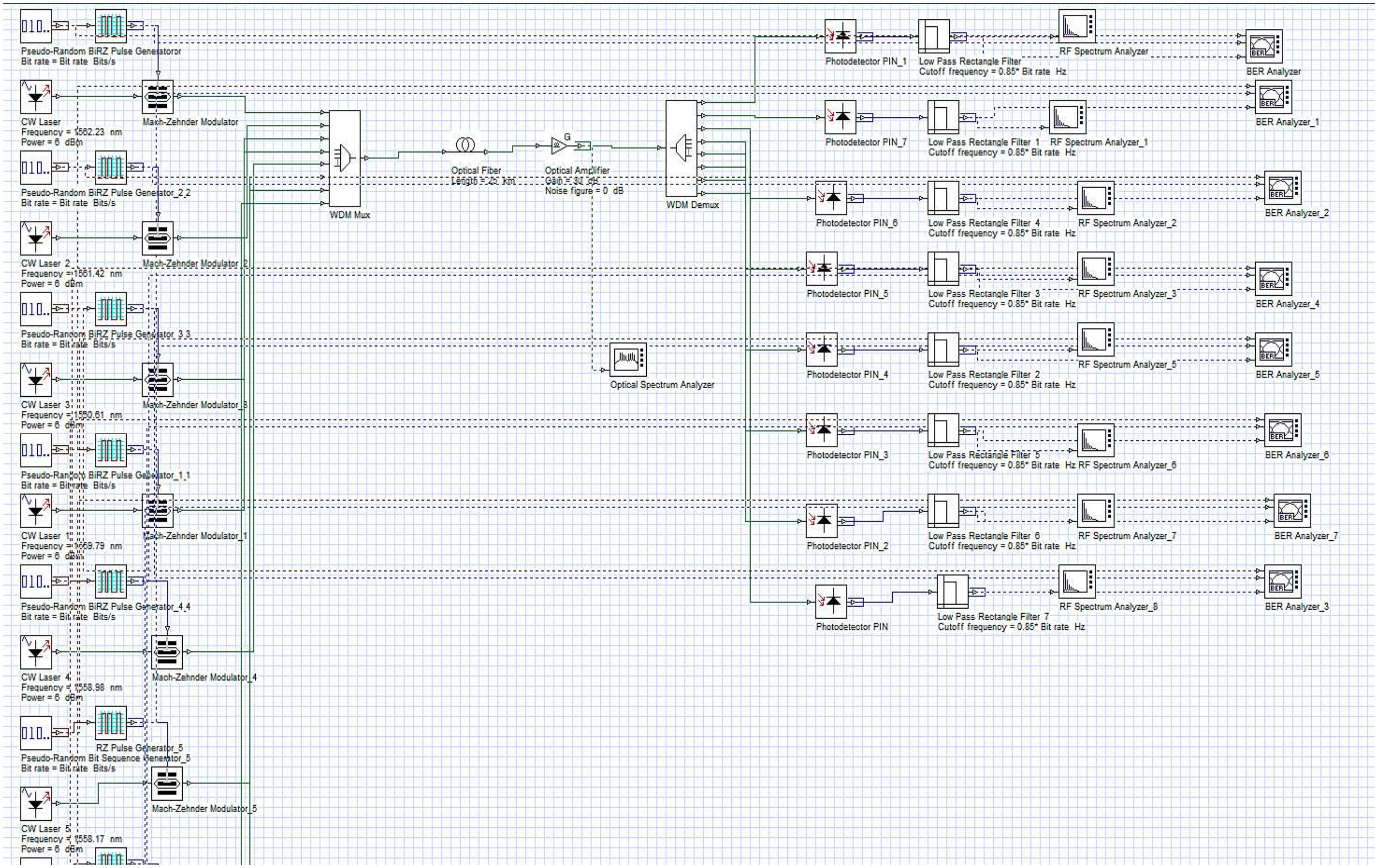

Fig. 5.16. WDM RoF with 8 users simulation

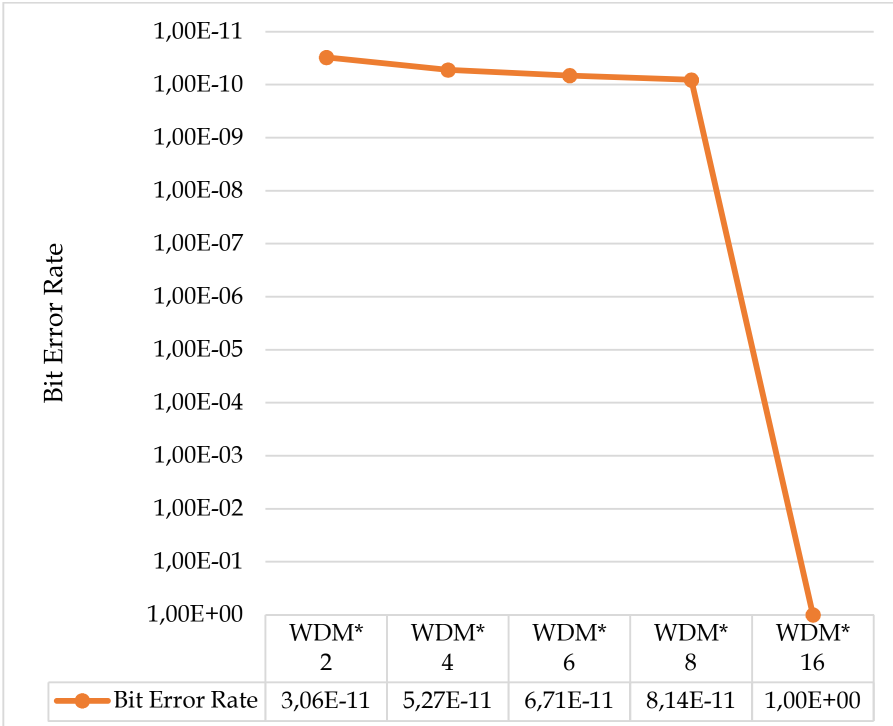

Fig. 5.18. BER Vs WDM outputs

5.5. OFDM and UFMC Simulation

In order to compare different multiplexing schemes, some simulations such as OFDM and UFMC were performed regarding SER (Symbol Error Rate) vs SNR (Signal to Noise Ratio). In Appendix D, there are the main results of a work developed in [186], which is derived from this PhD Thesis.

6. CONCLUSIONS AND FUTURE WORK

6.1. Conclusions

This PhD Thesis was developed mainly in Telecommunications and High Frequency (CMUN) Research Group of the Universidad Nacional de Colombia and had a special collaboration of the Metro Access and Short Range Systems Research Group of the Department of Photonics Engineering of the Technical University of Denmark DTU.

Throughout this thesis, the state of the art of hybrid Fiber-Wireless links has been expanded, disaggregating and defining each of its parts as the central station, the base station, the wireless transmission and the wireless receiver. In chapters 2 and 3, the basic concepts of the Radio over Fiber systems and latency were described and the latency concept that would be used in the experiments was defined in order to to achieve a research of how to implement hybrid links with low latency.

The main objective of this thesis was to validate experimentally a hybrid optical Fiber-Wireless link that had 1 ms latency, taking into account the system requirements to support Tactile Internet. The first challenge was to find an adequate procedure to measure latency in hybrid networks in the laboratory. Therefore, the main contribution of this work was to develop a procedure to measure latency, including software defined radio as a mean to measure latency and to generate data signal. In this way, the modulation and multiplexing techniques were varied and measured in order to achieve 1 ms latency in hybrid Fiber-Wireless communications.

In order to measure the delay contribution from individual elements in the W-band hybrid system, and estimate the overall system latency, identifying potential sources of delay, a real-time transmission with low complexity in W-band was demonstrated. Additionally, the potential in the generation of mmw links was evidenced and latency and Bit error Rate for these systems were measured.

It is important to mention that due to the hardware, specifically the USRP used in each of the experiments, it was not possible to increase the data rate. However, theoretically it is known that if the data rate is increased, the latency decreases. The selection of the electrical modulation of the signal affects the latency in the system, this was identified as a potential source of delay in all the experiments. The lowest latency achieved in the W-band experiment was approximately 2 ms using the QAM16 modulation. In chapter 4 each delay according to the latency definition was presented.

Three experiments were analyzed where the multiplexing and modulation of the electrical signal and the optical signal were varied in two different frequency bands. Despite the fact that the first experiment was performed in another frequency band, and another USRP equipment was used for the WDM experiment, the procedures to measure BER and latency were standardized and used in the same way in all the experiments. For this reason, it is possible to perform a compilation in terms of reliability in terms of Bit Error Rate and other comparison in terms of latency, taking into account the modulations and multiplexing format of the electrical signal and the optical modulation techniques.

It can be concluded that with the experiments in which the multiplexing of the electrical signal was varied, more latency was obtained than in the experiment where the optical multiplexing WDM was included. Using the same modulation of the electric signal QPSK with the GFDM multiplexing, 1.3 ms was obtained while 1.7 ms was obtained with the OFDM multiplexing.

By including WDM with the same modulation of the electrical signal QPSK, the lowest latency of this work was obtained, which was 1.1 ms with the hybrid system, achieving a Fiber-Wireless system that supports tactile internet with 1 ms of latency.

On the other hand, measurements were made of only the wireless system vs the hybrid system and it was shown that in all the experiments the latency was not greatly affected when changing the transmission system. It can be concluded that the combination of photonics in hybrid mmw links allows to take advantage of the best of both worlds and is an enabler of the fifth generation (5G) networks as well as Tactile Internet.

In terms of Bit Error Rate (BER), all the experiments carried out included measurements in order to know how reliable the systems were. It can be concluded that BER increases with increasing M-ary modulation scheme of the electric signal. In general, all the experiments achieved a Bit Error Rate that matches with the 5G key performance.

Finally, it is important to mention that a significant contribution of this thesis is to include Software-Defined-Radio as an enabler of microwave photonics technology. The importance of including and using SDR in hybrid systems is the possibility to use reconfigurable radios or transceivers in the future. Therefore, this thesis showed that it is possible to have hybrid systems mmw that can include cognitive radio in the future.

6.2. Future Work

Regarding future work, it is important to mention that in Colombia, the hybrid Fiber-Wireless links have been very little researched compared to global tendencies. Therefore, everything related to promoting Microwavephotonics in Colombia can be considered as future work. Since Radio over Fiber is new in this country it is possible to investigate how to apply this technology in all IoT and 5G applications in Colombia. Hence, this becomes a challenge to appropriate and promote research in this field in my country.

Concerning to the PhD thesis future work, the following research lines are proposed to give continuity to this work. First, it is proposed to evaluate the same system described, with more than one base station. And over this system measure latency and Bit Error Rate. In this way, it will be established how much delay adds to the system when the signal jumps from one base station to another, and this will simulate a mobile 5G network or a fixed wireless network.

Second, it is proposed to use other FPGAs to increase the data rate. The hardware used in this work belongs to National Instruments, but there are FPGAs from other providers, which can achieve higher data rates. In addition, it is proposed to create an interface that allows to continue using Software Defined Radio, by programming them, for example, with Labview. At the same time, it is proposed to use SDR to generate reconfigurable transceivers that can be mixed with radio-on-fiber hybrid links.

Third, regarding modulations and multiplexing formats, it is proposed to analyze new multiplexing schemes such as non-orthogonal multiple access (NOMA) for cellular future radio access. In the same way, it is proposed to combine electrical multiplexing and optical signal in order to measure its latency and reliability.

Finally it is proposed to configure the most important findings of this work and introduce them into integrated photonics, in order to investigate how SDR can be mixed with Radio over Fiber in a photonic integrated circuit.

Publications and Research Internships

Publications results of this thesis

As results of this work 2 journal papers were published and 3 participation in conference proceedings were presented. In addition, it was presented a poster as non-archive paper in the IEEE Photonics Conference. Below are described the titles respectively.

- ✓ **Rico-Martínez Mónica**, Jesús Álvarez Guerrero, Ferney Amaya, Tafur Monroy Idelfonso, Varón Margarita. Latency and reliability measurements for a 3.5 GHz Optical-Wireless WDM-PON network using SDR. IEEE Photonics Conference. Virginia 2018.

- ✓ **Monica Rico-Martinez**, Christian Camilo Cano-Vasquez, Santiago Isaac Rodriguez, Margarita Varon-Duran, Idelfonso Tafur Comparison of Performance Between OFDM and GFDM in a 3.5Ghz Band 5g Hybrid Fiber-Wireless Link Using SDR. Microwave Photonics Conference. Toulouse 2018.

- ✓ J.D. Cepeda, S. I Rodrıguez, C.D. Muñoz, **M. Rico-Martinez**, M. Varon, and I. Tafur Monroy, “Performance Evaluation of a real time OFDM Radio Over Fiber System at 2.5 GHz using Software Defined Radio SDR” in International Microwave and Optoelectronics Conference (IMOC), 2017.

- ✓ **M. Rico-Martinez**, A. Morales, V. Mehmeri, R. Puerta, M. Varon, and I. Tafur Monroy, “Latency analysis on W-Band Radio over Fiber links” in 2017 IEEE Photonics Conference (IPC 2017-non archive poster).

- ✓ **M. Rico-Martinez**, A. Morales, V. Mehmeri, R. Puerta, M. Varon, and I. Tafur Monroy, “Latency concept and how to measure it in emergent networks” in Redin, Faculty of Engineering Journal, 2018.

- ✓ **M. Rico-Martinez**, A. Morales, V. Mehmeri, R. Puerta, M. Varon, and I. Tafur Monroy “Procedure to measure real time latency using software defined radio in W-Band Fiber-Wireless link,” in Microwave and Optical Technology Letters, 2017.

Research Internships

In addition, two international research internships were performed. On the one hand, in 2015, I was one year in the Metro Access research group at the Department of Fotonik, Technical University of Denmark (DTU, Kgs. Lyngby, Denmark), for one year. On the other hand, I was two months at the Institut Supérieur de l'Aéronautique el de L'Espace (ISAE) - Supaero, Department of Electronic Optronic and Signal (DEOS). Furthermore, I made the last experimental part of the presented work, at the Universidad Pontificia Bolivariana (Medellin- Colombia). All the internships were fundamental pieces in the experimental development of this thesis. It was also very important to make connections with others research groups both in Colombia and in others countries around the world.

Related Products

Other products results of this research are listed below:

- Internal project of National University of Colombia (Código Hermes: 25364 "Modelo para orientar la optimización de las redes radio sobre fibra de última milla mediante el estudio de los parámetros de multiplexación, modulación y asignación de ancho de banda")
- 2 works of undergraduated students:
    - Cepeda Juan David, "Comparación de dos técnicas de generación de forma de onda OFDM y UFMC para un enlace de LTE sobre fibra óptica" 2016
    - Cabrera Ojeda Daniel, "Diseño e implementación de un enlace de RoF entre un vehículo y una estación base para la transmisión en tiempo real de datos de internet, multimedia y localización". 2019

Appendix A. USRP N210 and B205 Datasheet

1. USRP N210 [187]

The Ettus Research™ USRP™ N200 and N210 are the highest performing class of hardware of the USRP™ (Universal Software Radio Peripheral) family of products, which enables engineers to rapidly design and implement powerful, flexible software radio systems. The N200 and N210 hardware is ideally suited for applications requiring high RF performance. Such applications include physical layer prototyping, dynamic spectrum access and cognitive radio, spectrum monitoring, record and playback, and even networked sensor deployment. The Networked Series products offers MIMO capability with high bandwidth and dynamic range. The Gigabit Ethernet interface serves as the connection between the N200/N210 and the host computer. This enables the user to realize 50 MS/s of real-time bandwidth in the receive and transmit directions, simultaneously (full duplex).

Fig. B.1. USRP N210[187]

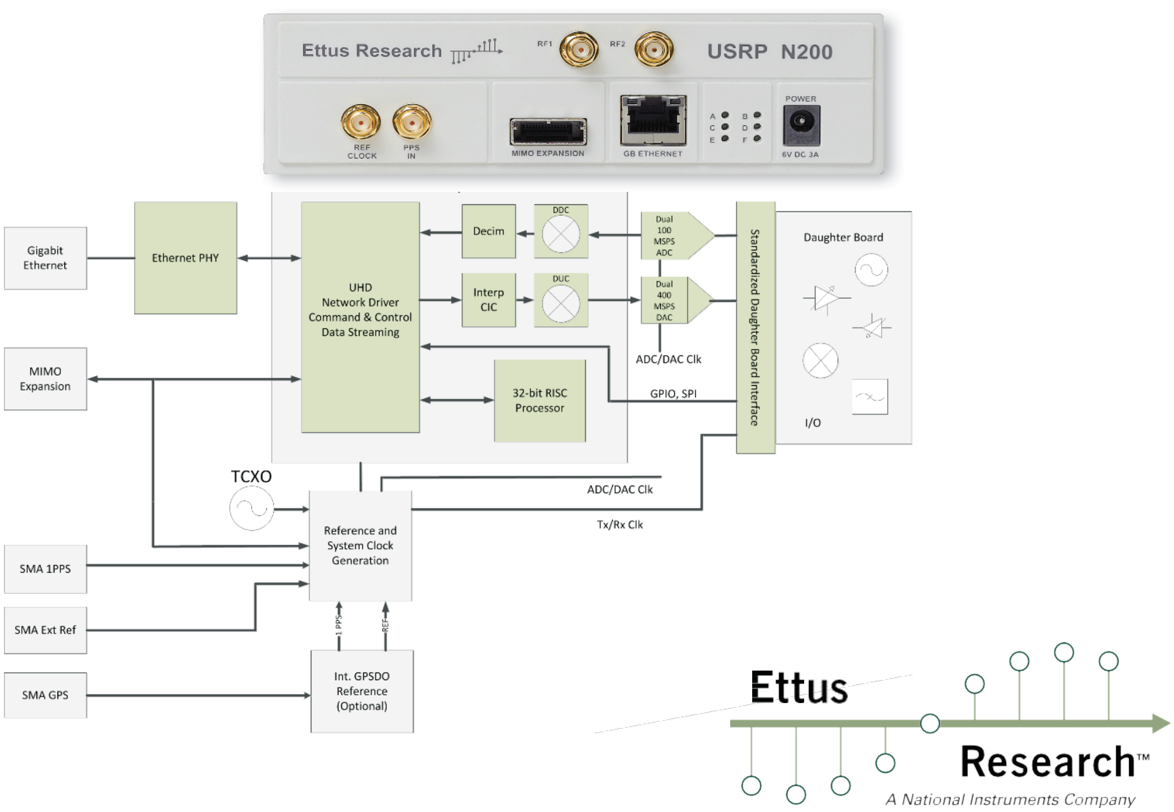

The Networked Series MIMO connection is located on the front panel of each unit. Two Networked Series units may be connected to realize a complete 2x2 MIMO configuration using the optional MIMO cable. External PPS and reference inputs can also be used to create larger multi-channel systems. The N200 and N210 are largely the same, except that the N210 features a larger FPGA for customers that intend to integrate custom FPGA functionality. The USRP Hardware Driver™ is the official driver for all Ettus Research products. The USRP Hardware Driver supports Linux, Mac OSX, Windows.

2. USRP B205[188]

The USRP B200mini Series delivers a 1x1 software defined radio/cognitive radio in the size of a business card. With a wide frequency range from 70 MHz to 6 GHz and a user-programmable Xilinx Spartan-6 FPGA, this flexible and compact platform is ideal for both hobbyist and OEM applications. The RF front end uses the Analog Devices AD9364 RFIC transceiver with 56 MHz of instantaneous bandwidth. The board is bus-powered by a high-speed USB 3.0 connection for streaming data to the host computer. The USRP B200mini Series also includes connectors for GPIO, JTAG, and synchronization with a 10 MHz clock reference or PPS time reference input signal. There are three configurations in this product family with options for a larger or industrial-grade FPGA. The USRP Hardware Driver™ (UHD) software API supports all USRP products and enables users to efficiently develop applications then seamlessly transition designs between platforms as requirements expand.

Fig. B.2. USRP B205[188]

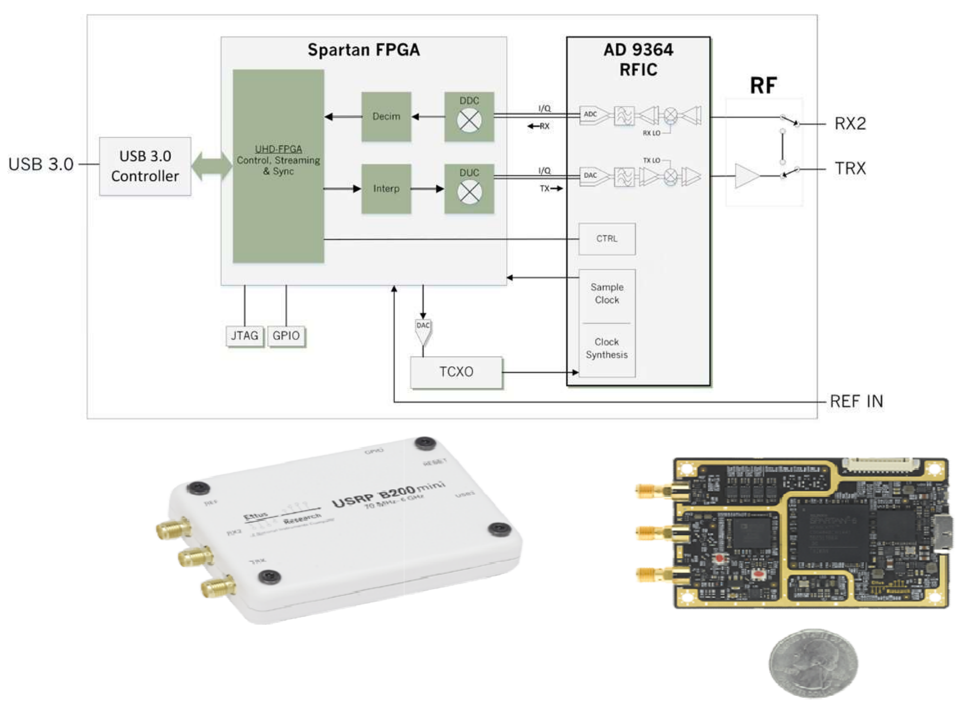

Appendix B. Matlab Code to measure BER

```
clear all; close all;

prbs7=load('PRBS7tx.txt');
prbs_size=length(prbs7);
rx_temp=load('recepcion16qam200-8');
[m n] = size(rx_temp);
tx=repmat(prbs7,[floor(m/128), n]);

rx=rx_temp(1:length(tx));

Matrix=NaN(length(tx), 3);
Matrix(:,1)=tx;
Matrix(:,2)=rx;
Matrix(:,3)=double(xor(tx,rx));

% rx_test=rx(43692:65535);
% tx_test_temp=repmat(prbs7, [floor(21844/128)+1, 1]);
% tx_test=tx_test_temp(1:length(rx_test));
%
% rx_test = circshift(rx_test,-finddelay(tx_test,rx_test));

[index z]=find(rx>1.5);
index_aux=[1;index+1;length(rx)];
delay=0;

for ii=1:length(index_aux)-1
  rx_aux_temp=rx(index_aux(ii):index_aux(ii+1)-2);
  NPRBS=floor(length(rx_aux_temp)/prbs_size);

  tx_aux=prbs7;
  rx_aux=rx_aux_temp(1:prbs_size);

  delay_aux(ii,1)=finddelay(tx_aux,rx_aux);
  delay = [delay; finddelay(tx_aux,rx_aux)];

  datarx = circshift(rx_aux,-finddelay(tx_aux,rx_aux));
  numerror(ii, 1) = sum(double(xor(tx_aux,datarx)));
  numbits(ii, 1) = length(rx_aux);

  for jj=2:NPRBS
```

```
    if ii==4 & jj==170
        %
    end

    rx_aux=rx_aux_temp(prbs_size*(jj-1)+1:prbs_size*(jj-1)+prbs_size);

    delay_aux(ii,jj)=finddelay(tx_aux,rx_aux);

    datarx = circshift(rx_aux,-finddelay(tx_aux,rx_aux));

    MatrixB=NaN(length(tx_aux), 3);
    MatrixB(:,1)=tx_aux;
    MatrixB(:,2)=datarx;
    MatrixB(:,3)=double(xor(tx_aux,datarx));

    delay = [delay; finddelay(tx_aux,rx_aux)];

    numerror(ii,jj) = sum(MatrixB(:,3));
    numbits(ii,jj) = length(rx_aux);

  end

end

  [m, n] = size(delay_aux);
  mask = ones(m,n);
  for ii=1:m
    for jj=2:n
        if delay_aux(ii,jj) ~= delay_aux(ii,jj-1)
            mask(ii,jj)=0;
            mask(ii,jj-1)=0;
        end
    end
  end

  numerrorF=mask.*numerror;
  numbitsF=mask.*numbits;
  Finalnumerror=sum(sum(numerrorF));
  Finalnumbits=sum(sum(numbitsF));
  BER=Finalnumerror/Finalnumbits;
```

Appendix C. GNU Radio Multiplexing Schemes

1. GFDM

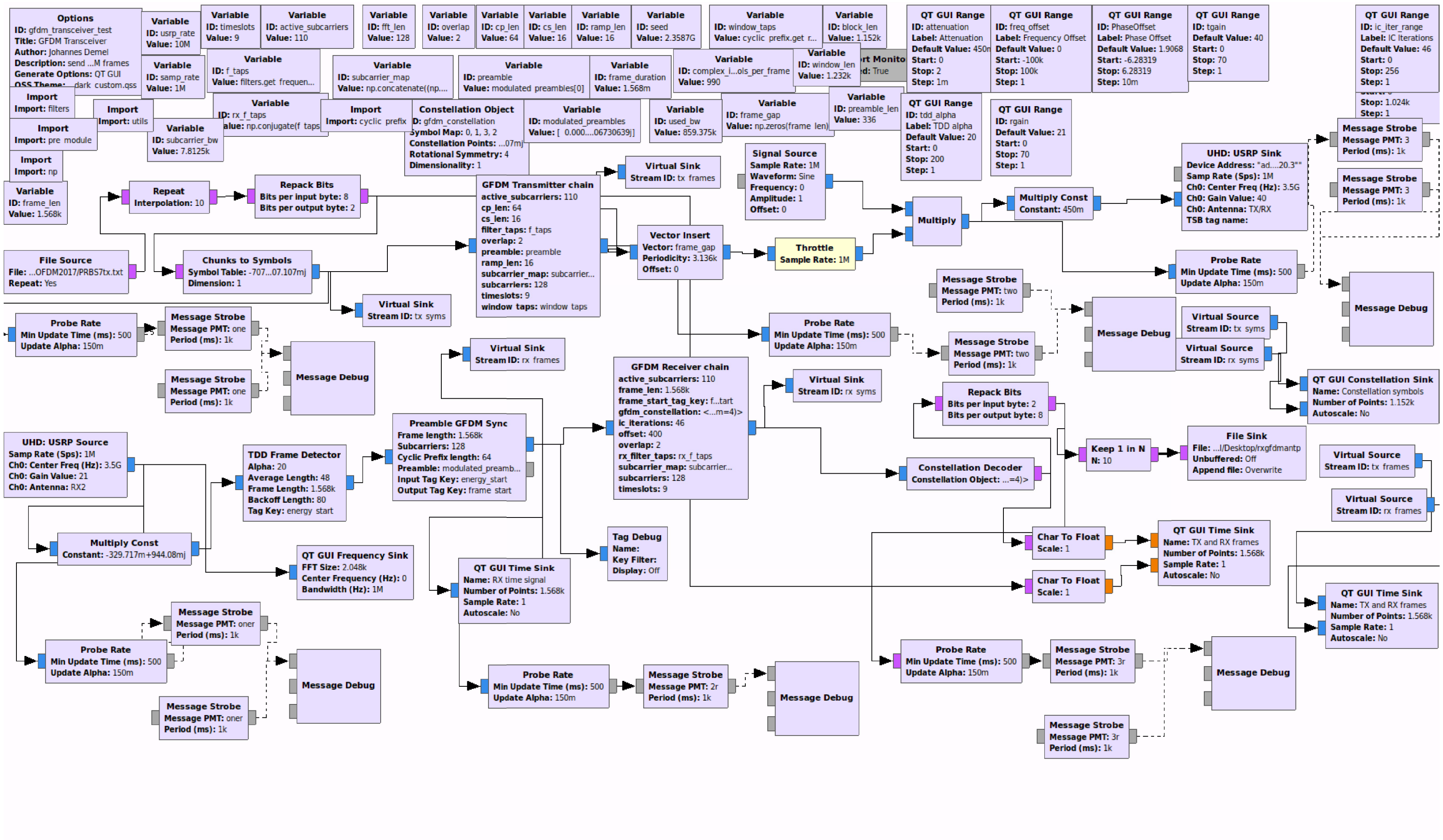

2. OFDM

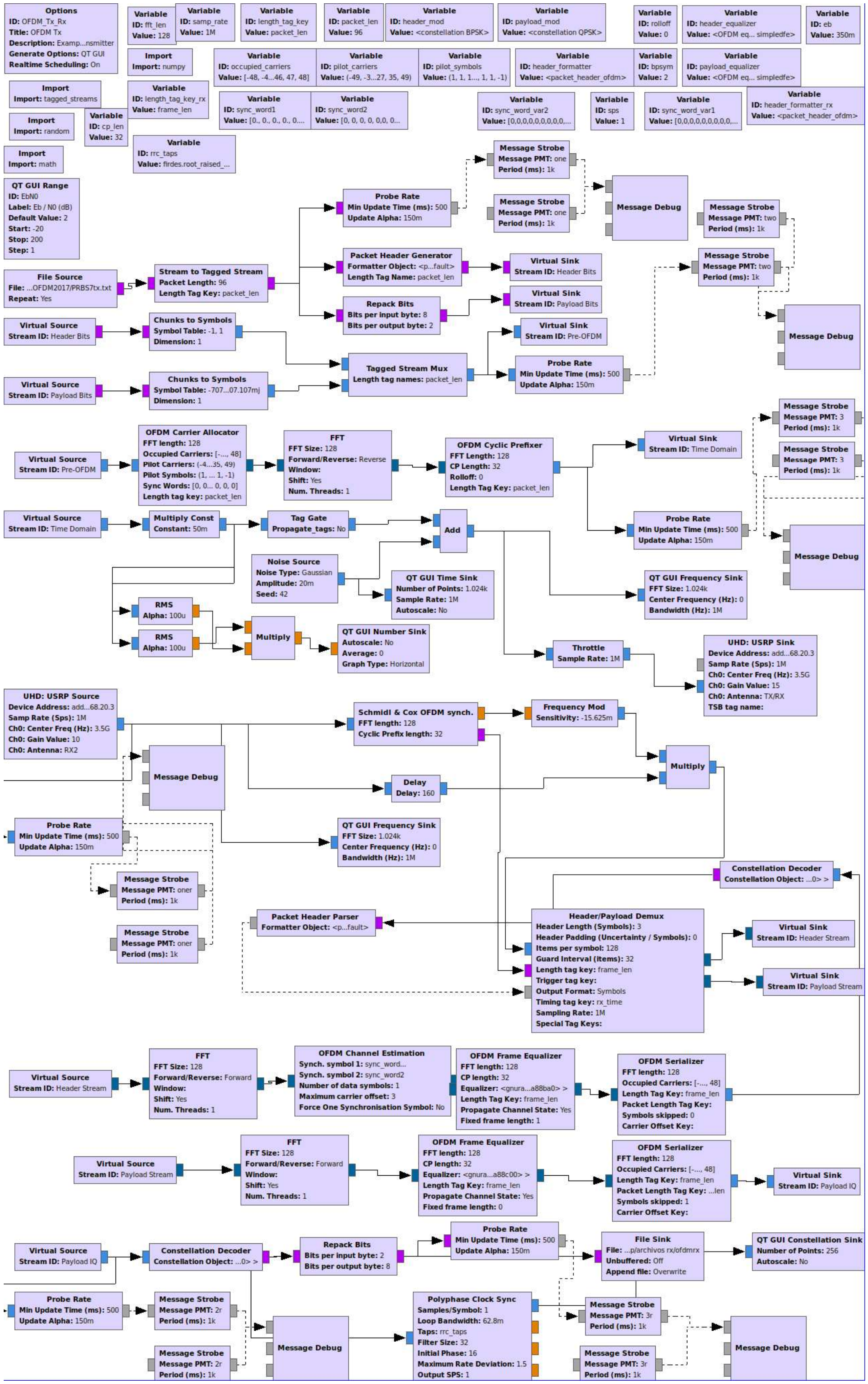

Appendix D. OFDM and UFMC Simulation

The simulations of comparison between OFDM and UFMC were made in Matlab, and they were based on the script provided by Alcatel - Germany, which includes the functionality of a transceiver of OFDM and UFMC[189]. This section presents the simulations parameters, the modeling of the channel, the measurement of the SER vs SNR, as well as the main results and conclusions of the simulations.

1. Simulation Parameters

It was necessary to define parameters that would allow a similarity of the systems. It is important to mention that this simulations were made taking into account an LTE system, then the parameters selected are for a LTE RoF link. The LTE standard establishes a series of FFT size and sampling rates for each bandwidth. In this case, an FFT value of 1024 was chosen for the simulation, which allows up to 1024 information subcarriers. Table D.1 shows the parameters chosen for both multiplexing schemes.

Table D.1. OFDM and UFMC Parameters

a) OFDM Parameters

OFDM		
Parameter	Symbol	Value
FFT size	N	1024
Modulation		QPSK
Bits per symbol	M	2
Filter length	LFIR	1
Cyclic prefix	CP	73
TTI number	NTTI	100
Symbols per TTI	NsymsperTTI	14

b) UFMC Parameters

UFMC		
Parameter	**Symbol**	**Value**
FFT size	N	1024
Modulation		QPSK
Bits per symbol	M	2
Filter length	LFIR	73
Number of bands	PRB	10
Carriers per band		12
TTI number	NTTI	100
Symbols per TTI	NsymsperTTI	14

The number of subcarriers used directly influences the efficiency of the system, for the simulations made, thus only 120 subcarriers were used. The digital modulation format chosen was QPSK, which transmits two bits per symbol. Additionally, LTE interval guard is chosen as 7% of the size of the FFT, therefore the length of the cyclic prefix is 73. The TTI parameters (Transmission Time Interval) were chosen for transmitting a predicted amount of information.

2. Channel Model

In this simulation, an AWGN channel model that describes a White Gaussian Noise is used. The noise signal is represented through a matrix of the size of the OFDM or UFMC symbol and the number of symbols to be transmitted per TTI.

The function *randn* of Matlab was used to generate the matrix of Gaussian distribution, as indicated in the next equation:.

$$n = nvar * \frac{1}{\sqrt{2}}\big(randn(N + CP, Nsyms)\big) + i * \big(randn(N + CP, Nsyms)\big) \quad (1),$$

where $nvar$ is the number of variables and is a noise factor that establishes the amplitude of the random variable, N is the FFT size, CP is the cyclic prefix and $Nsyms$ is the number of symbols per TTI, defined in the previous tables. This matrix is created in each cycle. In addition, the noise factor is determined by $nvar$, which is obtained from the SNR cycle. Then, the signal n, which represents the noise of the channel is added to the transmission signal.

3. SNR and SER evaluation

The evaluation of the SNR and the SER are carried out simultaneously in each decoding cycle of the signal. Regarding the estimation of SNR, it consists of two parts. First, we assigned a value of SNR in the outer cycle of the cycles according to criteria such as typical values of SNR used in communications. This SNR value defines the variable $nvar$ previously mentioned and can be derived by:

$$nvar = \frac{1}{\sqrt{10^{0.1*SNR}}} \quad (2),$$

It can be observed that at a higher signal-to-noise ratio, this factor of noise will be much smaller, thus the signal will be less affected.

Second, the other part of the SNR estimation is given by the energy of bit known as Eb. This energy is derived directly from the OFDM or UFMC symbols in time. The energy of each symbol is obtained with the multiplication of the transmission matrix by its transpose and obtaining the positions of the diagonal. Then, it is normalized according to the number of bits per digital symbol and the number of subcarriers used.

Finally, for the estimation of SER, a matrix is created for recording the errors as an account of the times in which a symbol is different from the original ones. Another matrix called *SymErr* keeps in each column the error for each SNR level.

4. Results

Figure D.1., shows the spectrum of the OFDM and UFMC signal. Red line is the UFMC spectrum and blue line is the OFDM spectrum. It can be observed that there is a great difference in the drops of the spectrum, once the number of subcarriers used has been completed. In the case of UFMC, the fall is much more pronounced than in OFDM due to the presence of the filter that is implemented per sub-band.

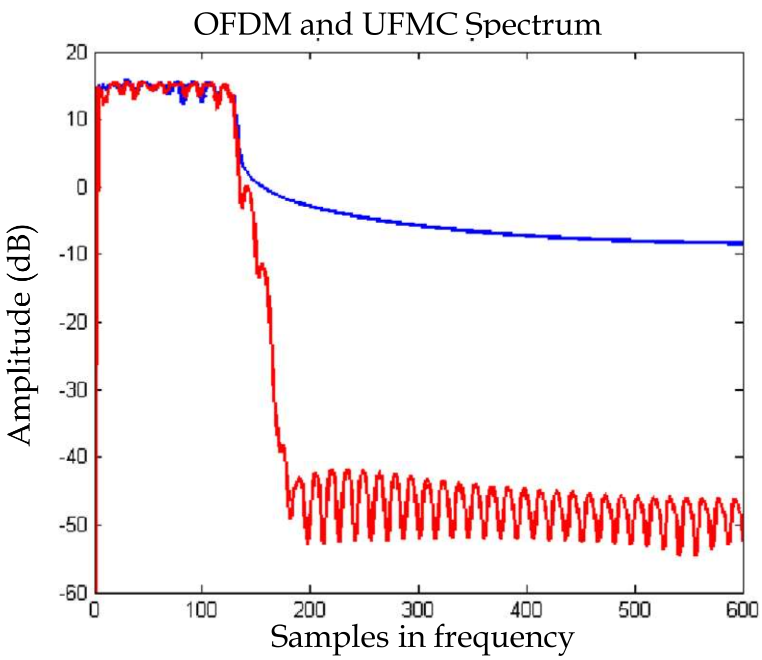

Fig. D.1. OFDM and UFMC Spectrum
Source:[186]

However, UFMC has an advantage over OFDM, because in each band, this pronounced fall, means a considerable reduction of the interference between sub-bands. This is very important, because in LTE, these sub-bands exist and are called Physics Resource Blocks, which provide services to different users.

FigureD.2 (a) shows the representation of the OFDM symbol in time. The red sections are the repetition of the final part of the symbol at the beginning. Similarly, Figure D.2 (b) shows UFMC in time, where the sections in red color indicate a slight transition between symbols.

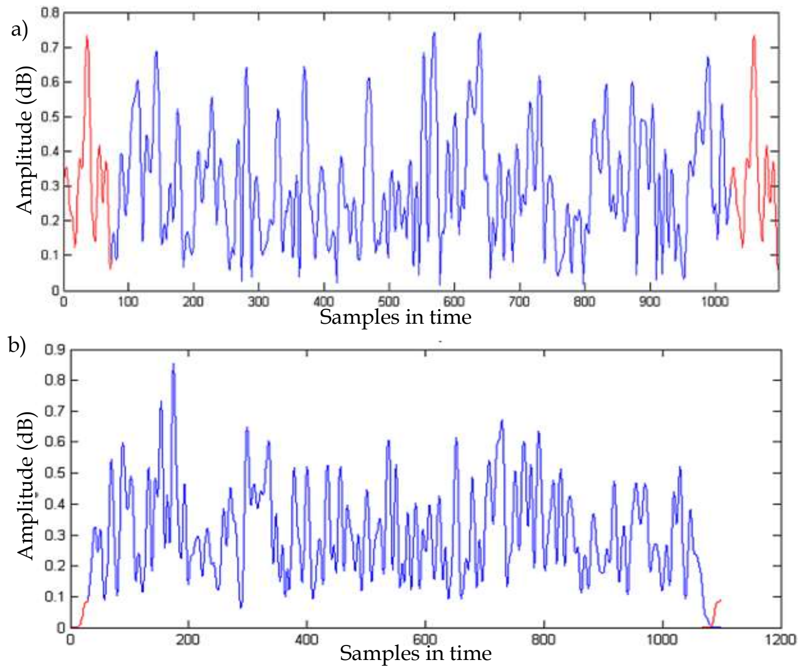

Fig. D.2. OFDM and UFMC in time
Source:[186]

In order to analyze SER against SNR, it is necessary to define the Carrier Frequency Offset (CFO). CFO consists of a displacement of the frequency in the receiver. This shift, influences in the recovery of the symbols and in the orthogonality between subcarriers. CFO is caused mainly by the Doppler Effect and, in other cases, by imbalances between the transmission and the reception oscillators. CFO, as well as CFO normalized, can be expressed as follows:

$$f_{offset} = f_c - f_c' \qquad (3),$$
$$CFO = \frac{f_{offset}}{\Delta f}$$

where f_c is the carrier frequency, f_c' is the carrier frequency displaced, and Δf is the space between subcarriers and is used to normalize CFO.

To compare the performance of both multiplexing techniques, they were subjected to different rCFO (rCFO is the same that CFO, the first one was used in the Matlab Code) values to observe their response in the SER Vs SNR curves.

Figure D.3., shows the curves of SER vs. SNR for different offsets such as 0.0, 0.1 and 0.2, which were simulated through Matlab. It is clear that the behavior of the curves will deteriorate as the offset increases, producing a higher Error Rate even at high SNR values. However, it cannot be concluded that UFMC presents improvements over OFDM. Only that its curve is slightly below that of OFDM for an offset greater than 0.0.

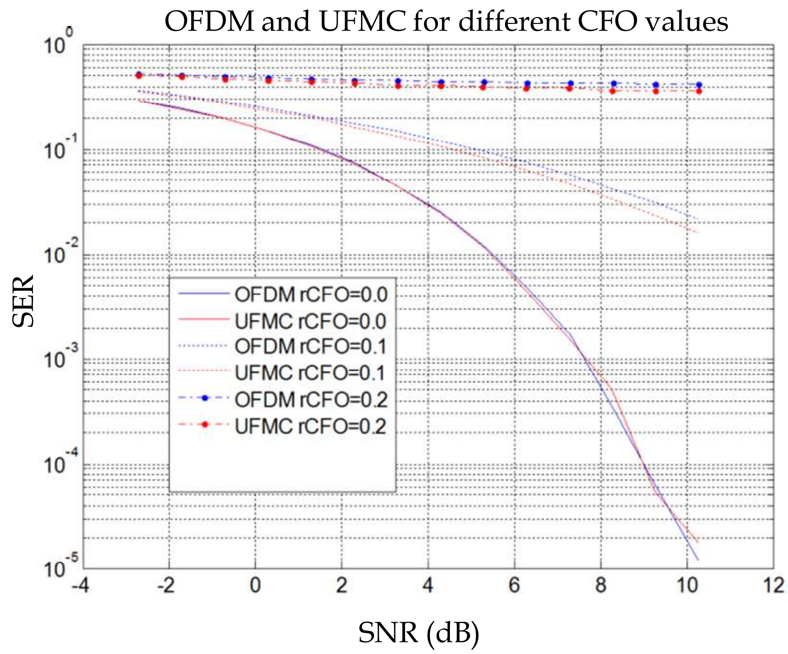

Fig. D.3. OFDM and UFMC for different CFO Values
Source:[186]

In terms of the effect of CFO on the symbol transmitted, Figure D.4., shows the constellation diagrams of QPSK with different values of CFO. It can be observed that with a CFO of 0.0, the symbols remain scattered around the original value, while for 0.1, the points suffer a rotation due to the phase introduced.

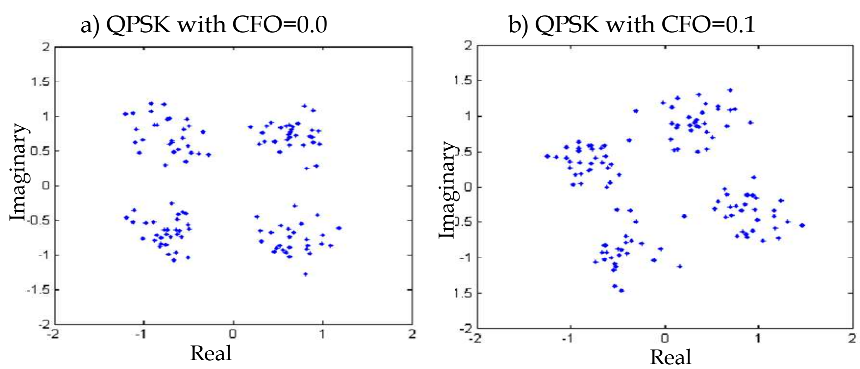

Fig. D.4. QPSK Diagram Constellation for different CFO Values.
a) CFO=0.0, b)CFO=0.1
Source:[186]

Until here the analysis of the offset in frequency has been displayed. Similarly, other simulations regarding offset in time were done. For this reason, it is important to define Symbol Time Offset (STO), which introduces a delay in the transmitted signal. In other words, the signal arrives to the receiver or to its corresponding window before or after the time expected. The main cause is the multiple paths that add delay to the response of the channel. This delay can be represented as a constant phase, which affects the symbols decode. STO can be expressed as follows:

$$STO = \frac{1}{N} \sum_{n=0}^{N-1} x_1[n + \delta]\, e^{\frac{-j2\pi nk}{N}} \tag{4}$$

where N is the FFT size, $x_1[n]$ is the original signal and δ is the number of delay samples that are introduced into the system. The exponential term represents the Fourier transform, which converts the time samples to the frequency. Figure D.5 shows the comparison between OFDM and UFMC with different STO values for both.

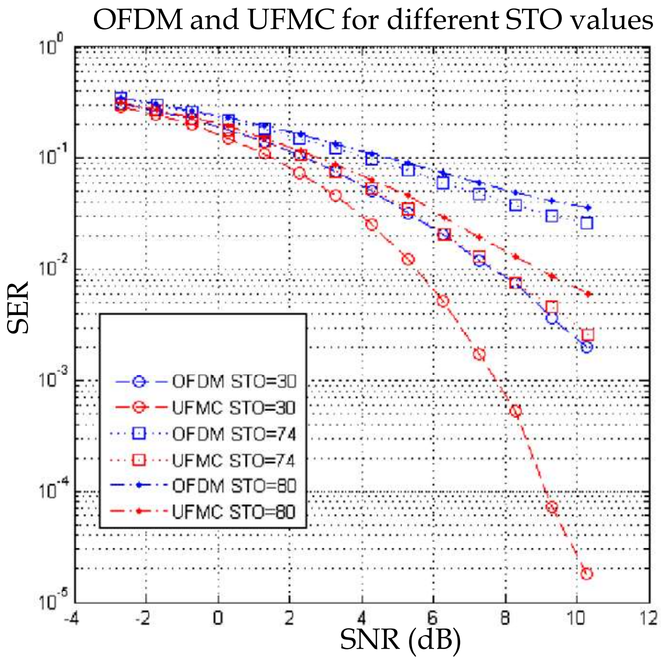

Fig. D.5. OFDM and UFMC for different STO Values
Source:[186]

To make the previous figure, it was taken into account that the decoding of the digital symbols is simply an aggregated mismatch proportional to the delay. For comparison purposes, simulations with delay of 30, 74 and 80 samples were carried out. As a result, Figure D.5 shows an improvement of UFMC curves compared to those of OFDM. For instance, in case of an offset of 30 samples and an SNR of 10, the UMFC SER is in the range of 10E-5; while for OFDM this SER is in 10E-3. This demonstrates that a multiplexing like UFMC has requirements of synchronization much less strict than OFDM.

Appendix E. W-band RoF Measurements Results

1. GMSK

200kbps						
Transmission Throughput measured		**Reception Throughput measured**		**Delay in ms in the Transmission**	**Delay in ms in the Reception**	**End To End Latency**
1	45463,3	1	452183	1,407728871	4,529139751	6,719177348
2	695318	2	213968	0,184088431	0,598220295	
1	51480,7	1	469975	1,243184339	4,3576786	6,351355509
2	691130	2	226433	0,185203941	0,565288628	
1	45476,7	1	468115	1,407314075	4,374993324	6,519517449
2	696375	2	231297	0,183809011	0,553401038	
1	42988,3	1	447061	1,488777179	4,581030329	6,843485432
2	655846	2	221258	0,195167768	0,578510156	
1	37727,6	1	485154	1,696370827	4,221340028	6,660192317
2	604817	2	2,41E+05	0,211634263	0,530847199	
1	47935,9	1	444547	1,33511627	4,606936949	6,694591069
2	736811	2	221141	0,173721619	0,57881623	
1	35598,9	1	493802	1,797808359	4,147411311	6,737919756
2	556113	2	227543	0,230169048	0,562531038	
1	58691,4	1	462799	1,090449367	4,425247246	6,244893529
2	815077	2	223715	0,157040378	0,572156538	
1	51639,7	1	463916	1,239356542	4,414592297	6,403156011
2	7,02E+05	2	225757	0,18222586	0,566981312	
1	55732,5	1	403655	1,148342529	5,073639618	7,01926877
2	678600	2	210297	0,188623637	0,608662986	6,619355719
500 kbps						
1	127183	1	554046	0,503211907	0,80859712	3,047672978
2	509487	2	525357	1,004932412	0,730931538	
1	101428	1	538408	0,63098947	0,832082733	2,962022499
2	677539	2	516633	0,755676057	0,743274239	
1	81323,7	1	544435	0,786978458	0,822871417	2,999461962
2	6,21E+05	2	679993	0,824900392	0,564711696	
1	116728	1	533574	0,548283188	0,839621121	2,677613825

2	9,27E+05	2	520610	0,552113235	0,737596281	
1	135687	1	556382	0,471673779	0,805202181	2,653951605
2	782612	2	5,31E+05	0,65421946	0,722856186	
1	122344	1	572915	0,523115151	0,781965911	2,739388605
2	7,17E+05	2	533343	0,714320593	0,71998695	
1	129705	1	556196	0,493427393	0,805471453	2,599411527
2	8,78E+05	2	535107	0,582899195	0,717613487	
1	100135	1	602964	0,639137165	0,742996265	2,757445746
2	7,90E+05	2	527821	0,647792949	0,727519367	
1	116905	1	570007	0,54745306	0,78595526	2,687281755
2	8,31E+05	2	520348	0,615905766	0,737967668	
1	125407	1	602964	0,510338338	0,742996265	2,604425967
2	8,21E+05	2	527821	0,623571996	0,727519367	2,772867647
700kbps						
1	125760,5	1	1,53E+06	0,508903829	1,339612768	2,137729957
2	1,02E+06	2	780765	0,125271585	0,163941775	
1	116942	1	1,41E+06	0,547279848	1,450311945	2,235135218
2	1,76E+06	2	7,77E+05	0,07289626	0,164647166	
1	116550,2	1	1,46E+06	0,549119607	1,406467829	2,221625685
2	1474370	2	714200	0,086816742	0,179221507	
1	115960,2	1	1,51E+06	0,551913501	1,358414476	2,167765322
2	1576700	2	726220	0,081182216	0,176255129	
1	165160,1	1	1,35E+06	0,387502793	1,519321647	2,180950043
2	1,21E+06	2	7,61E+05	0,106015554	0,168110049	
1	118570,1	1	1,52E+06	0,539765084	1,348148928	2,130092292
2	1,59E+06	2	791110	0,080380299	0,16179798	
1	106080,5	1	1,51E+06	0,603315407	1,355196464	2,205920475
2	1,60E+06	2	764992	0,080086594	0,167322011	
1	112573	1	1,52E+06	0,568519983	1,350308896	2,161835905
2	1,89E+06	2	729730	0,067599683	0,175407342	
1	122754	1	1,43E+06	0,521367939	1,433531191	2,205427781
2	1,69E+06	2	731660	0,075584005	0,174944646	
1	115504	1	1,48E+06	0,554093365	1,381347758	2,183436647
2	1,80E+06	2	723333	0,071036917	0,176958607	2,182991932

2. DQPSK

200kbps						
Transmission Throughput measured		Reception Throughput measured		Delay in ms in the Transmission	Delay in ms in the Reception	End To End Latency
1	64721,3	1	217844	0,988855292	2,056517508	5,974795067
2	443018	2	216495	1,155709249	1,773713019	
1	64537,6	1	222585	0,991669972	2,012714244	6,068741308
2	408973	2	211869	1,251916386	1,812440706	
1	51611	1	221632	1,240045727	2,021368755	6,162143912
2	450457	2	217674	1,136623473	1,764105957	
1	68615,2	1	218364	0,932737936	2,05162023	6,009876904
2	455180	2	202032	1,124829738	1,900689	
1	61817,2	1	219348	1,035310561	2,042416617	6,173562739
2	391422	2	2,15E+05	1,308051157	1,787784404	
1	63463,3	1	219890	1,008456856	2,037382328	6,070374047
2	407606	2	217143	1,256114974	1,768419889	
1	53628,2	1	218300	1,193401979	2,052221713	6,091745431
2	473496	2	217588	1,081318533	1,764803206	
1	53088,5	1	215552	1,205534155	2,078384798	6,297797247
2	417643	2	214771	1,225927407	1,787950887	
1	74365,1	1	219576	0,860618758	2,040295843	5,577245664
2	5,55E+05	2	218928	0,922329747	1,754001316	
1	72261,6	1	222320	0,885670951	2,01511335	5,823036594
2	446051	2	216411	1,147850806	1,774401486	6,024931891
500 kbps						
1	105050	1	1,15E+06	0,609233698	1,784314067	2,773508372
2	1,46E+06	2	437987	0,087714489	0,292246117	
1	108180	1	1,25E+06	0,591606582	1,643053126	2,563443254
2	1,62E+06	2	512778	0,079162853	0,249620694	
1	85792	1	1,15E+06	0,745990302	1,776744428	2,750504165
2	1,56E+06	2	876928	0,081805342	0,145964093	
1	104703	1	1,23E+06	0,611252782	1,664337028	2,607590784
2	1,57E+06	2	510649	0,081339561	0,250661413	
1	107812	1	1,10E+06	0,593625941	1,859721768	2,674287327

2	1,52E+06	2	9,35E+05	0,084005487	0,13693413	
1	92933,5	1	1,22E+06	0,688664475	1,676736913	2,607508794
2	1,35E+06	2	869712	0,09493225	0,147175157	
1	103541	1	1,10E+06	0,618112632	1,868425614	2,819843364
2	1,34E+06	2	538313	0,09552524	0,237779879	
1	93176,4	1	1,01E+06	0,686869207	2,033824245	3,043727331
2	1,41E+06	2	550786	0,09063872	0,232395159	
1	93255,6	1	1,14E+06	0,686285864	1,79705872	2,827485094
2	1,32E+06	2	518220	0,097141166	0,246999344	
1	109358	1	1,13E+06	0,585233819	1,806107961	2,708383422
2	1,54E+06	2	547076	0,083070493	0,233971148	2,737628191
700kbps						
1	76825,1	1	772450,3	0,83306107	0,579972589	2,358626775
2	1263400	2	710667	0,405255659	0,540337458	
1	155241	1	756707	0,412262225	0,592038927	2,065756398
2	1,19E+06	2	608087	0,429966661	0,631488586	
1	133793	1	709200	0,478350885	0,631697688	2,104120668
2	1,14E+06	2	705071	0,449446093	0,544626002	
1	162558	1	680870	0,393705631	0,6579817	2,05956532
2	1,23E+06	2	650670	0,417717078	0,590160911	
1	120710	1	741070	0,530196338	0,604531286	2,121652757
2	1,19E+06	2	6,89E+05	0,429353705	0,557571428	
1	159927	1	703067	0,400182583	0,637208118	1,991846723
2	1,26E+06	2	702364	0,407730961	0,54672506	
1	90072,5	1	802364	0,710538733	0,558350076	2,143210024
2	1,29E+06	2	801818	0,395409542	0,478911673	
1	155344	1	702326	0,411988876	0,637880415	2,017398479
2	1,22E+06	2	702261	0,420723941	0,546805248	
1	146051	1	702000	0,438203093	0,638176638	2,158463711
2	1,14E+06	2	605100	0,447478129	0,63460585	
1	167225	1	702364	0,382717895	0,637845903	2,070216208
2	1,31E+06	2	583380	0,391419354	0,658233056	2,109085706

3. 8PSK

200kbps						
Transmission Throughput measured		**Reception Throughput measured**		**Delay in ms in the Transmission**	**Delay in ms in the Reception**	**End To End Latency**
1	83522,4	1	325733	0,862044194	0,884159726	4,604568146
2	409332	2	212980	1,055378031	1,802986196	
1	96427,1	1	328005	0,74667806	0,878035396	4,337440581
2	477368	2	212417	0,904962209	1,807764915	
1	109038	1	318623	0,660320255	0,90388955	4,255630056
2	500218	2	210089	0,86362346	1,827796791	
1	94953,3	1	305170	0,758267485	0,943736278	4,676114836
2	353166	2	219317	1,223220808	1,750890264	
1	89567,1	1	323665	0,803866598	0,889808907	4,794598602
2	339160	2	2,10E+05	1,27373511	1,827187986	
1	97673	1	327237	0,737153563	0,880096077	4,3425125
2	455209	2	216186	0,949014628	1,776248231	
1	105814	1	328049	0,680439261	0,877917628	4,346705941
2	422975	2	217316	1,021336958	1,767012093	
1	67671,1	1	325424	1,063969701	0,884999263	4,612849535
2	486697	2	216184	0,887615909	1,776264663	
1	95205,5	1	317804	0,75625883	0,906218927	4,462331934
2	434373	2	212705	0,994536953	1,805317223	
1	111566	1	313518	0,645357905	0,918607544	4,245190063
2	472395	2	217350	0,914488934	1,76673568	4,467794219
500 kbps						
1	139492	1	363436	0,516158633	0,792436633	2,869928749
2	549062	2	495780	0,786796391	0,774537093	
1	142863	1	366084	0,503979337	0,786704691	2,557459878
2	789921	2	533418	0,546890132	0,719885718	
1	171239	1	358283	0,420464964	0,803833841	2,571448562
2	657301	2	556589	0,65723314	0,689916617	
1	125828	1	361263	0,572209683	0,797203146	2,79710339
2	572147	2	570885	0,755050712	0,672639849	
1	169574	1	366387	0,424593393	0,78605409	2,419253371
2	797927	2	575537	0,54140291	0,667202977	
1	170011	1	364442	0,423502009	0,790249203	2,425142431
2	811786	2	565345	0,532159953	0,679231266	

1	164860	1	361622	0,436734199	0,796411723	2,455083141
2	789483	2	569105	0,547193543	0,674743676	
1	135914	1	366378	0,529746752	0,7860734	2,725818099
2	589956	2	566589	0,732257999	0,677739949	
1	187254	1	358753	0,38450447	0,802780743	2,382442929
2	809798	2	580331	0,533466371	0,661691345	
1	143689	1	363873	0,501082198	0,791484941	2,643146848
2	712673	2	515844	0,606168607	0,744411101	2,58468274
700kbps						
1	175368	1	496865	0,410565211	0,724542884	2,124491501
2	891607	2	748715	0,484518403	0,504865002	
1	193762	1	501886	0,371589889	0,717294366	2,084703574
2	808770	2	818758	0,534144442	0,461674878	
1	193726	1	504477	0,371658941	0,713610333	2,032304863
2	898993	2	810293	0,480537668	0,466497921	
1	188691	1	512209	0,381576228	0,702838099	2,018104844
2	967403	2	775967	0,446556399	0,487134118	
1	183508	1	8,10E+05	0,392353467	0,44460582	2,08324825
2	8,78E+05	2	5,01E+05	0,492136636	0,754152327	
1	147778	1	816137	0,487217312	0,441102413	2,134385307
2	854650	2	539541	0,505470075	0,700595506	
1	170366	1	804909	0,422619537	0,447255528	2,051787726
2	818285	2	578000	0,527933422	0,653979239	
1	184801	1	817058	0,389608281	0,440605196	2,010464595
2	989968	2	508151	0,436377742	0,743873376	
1	143689	1	815402	0,501082198	0,441500021	2,161521412
2	905596	2	509499	0,477033909	0,741905283	
1	176580	1	819724	0,407747197	0,439172209	2,039553427
2	970809	2	505588	0,444989694	0,747644327	2,07405655

4. 16QAM

200kbps						
Transmission Throughput measured		Reception Throughput measured		Delay in ms in the Transmission	Delay in ms in the Reception	End To End Latency
1	114474	1	430179	0,559078917	0,297550555	3,801863674
2	445068	2	216030	0,575193004	2,370041198	
1	95571,6	1	431748	0,669655002	0,296469237	4,045104711
2	373599	2	213890	0,685226674	2,393753799	
1	122669	1	428488	0,521729206	0,298724818	3,825369946
2	446300	2	210586	0,573605198	2,431310723	
1	104150	1	432812	0,61449832	0,295740414	3,976918982
2	369507	2	215682	0,692815021	2,373865228	
1	117197	1	428085	0,546089064	0,299006039	3,814231984
2	445467	2	2,14E+05	0,57467781	2,394459072	
1	104597	1	434772	0,611872233	0,294407184	3,989276719
2	351706	2	217399	0,727880673	2,355116629	
1	117181	1	435745	0,546163627	0,293749785	4,007990236
2	329290	2	214168	0,777430229	2,390646595	
1	122050	1	427143	0,524375256	0,299665452	3,924847444
2	380940	2	210805	0,672021841	2,428784896	
1	107909	1	435416	0,593092328	0,293971742	3,887645203
2	3,93E+05	2	217875	0,65060982	2,349971314	
1	120167	1	422026	0,532592143	0,303298849	3,827440625
2	403224	2	217256	0,634882844	2,356666789	3,910068953
500 kbps						
1	145016	1	287566	0,441330612	0,445115208	2,36353178
2	439813	2	572054	0,58206556	0,8950204	
1	152844	1	283401	0,418727592	0,45165684	2,364634598
2	463207	2	543766	0,552668677	0,941581489	
1	139572	1	288032	0,458544694	0,444395067	2,440551745
2	410085	2	560573	0,624260824	0,91335116	
1	156697	1	272589	0,408431559	0,469571406	2,366797707
2	450927	2	555872	0,567719387	0,921075355	
1	136040	1	287530	0,470449868	0,445170939	2,369986616
2	455883	2	5,73E+05	0,56154759	0,892818219	
1	154264	1	287854	0,414873204	0,444669867	2,276841354

2	491112	2	571408	0,521266025	0,896032257	
1	150201	1	274839	0,426095698	0,465727208	2,332814696
2	480007	2	564084	0,533325556	0,907666234	
1	155081	1	279403	0,412687563	0,458119634	2,335892565
2	446319	2	574310	0,57358078	0,891504588	
1	156422	1	284194	0,409149608	0,45039656	2,343884314
2	4,27E+05	2	578880	0,59987159	0,884466556	
1	152143	1	281015	0,420656882	0,4554917	2,286225651
2	509566	2	564070	0,502388307	0,907688762	2,348116102
700kbps						
1	269454	1	376003	0,23751735	0,510634224	2,065982136
2	769860	2	779456	0,332527992	0,98530257	
1	269272	1	385091	0,237677887	0,498583452	2,003410848
2	791627	2	813762	0,323384624	0,943764885	
1	268122	1	378542	0,238697309	0,50720924	2,012048273
2	794791	2	813521	0,322097256	0,944044468	
1	260932	1	381342	0,245274631	0,503485061	2,013196715
2	805476	2	811314	0,317824491	0,946612532	
1	262472	1	383060	0,243835533	0,501226962	2,033638303
2	770307	2	8,03E+05	0,33233503	0,956240778	
1	266256	1	372411	0,24037017	0,515559422	2,021373453
2	801654	2	811750	0,319339765	0,946104096	
1	267329	1	372647	0,239405377	0,515232915	2,009413356
2	808874	2	818514	0,316489342	0,938285723	
1	262355	1	379200	0,243944274	0,506329114	2,028632317
2	798574	2	801848	0,320571419	0,957787511	
1	261875	1	379222	0,244391408	0,50629974	2,063587788
2	7,22E+05	2	801326	0,354485207	0,958411433	
1	260683	1	367583	0,245508913	0,522331011	1,766702095
2	829766	2	833214	0,077130179	0,921731992	2,001798529

References

[1] D. Soldani and A. Manzalini, “Horizon 2020 and Beyond: On the 5G Operating System for a True Digital Society,” *IEEE Veh. Technol. Mag.*, vol. 10, no. 1, pp. 32–42, Mar. 2015.

[2] S. Talwar, D. Choudhury, K. Dimou, E. Aryafar, B. Bangerter, and K. Stewart, “Enabling technologies and architectures for 5G wireless,” in *2014 IEEE MTT-S International Microwave Symposium (IMS2014)*, 2014, pp. 1–4.

[3] G. Carpintero *et al.*, “Microwave Photonic Integrated Circuits for Millimeter-Wave Wireless Communications,” *J. Light. Technol.*, vol. 32, no. 20, pp. 3495–3501, Oct. 2014.

[4] T. I. IEEE Internet Initiative, “Towards a definition of the Internet of Things (IoT).” May-2015.

[5] “Internet of Things in 2020 A ROADMAP FOR THE FUTURE,” Sep. 2008.

[6] N. Bari, G. Mani, and S. Berkovich, “Internet of Things as a Methodological Concept,” in *Geo), 2013 Fourth International Conference on Computing for Geospatial Research and Application (COM*, 2013, pp. 48–55.

[7] D. Szabo, A. Gulyas, F. H. P. Fitzek, F. H. P. Fitzek, and D. E. Lucani, “Towards the Tactile Internet: Decreasing Communication Latency with Network Coding and Software Defined Networking,” in *European Wireless 2015; 21th European Wireless Conference; Proceedings of*, 2015, pp. 1–6.

[8] M. Rico-Martínez, A. Morales, V. Mehmeri, R. Puerta, M. Varón, and I. T. Monroy, “Procedure to measure real time latency using software defined radio in a W-band fiber-wireless link,” *Microw. Opt. Technol. Lett.*, vol. 59, no. 12, pp. 3147–3151, Dec. 2017.

[9] G. P. Fettweis, “The Tactile Internet: Applications and Challenges,” *IEEE Veh. Technol. Mag.*, vol. 9, no. 1, pp. 64–70, Mar. 2014.

[10] R. M. Assumpção, O. C. Branquinho, F. Abbade, and D. G. Lona, “Impact Evaluation of Radio over Fiber Technology in Wireless Sensor Networks,” *Comput. Eng.*, pp. 618–622, Oct. 2011.

[11] J. Yao, “Microwave Photonics,” *J. Light. Technol.*, vol. 27, no. 3, pp. 314–335, Feb. 2009.

[12] C. S. Arismar, D. C. V. e Silva, M. A. Q. R. Fortes, L. F. da Silva, O. C. Branquinho, and M. L. F. Abbade, “Radio over Fiber system applied to IEEE 802.15.4 standard,” in *2009 SBMO/IEEE MTT-S International Microwave and Optoelectronics Conference (IMOC)*, 2009, pp. 838–840.

[13] R. Karthikeyan, S. Prakasam, and A. Professor, “A Survey on Radio over Fiber (RoF) for Wireless Broadband Access Technologies,” *Int. J. Comput. Appl.*, vol. 64, no. 12, pp. 975–8887, 2013.

[14] Y. Horiuchi, “ROF Application to 3G Mobile Systems in Offices and Outdoors,” *2005 Int. Top. Meet. Microw. Photonics*, pp. 3–3, 2005.

[15] C. Lim, A. Nirmalathas, M. Bakaul, P. Gamage, D. Novak, and R. Waterhouse, “Fiber-Wireless Networks and Subsystem Technologies,” *J. Light. Technol.*, vol. 28, no. 4, pp. 390–

405, Feb. 2010.

[16] N. Ghazisaidi, M. Maier, and C. M. Assi, "Fiber-Wireless (FiWi) Access Networks: A survey," *Commun. Mag. IEEE*, vol. 47, no. February, pp. 160–167, 2009.

[17] M. Simsek, A. Aijaz, M. Dohler, J. Sachs, and G. Fettweis, "5G-Enabled Tactile Internet," *IEEE J. Sel. Areas Commun.*, vol. 34, no. 3, pp. 460–473, Mar. 2016.

[18] V. Sharma, A. Singh, and A. K. Sharma, "Challenges to radio over fiber (RoF) technology and its mitigation schemes – A review," *Opt. - Int. J. Light Electron Opt.*, vol. 123, no. 4, pp. 338–342, Feb. 2012.

[19] H. Al-Raweshidy and S. Komaki, *Radio over fiber technologies for mobile communications networks*. Artech House, 2002.

[20] S. K. Yong and C.-C. Chong, "An Overview of Multigigabit Wireless through Millimeter Wave Technology: Potentials and Technical Challenges," *EURASIP J. Wirel. Commun. Netw.*, vol. 2007, no. 1, pp. 1–10, 2007.

[21] M. Lucente *et al.*, "Analysis and design of a point-to-point radio-link at W band for future satellite telecommunication experiments," in *2011 Aerospace Conference*, 2011, pp. 1–10.

[22] I. Aldaya, A. Arag, and G. Campuzano, "Millimeter-Wave Frequency Radio over Fiber Systems: A Survey," *IEEE Communications Survey&Tutorials*, vol. 15, no. 4, pp. 1593–1619, 2013.

[23] N. Kumari and P. K. Kaushik, "A REVIEW ON RADIO OVER FIBER TECHNOLOGY," *Int. J. Adv. Res. Sci. Eng. http//www.ijarse.com IJARSE*, no. 32, 2014.

[24] C. Lim, A. Nirmalathas, Y. Yang, D. Novak, and R. Waterhouse, "Radio-over-Fiber Systems," *Commun. Photonics Conf. Exhib. (ACP), 2009 Asia (Volume2009-Supplement)*, vol. 7632, pp. 1–10, 2009.

[25] N. Kumar, A. Garg, S. Panwar, D. O. Electronics, and C. H. C. T. M. Kaithal, "A Review Paper On Radio Over Fibre Technology," vol. 7, no. 11, pp. 7–10, 2012.

[26] J. Guillory, T. Advisor, C. Algani, A. Pizzinat, P. G. Tartarini, and B. Charbonnier-Engineer, "Radio over Fiber for the future Home Area Networks," 2012.

[27] N. Mohamed, S. M. Idrus, and A. B. Mohammad, "Review on system architectures for the millimeter-wave generation techniques for RoF communication link," *2008 IEEE Int. RF Microw. Conf.*, pp. 326–330, Dec. 2008.

[28] X. N. Fernando, *Radio over fiber for wireless communications: from fundamentals to advanced topics*, First Edit. Wiley-IEEE Press, 2014.

[29] L. A. (Larry A. . Coldren, S. W. (Scott W. . Corzine, and M. Mashanovitch, *Diode lasers and photonic integrated circuits*. Wiley, 2012.

[30] K. K.-D. Rahman Mohammad Shaifur , Lee Jung Hyun , Park Youngil, "Radio over Fiber as a Cost Effective Technology for Transmission of WiMAX Signals," in *World Academy of Science, Engineering and Technology*, 2009, p. 32.

[31] B. A. Forouzan, *Data Communications and Networking*. Huga Media, 2007.

[32] Coronel Rico Juan Fernando, "Injection Locked VCSEL Based Oscillator – ILVBO," Universidad Nacional de Colombia Faculty of Eng, 2016.

[33] W. W.-I. T. on Communications and undefined 1993, "Optical fiber-based microcellular systems: An overview," *search.ieice.org*.

[34] R. Deiterding, R. Glowinski, H. Oliver, and S. Poole, "A Reliable Split-Step Fourier Method for the Propagation Equation of Ultra-Fast Pulses in Single-Mode Optical Fibers," *J. Light. Technol.*, vol. 31, no. 12, pp. 2008–2017, Jun. 2013.

[35] U. S. Kumar, V. Saminadan, and P. Williams, "Performance Evaluation of Millimeter Wave and UWB Signals over Fiber Radio Networks " IEEE," pp. 104–107, 2012.

[36] L. Yang, X. Zhu, and S. Liu, "Measurement Techniques for Spurious Free Dynamic Range of Analog to Digital Converter," *IERI Procedia*, vol. 4, pp. 195–200, Jan. 2013.

[37] Q. Gu, *RF system design of transceivers for wireless communications*. Springer, 2005.

[38] S. Lee, M. Chuang, C. Lee, and C. Sun, "Design and Applications of Radio-Over-Fiber

Schemes to Indoor Wireless Coverage and High- Speed Rails," vol. 2, no. October, pp. 1–3, 2012.

[39] D. Xu, J. Zhang, X. Gao, P. Zhang, and Y. Wu, "Indoor Office Propagation Measurements and Path Loss Models at 5.25 GHz," in *2007 IEEE 66th Vehicular Technology Conference*, 2007, pp. 844–848.

[40] D. M. J. Devasirvatham, C. Banerjee, M. J. Krain, and D. A. Rappaport, "Multi-frequency radiowave propagation measurements in the portable radio environment," in *IEEE International Conference on Communications, Including Supercomm Technical Sessions*, pp. 1334–1340.

[41] I. I. of technology G. Institute, "Multipath Wave Propagation and Fading." [Online]. Available: http://www.iitg.ac.in/scifac/qip/public_html/cd_cell/chapters/a_mitra_mobile_communication/chapter5.pdf.

[42] W. T. Barnett, "Multipath Propagation at 4, 6, and 11 GHz," *Bell Syst. Tech. J.*, vol. 51, no. 2, pp. 321–361, Feb. 1972.

[43] A. A. M. Saleh and R. Valenzuela, "A Statistical Model for Indoor Multipath Propagation," *IEEE J. Sel. Areas Commun.*, vol. 5, no. 2, pp. 128–137, Feb. 1987.

[44] I. Cox and Cambridge University Press., *Analog Optical Links□: Theory and Practice*. Cambridge University Press, 2004.

[45] C. H. Cox, E. I. Ackerman, G. E. Betts, and J. L. Prince, "Limits on the performance of RF-over-fiber links and their impact on device design," *IEEE Trans. Microw. Theory Tech.*, vol. 54, no. 2, pp. 906–920, Feb. 2006.

[46] T. Ismail, C.-P. Liu, J. E. Mitchell, and A. J. Seeds, "High-Dynamic-Range Wireless-Over-Fiber Link Using Feedforward Linearization," *J. Light. Technol.*, vol. 25, no. 11, pp. 3274–3282, Nov. 2007.

[47] A. Karim and J. Devenport, "High Dynamic Range Microwave Photonic Links for RF Signal Transport and RF-IF Conversion," *J. Light. Technol.*, vol. 26, no. 15, pp. 2718–2724, Aug. 2008.

[48] R. F. Kalman, J. C. Fan, and L. G. Kazovsky, "Dynamic range of coherent analog fiber-optic links," *J. Light. Technol.*, vol. 12, no. 7, pp. 1263–1277, Jul. 1994.

[49] V. J. Urick, F. Bucholtz, P. S. Devgan, J. D. McKinney, and K. J. Williams, "Phase Modulation With Interferometric Detection as an Alternative to Intensity Modulation With Direct Detection for Analog-Photonic Links," *IEEE Trans. Microw. Theory Tech.*, vol. 55, no. 9, pp. 1978–1985, Sep. 2007.

[50] Y. Li and P. Herczfeld, "Coherent PM Optical Link Employing ACP-PPLL," *J. Light. Technol.*, vol. 27, no. 9, pp. 1086–1094, May 2009.

[51] B. M. Haas, V. J. Urick, J. D. McKinney, and T. E. Murphy, "Dual-Wavelength Linearization of Optically Phase-Modulated Analog Microwave Signals," *J. Light. Technol.*, vol. 26, no. 15, pp. 2748–2753, Aug. 2008.

[52] T. R. Clark, S. R. O'Connor, and M. L. Dennis, "A Phase-Modulation I/Q-Demodulation Microwave-to-Digital Photonic Link," *IEEE Trans. Microw. Theory Tech.*, vol. 58, no. 11, pp. 3039–3058, Nov. 2010.

[53] A. Ramaswamy *et al.*, "Demonstration of a linear ultra-compact integrated coherent receiver," in *2010 IEEE International Topical Meeting on Microwave Photonics*, 2010, pp. 31–34.

[54] Y. Yang, M. J. Crisp, T. Li, R. V. Penty, and I. H. White, "MIMO capable RoF system with improved SFDR using quadruple sidebands," in *2017 International Topical Meeting on Microwave Photonics (MWP)*, 2017, pp. 1–3.

[55] S. Chen *et al.*, "Experimental Investigation on Improved Predistortion Circuit for Directly Modulated Radio Over Fiber System," *IEEE Photonics J.*, vol. 9, no. 5, pp. 1–9, Oct. 2017.

[56] B. Hraimel and X. Zhang, "Performance Improvement of Radio-Over Fiber Links Using Mixed-Polarization Electro-Absorption Modulators," *IEEE Trans. Microw. Theory Tech.*, vol.

59, no. 12, pp. 3239–3248, Dec. 2011.
[57] A. Stohr, "10 Gbit/s wireless transmission using millimeter-wave over optical fiber systems," in *Optical Fiber Communication Conf., Los Angeles, CA*, 2011, pp. 10–12.
[58] W. Jiang *et al.*, "32.65-Gbps OFDM RoF signal generation at 60GHz employing an adaptive I/Q imbalance correction," in *36th European Conference and Exhibition on Optical Communication*, 2010, pp. 1–3.
[59] A. Ng'oma *et al.*, "31 Gbps RoF system employing adaptive bit-loading OFDM modulation at 60 GHz," *Opt. Fiber Commun. Conf. Expo. (OFC/NFOEC), 2011 Natl. Fiber Opt. Eng. Conf.*, pp. 1–3, 2011.
[60] A. Hirata *et al.*, "Transmission Characteristics of 120-GHz-Band Wireless Link Using Radio-on-Fiber Technologies," *J. Light. Technol.*, vol. 26, no. 15, pp. 2338–2344, Aug. 2008.
[61] I. Aldaya, J. Beas, G. Castañón, G. Campuzano, and A. Aragón-Zavala, "A survey of key-enabling components for remote millimetric wave generation in radio over fiber networks," *Opt. Laser Technol.*, vol. 49, pp. 213–226, Jul. 2013.
[62] H. Chen, R. Lin, and J. Ye, "Millimeter-wave Radio over Fiber System for Broadband Wireless Communication," China, 2009.
[63] Qualcomm Technologies, "Spectrum for4G and 5G," *December*, 2017. [Online]. Available: https://www.qualcomm.com/media/documents/files/spectrum-for-4g-and-5g.pdf. [Accessed: 08-Feb-2018].
[64] A. Kühn, "5G and IMT Identification -Views from CEPT," *ITU*, 2017. [Online]. Available: https://www.itu.int/en/ITU-R/seminars/rrs/2017-Africa/Forum/CEPT-ECC.pdf. [Accessed: 14-Apr-2018].
[65] Ulrich Rehfuess, "5G will change the world," *Nokia-ITU*, 2017. [Online]. Available: https://www.itu.int/en/ITU-D/Regionalpresence/Europe/Documents/Events/2017/SpectrumManagement/Ulrich__Nokia__5G_in 700w.pdf. [Accessed: 14-Apr-2018].
[66] L. Cavalcante, "Wavelet-Coding for Radio over Fibre," Technical University of Denmark, 2017.
[67] ITU, RESOLUTION 238 (WRC-15) Studies on frequency-related matters for International Mobile Telecommunications identification including possible additional allocations to the mobile services on a primary basis in portion(s) of the frequency range between 24.25 , vol. 238. 2015.
[68] F.-M. Kuo *et al.*, "Remotely Up-Converted 20-Gbit/s Error-Free Wireless On–Off-Keying Data Transmission at W-Band Using an Ultra-Wideband Photonic Transmitter-Mixer," *IEEE Photonics J.*, vol. 3, no. 2, pp. 209–219, Apr. 2011.
[69] I. Sarkas *et al.*, "An 18-Gb/s, Direct QPSK Modulation SiGe BiCMOS Transceiver for Last Mile Links in the 70–80 GHz Band," *IEEE J. Solid-State Circuits*, vol. 45, no. 10, pp. 1968–1980, Oct. 2010.
[70] Jin-Wei Shi *et al.*, "A W-Band Photonic Transmitter-Mixer Based on High-Power Near-Ballistic Uni-Traveling-Carrier Photodiodes for BPSK and QPSK Data Transmission Under Bias Modulation," *IEEE Photonics Technol. Lett.*, vol. 21, no. 15, pp. 1039–1041, Aug. 2009.
[71] R. W. Ridgway, D. W. Nippa, and S. Yen, "Data Transmission Using Differential Phase-Shift Keying on a 92 GHz Carrier," *IEEE Trans. Microw. Theory Tech.*, vol. 58, no. 11, pp. 3117–3126, Nov. 2010.
[72] A. Kanno *et al.*, "20-Gb/s QPSK W-band (75-110GHz) wireless link in free space using radio-over-fiber technique," *IEICE Electron. Express*, vol. 8, no. 8, pp. 612–617, 2011.
[73] J. Federici and L. Moeller, "Review of terahertz and subterahertz wireless communications," *J. Appl. Phys.*, vol. 107, no. 11, p. 111101, Jun. 2010.
[74] H. Singh, J. Oh, C. Kweon, X. Qin, H.-R. Shao, and C. Ngo, "A 60 GHz wireless network for enabling uncompressed video communication," *IEEE Commun. Mag.*, vol. 46, no. 12, pp. 71–78, Dec. 2008.

[75] A. Ghosh *et al.*, “Millimeter-Wave Enhanced Local Area Systems: A High-Data-Rate Approach for Future Wireless Networks,” *IEEE J. Sel. Areas Commun.*, vol. 32, no. 6, pp. 1152–1163, Jun. 2014.

[76] X. Pang *et al.*, “100 Gbit/s hybrid optical fiber-wireless link in the W-band (75–110 GHz),” *Opt. Express*, vol. 19, no. 25, p. 24944, Dec. 2011.

[77] T. Pfeiffer, “Next Generation Mobile Fronthaul Architectures,” in *Optical Fiber Communication Conference*, 2015, p. M2J.7.

[78] C. Paoloni, F. Magne, F. André, … X. B.-N. and, and undefined 2017, “TWEETHER future generation W-band backhaul and access network technology,” *ieeexplore.ieee.org*.

[79] J. G. Andrews *et al.*, “What Will 5G Be?,” *IEEE J. Sel. Areas Commun.*, vol. 32, no. 6, pp. 1065–1082, Jun. 2014.

[80] P. Pirinen, “A brief overview of 5G research activities,” in *1st International Conference on 5G for Ubiquitous Connectivity*, 2014, pp. 17–22.

[81] D. Szabo, A. Gulyas, F. H. P. Fitzek, and D. E. Lucani, “Towards the Tactile Internet: Decreasing Communication Latency with Network Coding and Software Defined Networking,” in *Proceedings of European Wireless 2015; 21th European Wireless Conference*, 2015, pp. 1–6.

[82] T. W. D. Itu-T, “The Tactile Internet,” *ITU*, 2014. [Online]. Available: http://www.itu.int/ITU-T/techwatch. [Accessed: 15-Apr-2018].

[83] M. Maier, M. Chowdhury, B. P. Rimal, and D. P. Van, “The tactile internet: vision, recent progress, and open challenges,” *IEEE Commun. Mag.*, vol. 54, no. 5, pp. 138–145, May 2016.

[84] R. Waterhouse and D. Novack, “Realizing 5G: Microwave Photonics for 5G Mobile Wireless Systems,” *IEEE Microw. Mag.*, vol. 16, no. 8, pp. 84–92, Sep. 2015.

[85] M. Elkashlan, T. Q. Duong, and H.-H. Chen, “Millimeter-wave communications for 5G: fundamentals: Part I [Guest Editorial],” *IEEE Commun. Mag.*, vol. 52, no. 9, pp. 52–54, Sep. 2014.

[86] M. Elkashlan, T. Q. Duong, and H. Chen, “Millimeter-wave communications for 5G – Part 2: applications [Guest Editorial],” *IEEE Commun. Mag.*, vol. 53, no. 1, pp. 166–167, Jan. 2015.

[87] M. Fiorani *et al.*, “Challenges for 5G transport networks,” in *2014 IEEE International Conference on Advanced Networks and Telecommuncations Systems (ANTS)*, 2014, pp. 1–6.

[88] A. De La Oliva *et al.*, “Xhaul: toward an integrated fronthaul/backhaul architecture in 5G networks,” *IEEE Wirel. Commun.*, vol. 22, no. 5, pp. 32–40, Oct. 2015.

[89] R. Taori and A. Sridharan, “Point-to-multipoint in-band mmwave backhaul for 5G networks,” *IEEE Commun. Mag.*, vol. 53, no. 1, pp. 195–201, Jan. 2015.

[90] C. Liu, J. Wang, L. Cheng, M. Zhu, and G.-K. Chang, “Key Microwave-Photonics Technologies for Next-Generation Cloud-Based Radio Access Networks,” *J. Light. Technol.*, vol. 32, no. 20, pp. 3452–3460, Oct. 2014.

[91] F. E. Froehlich and A. Kent, *The Froehlich/Kent encyclopedia of telecommunications*. M. Dekker, 1991.

[92] A. P. (Antony P. . Oodan and Institution of Electrical Engineers., *Telecommunications quality of service management□: from legacy to emerging services*. Institution of Electrical Engineers, 2003.

[93] Nokia Siemens Networks, “White paper. Latency. The impact of latency on application performance - PDF,” Finland, 2009.

[94] A. Maiti, A. A. Kist, and A. D. Maxwell, “Estimation of round trip time in distributed real time system architectures,” in *2013 Australasian Telecommunication Networks and Applications Conference (ATNAC)*, 2013, pp. 57–62.

[95] S. Mumtaz and J. Rodriguez, *Green communication in 4G wireless systems / monograph.* River Publishers, 2013.

[96] B. Briscoe *et al.*, “Reducing Internet Latency: A Survey of Techniques and Their Merits,” *IEEE Commun. Surv. Tutorials*, vol. 18, no. 3, pp. 2149–2196, 2016.

[97] F. E. Froehlich and A. Kent, *The Froehlich/Kent Encyclopedia of Telecommunications: Volume 3 - Codes for the Prevention of Errors to Communications Frequency Standards*. CRC Press, 1991.

[98] B. M. Siddharth Mohan, Rohit Kapoor, "Latency in HSPA Data Networks | Qualcomm," *Jul* , 2013. [Online]. Available: https://www.qualcomm.com/documents/qualcomm-research-latency-hspa-data-networks. [Accessed: 08-Sep-2017].

[99] F. Fresolone, R. Kloibhofer, A. Ralbovsky, P. Farkas, M. Rakus, and T. Palenik, "Throughput and one-way latency measurements in a 3G/4G live-network hi-mobility uplink," in *2016 39th International Conference on Telecommunications and Signal Processing (TSP)*, 2016, pp. 44–49.

[100] R. Goonatilake and R. A. Bachnak, "Modeling Latency in a Network Distribution," *Netw. Commun. Technol.*, vol. 1, no. 2, Aug. 2012.

[101] H. Holma and A. Toskala, *WCDMA for UMTS: HSPA Evolution and LTE*. John Wiley & Sons, 2007.

[102] A. Osseiran, J. F. Monserrat, and P. Marsch, *5G Mobile and Wireless Communications Technology*. Cambridge University Press, 2016.

[103] K. R. Venugopal and L. M. Patnaik, *Wireless Networks and Computational Intelligence: 6th International Conference on Information Processing, ICIP 2012, Bangalore, India, August 10-12, 2012. Proceedings*. Springer, 2012.

[104] M. Laner, P. Svoboda, P. Romirer-Maierhofer, N. Nikaein, F. Ricciato, and M. Rupp, "A comparison between one-way delays in operating HSPA and LTE networks," in *2012 10th International Symposium on Modeling and Optimization in Mobile, Ad Hoc and Wireless Networks (WiOpt)*, 2012, pp. 286–292.

[105] S. Konishi, X. Wang, T. Kitahara, H. Nakamura, and T. Suzuki, "A Study on Ultra Low-Latency Mobile Networks," *Wirel. Pers. Commun.*, vol. 44, no. 1, pp. 57–73, Dec. 2007.

[106] P. Chanclou *et al.*, "Optical fiber solution for mobile fronthaul to achieve Cloud Radio Access Network," in *Future Network & Mobile Summit*, 2013, pp. 1–11.

[107] M. C. Yuang *et al.*, "OPMDC: Architecture Design and Implementation of a New Optical Pyramid Data Center Network," *J. Light. Technol.*, vol. 33, no. 10, pp. 2019–2031, May 2015.

[108] E. Lahetkangas *et al.*, "Achieving low latency and energy consumption by 5G TDD mode optimization," in *2014 IEEE International Conference on Communications Workshops (ICC)*, 2014, pp. 1–6.

[109] I. Gaspar, L. Mendes, M. Matthé, N. Michailow, A. Festag, and G. Fettweis, "LTE-compatible 5G PHY based on generalized frequency division multiplexing," in *2014 11th International Symposium on Wireless Communications Systems (ISWCS)*, 2014, pp. 209–213.

[110] I. Gaspar, L. Mendes, M. Matthe, N. Michailow, A. Festag, and G. Fettweis, "LTE-compatible 5G PHY based on generalized frequency division multiplexing," in *2014 11th International Symposium on Wireless Communications Systems (ISWCS)*, 2014, pp. 209–213.

[111] X. Liu, Q. X. Deng, and Z. K. Wang, "Design and FPGA Implementation of High-Speed, Fixed-Latency Serial Transceivers," *IEEE Trans. Nucl. Sci.*, vol. 61, no. 1, pp. 561–567, Feb. 2014.

[112] J. W. Gu and Measurement Data Acquisition Group, "The optical fiber latency," UK, 2011.

[113] C. Y. Yeoh, M. H. Mokhtar, A. A. A. Rahman, and A. K. Samingan, "Performance study of LTE experimental testbed using OpenAirInterface," in *2016 18th International Conference on Advanced Communication Technology (ICACT)*, 2016, pp. 617–622.

[114] P. Assimakopoulos, M. K. Al-Hares, and N. J. Gomes, "Switched Ethernet Fronthaul Architecture for Cloud-Radio Access Networks," *J. Opt. Commun. Netw.*, vol. 8, no. 12, pp. B135–B146, Dec. 2016.

[115] T. Pögel, J. Lübbe, and L. Wolf, "Passive client-based bandwidth and latency measurements in cellular networks," in *2012 Proceedings IEEE INFOCOM Workshops*, 2012, pp. 37–42.

[116] I. Bravo, M. Mazo, J. L. Lazaro, P. Jimenez, A. Gardel, and M. Marron, "Novel HW Architecture Based on FPGAs Oriented to Solve the Eigen Problem," *IEEE Trans. Very Large*

Scale Integr. Syst., vol. 16, no. 12, pp. 1722–1725, Dec. 2008.

[117] A. K. Panda and K. C. Ray, "FPGA Prototype of Low Latency BBS PRNG," in *2015 IEEE International Symposium on Nanoelectronic and Information Systems*, 2015, pp. 118–123.

[118] N. Systems, "Mobile Network Protocol Tester - Absolute Analysis Representatives NextGig Systems, Inc.," *NextGig Systems*. [Online]. Available: http://www.nextgigsystems.com/protocol_testing/mobile_tester.html. [Accessed: 12-Mar-2017].

[119] "GNU Radio Manual and C++ API Reference: high_res_timer.h Source File." .

[120] G. Jackson, P. Keleher, and A. Sussman, "A Ping Too Far: Real World Network Latency Measurement," in *2015 IEEE 11th International Conference on e-Science*, 2015, pp. 580–588.

[121] S. Hu, W. Bai, K. Chen, C. Tian, Y. Zhang, and H. Wu, "Providing bandwidth guarantees, work conservation and low latency simultaneously in the cloud," in *IEEE INFOCOM 2016 - The 35th Annual IEEE International Conference on Computer Communications*, 2016, pp. 1–9.

[122] T. Wirth, M. Mehlhose, J. Pilz, B. Holfeld, and D. Wieruch, "5G New Radio and Ultra Low Latency Applications : A PHY Implementation Perspective," *2016 50th Asilomar Conf. Signals, Syst. Comput.*, pp. 1409–1413, Nov. 2016.

[123] N. B. Truong, Y. J. Suh, and C. Yu, "Latency Analysis in GNU Radio/USRP-Based Software Radio Platforms," in *MILCOM 2013 - 2013 IEEE Military Communications Conference*, 2013, pp. 305–310.

[124] M. Laner, P. Svoboda, and M. Rupp, "Latency analysis of 3G network components," in *European Wireless 2012; 18th European Wireless Conference 2012*, 2012, pp. 1–8.

[125] T. Schmid, O. Sekkat, and M. B. Srivastava, *An Experimental Study of Network Performance Impact of Increased Latency in Software Defined Radios*. .

[126] Opensignal, "State of Mobile Networks: USA - OpenSignal," 2018. [Online]. Available: https://opensignal.com/reports/2018/07/usa/state-of-the-mobile-network. [Accessed: 27-Jul-2018].

[127] R. A. Cacheda *et al.*, "QoS Requirements For Multimedia Services," in *Resource Management in Satellite Networks*, Boston, MA: Springer US, pp. 67–94.

[128] Dang Nam-Khanh; Tran Xuan-Tu; Le-Van Thanh-Vu, "FPGA Implementation of a Low Latency and High Throughput Network-on-Chip Router Architecture," *IEICE ICDV*, pp. 11–16, 2011.

[129] P. Zetterberg and R. Fardi, "Open Source SDR Frontend and Measurements for 60-GHz Wireless Experimentation," *IEEE Access*, vol. 3, pp. 445–456, 2015.

[130] A. A. Abidi, "The Path to the Software-Defined Radio Receiver," *IEEE J. Solid-State Circuits*, vol. 42, no. 5, pp. 954–966, May 2007.

[131] Ettus Research, "USRP Hardware Driver and USRP Manual: Daughterboards," *Ettus Research*. [Online]. Available: https://files.ettus.com/manual/page_dboards.html. [Accessed: 15-Apr-2017].

[132] M. G. Solomon, D. Kim, P. and C. S. O. S. E. I. F. V. D. K. (In, and J. L. Carrell, *Fundamentals of Communications and Networking*. Jones & Bartlett Publishers, 2014.

[133] Zhichu Cui, "Allowable Limit of Error in Clinical Chemestry Quality Control," *Clin. Cehem*, vol. 35/4, pp. 630–631.

[134] M. A. Rico-Martínez *et al.*, "Latency analysis on W-band hybrid fiber-wireless link using software defined radio in real time," *Rev. Fac. Ing. Univ. Antioquia*, no. 87, pp. 16–22, Jun. 2018.

[135] R. Hofstetter, H. Schmuck, and R. Heidemann, "Dispersion effects in optical millimeter-wave systems using self-heterodyne method for transport and generation," *IEEE Trans. Microw. Theory Tech.*, vol. 43, no. 9, pp. 2263–2269, Sep. 1995.

[136] S. Rommel, L. C. P. Cavalcante, A. G. Quintero, A. K. Mishra, J. J. Vegas Olmos, and I. T. Monroy, "W-band photonic-wireless link with a Schottky diode envelope detector and bend insensitive fiber," *Opt. Express*, vol. 24, no. 11, p. 11312, May 2016.

[137] E. Dahlman *et al.*, "5G wireless access: Requirements and realization," *IEEE Commun. Mag.*, 2014.
[138] T. Yang, M. Gao, J. Qian, J. Zhang, and W. Chen, "A flexible millimeter-wave radio-over-fiber system for various transmission bit rate," *Opt. Laser Technol.*, vol. 96, pp. 132–140, Nov. 2017.
[139] J. Yao, "Microwave Photonics," *J. Light. Technol.*, vol. 27, no. 3, pp. 314–335, Feb. 2009.
[140] X. Yu *et al.*, "400-GHz Wireless Transmission of 60-Gb/s Nyquist-QPSK Signals Using UTC-PD and Heterodyne Mixer," *IEEE Trans. Terahertz Sci. Technol.*, vol. 6, no. 6, pp. 765–770, Nov. 2016.
[141] X. Pang *et al.*, "260 Gbit/s photonic-wireless link in the THz band," in *2016 IEEE Photonics Conference (IPC)*, 2016, pp. 1–2.
[142] J. Zhang, J. Yu, N. Chi, Z. Dong, X. Li, and G. K. Chang, "Multichannel 120-Gb/s Data Transmission Over 2× 2 MIMO fiber-wireless link at W-band," *IEEE Photonics Technol. Lett.*, vol. 25, no. 8, pp. 780–783, Apr. 2013.
[143] Z. Zhang, J. Ma, Q. Zhang, and S. Huang, "An analog mobile fronthaul based on low and high frequency hybrid network for next generation mobile system," *Opt. Fiber Technol.*, vol. 38, pp. 123–129, Nov. 2017.
[144] Qualcomm Technologies, "Discussing 5G spectrum on Capitol Hill | Qualcomm," *Qualcomm*, Jul-2017. [Online]. Available: https://www.qualcomm.com/news/onq/2017/07/20/discussing-5g-spectrum-capitol-hill.
[145] G. Ancans, V. Bobrovs, A. Ancans, and D. Kalibatiene, "Spectrum Considerations for 5G Mobile Communication Systems," *Procedia Comput. Sci.*, vol. 104, pp. 509–516, Jan. 2017.
[146] KA BR Omar, "Results and implications of World Radiocommunication Conference, 2015," *ITU*, Mar. 2017.
[147] GSMA, "Considerations for the 3.5 GHz IMT range: getting ready for use," May-2017. .
[148] M. Rico-Martinez, C. C. C. Vasquez, S. I. Rodriguez, G. M. V. Duran, and I. T. Monroy, "Comparison of performance between OFDM and GFDM in a 3.5GHz band 5G hybrid Fiber-Wireless link using SDR," in *2018 International Topical Meeting on Microwave Photonics (MWP)*, 2018, pp. 1–4.
[149] M. Rico-Martinez, M. Varon, J. A. Guerrero, F. Amaya, and I. T. Monroy, "Latency and Reliability Measurements for a 3.5 GHz Optical-Wireless WDM-PON Network using SDR," in *2018 IEEE Photonics Conference (IPC)*, 2018, pp. 1–2.
[150] J. D. Cepeda, S. I. Rodríguez, M. Rico-Martínez, C. D. Muñoz, M. Varón, and I. T. Monroy, "Performance evaluation of a real time OFDM radio over fiber system at 2.5 GHz using software defined radio SDR," in *2017 SBMO/IEEE MTT-S International Microwave and Optoelectronics Conference (IMOC)*, 2017, pp. 1–5.
[151] E. Krouk and S. Semenov, *Modulation and Coding Techniques in Wireless Communications*. John Wiley & Sons, 2011.
[152] X. N. Fernando, *Radio Over Fiber for Wireless Communications*. Chichester, UK: John Wiley & Sons, Ltd, 2014.
[153] J. Torres Nova, J. M. T. Nova, and H. P. Penagos, "Studying and comparing spectrum efficiency and error probability in GMSK and DBPSK modulation schemes," *Ing. e Investig.*, vol. 28, no. 3, pp. 75–80, Sep. 2008.
[154] T. M. Schmidl and D. C. Cox, "Robust frequency and timing synchronization for OFDM," *IEEE Trans. Commun.*, vol. 45, no. 12, pp. 1613–1621, Dec. 1997.
[155] J. Armstrong, "OFDM for Optical Communications," *J. Light. Technol.*, vol. 27, no. 3, pp. 189–204, Feb. 2009.
[156] H. Mahmoud, T. Yucek, and H. Arslan, "OFDM for cognitive radio: merits and challenges," *IEEE Wirel. Commun.*, vol. 16, no. 2, pp. 6–15, Apr. 2009.
[157] H. Mahmoud, T. Yucek, and H. Arslan, "OFDM for cognitive radio: merits and challenges,"

IEEE Wirel. Commun., vol. 16, no. 2, pp. 6–15, Apr. 2009.
[158] H. Arslan, Ed., *Cognitive Radio, Software Defined Radio, and Adaptive Wireless Systems*. Dordrecht: Springer Netherlands, 2007.
[159] M. Stecher and J. Wolf, “Detectors and procedures for the measurement of out-of-band emissions,” 2002, pp. 253–256.
[160] A. Farhang, N. Marchetti, and L. E. Doyle, “Low-Complexity Modem Design for GFDM,” *IEEE Trans. Signal Process.*, vol. 64, no. 6, pp. 1507–1518, Mar. 2016.
[161] S. K. Antapurkar, A. Pandey, and K. K. Gupta, “GFDM performance in terms of BER, PAPR and OOB and comparison to OFDM system,” 2016, p. 020039.
[162] A. Kumar, M. Magarini, and S. Bregni, “Improving GFDM Symbol Error Rate Performance using ¨Better than Nyquist¨Pulse Shaping Filters,” *IEEE Lat. Am. Trans.*, vol. 15, no. 7, pp. 1244–1249, 2017.
[163] N. Michailow, S. Krone, M. Lentmaier, and G. Fettweis, “Bit Error Rate Performance of Generalized Frequency Division Multiplexing,” in *2012 IEEE Vehicular Technology Conference (VTC Fall)*, 2012, pp. 1–5.
[164] J. Demel, C. Bockelmann, and A. Dekorsy, “Evaluation of a software defined GFDM implementation for industry 4.0 applications,” in *2017 IEEE International Conference on Industrial Technology (ICIT)*, 2017, pp. 1283–1288.
[165] N. ; Michailow *et al.*, “Generalized Frequency Division Multiplexing: A Flexible Multi-Carrier Modulation Scheme for 5th Generation Cellular Networks Generalized Frequency Division Multiplexing: A Flexible Multi-Carrier Modulation Scheme for 5th Generation Cellular Networks.”
[166] 3GPP, “Release 15. Technical specification Group services and systems aspects,” *3GPP*. [Online]. Available: http://www.3gpp.org/release-15. [Accessed: 12-Dec-2018].
[167] IEEE, “Standards - IEEE 5G,” *IEEE*. [Online]. Available: https://futurenetworks.ieee.org/standards. [Accessed: 12-Dec-2018].
[168] E. Martin *et al.*, “28 GHz 5G radio over fibre using UF-OFDM with optical heterodyning,” in *2017 International Topical Meeting on Microwave Photonics (MWP)*, 2017, pp. 1–4.
[169] “GitHub,” *GitHub*. .
[170] Z. Wang, L. Mei, X. Wang, and N. Zhang, “Bit error rate analysis of generalised frequency division multiplexing with weighted-type fractional Fourier transform precoding,” *IET Commun.*, vol. 11, no. 6, pp. 916–924, Apr. 2017.
[171] Z. Zhong and J. Guo, “Bit error rate analysis of a MIMO-generalized frequency division multiplexing scheme for 5th generation cellular systems,” in *2016 IEEE International Conference on Electronic Information and Communication Technology (ICEICT)*, 2016, pp. 62–68.
[172] N. Michailow, S. Krone, M. Lentmaier, and G. Fettweis, “Bit Error Rate Performance of Generalized Frequency Division Multiplexing,” in *2012 IEEE Vehicular Technology Conference (VTC Fall)*, 2012, pp. 1–5.
[173] “KPIs ‹ 5G-PPP.” [Online]. Available: https://5g-ppp.eu/kpis/. [Accessed: 28-Feb-2018].
[174] E. David Kennedy, “D2.6 Final report on programme progress and KPIs,” Euro 5G, Oct. 2017.
[175] ITU-T Standard, “End-to-end error performance parameters and objectives for international, constant bit-rate digital paths and connections.” .
[176] G. K. Chang *et al.*, “Key Technologies of WDM-PON for Future Converged Optical Broadband Access Networks [Invited],” *IEEE/OSA J. Opt. Commun. Netw.*, vol. 1, no. 4, pp. C35–C50, Sep. 2009.
[177] “G.694.1 : Spectral grids for WDM applications: DWDM frequency grid.” [Online]. Available: https://www.itu.int/rec/T-REC-G.694.1/. [Accessed: 29-Jan-2019].
[178] X. Chen and J. Yao, “Wavelength Reuse in a Symmetrical Radio Over WDM-PON Based on Polarization Multiplexing and Coherent Detection,” *J. Light. Technol.*, vol. 34, no. 4, pp. 1150–1157, Feb. 2016.

[179] KyungWoon Lee, Jung Ho Park, and HyunDo Jung, “Comparison of digitized and analog radio-over-fiber systems over WDM-PON networks,” in *2013 International Conference on ICT Convergence (ICTC)*, 2013, pp. 705–706.

[180] J. Zacharias and V. Narayanan, “Simulation of WDM-PON and radio over fiber with single mach zehnder modulator,” in *2015 International Conference on Control Communication & Computing India (ICCC)*, 2015, pp. 401–406.

[181] N. G. Gonzalez, D. Zibar, A. Caballero, and I. T. Monroy, “Experimental 2.5-Gb/s QPSK WDM Phase-Modulated Radio-Over-Fiber Link With Digital Demodulation by a K-Means Algorithm,” *IEEE Photonics Technol. Lett.*, vol. 22, no. 5, pp. 335–337, Mar. 2010.

[182] A. A. Abidi, “The Path to the Software-Defined Radio Receiver,” *IEEE J. Solid-State Circuits*, vol. 42, no. 5, pp. 954–966, May 2007.

[183] “Ettus Research - The leader in Software Defined Radio (SDR).” .

[184] C. Zhang, T. Ning, J. Li, L. Pei, C. Li, and S. Ma, “A full-duplex WDM-RoF system based on tunable optical frequency comb generator,” *Opt. Commun.*, vol. 344, pp. 65–70, Jun. 2015.

[185] G. H. Smith, D. Novak, and C. Lim, “A millimeter-wave full-duplex fiber-radio star-tree architecture incorporating WDM and SCM,” *IEEE Photonics Technol. Lett.*, vol. 10, no. 11, pp. 1650–1652, Nov. 1998.

[186] Cepeda Juan David, “Comparacion de dos tecnicas de generacion de f orma de onda OFDM y UFMC para un enlace de LTE sobre fibra optica,” Universidad Nacional de Colombia Faculty of Eng, Bogotá, 2016.

[187] “Ettus N200-210 Datasheet,” 2013.

[188] “USRP™ B200mini Series Product Overview,” 2015.

[189] Alcatel-Lucent Deutschland AG, “UFMC (Matlab files) | 5GNow,” *web page*, 2010. [Online]. Available: http://www.5gnow.eu/?page_id=424. [Accessed: 29-Jan-2017].